

CHROMATIN AND TRANSCRIPTIONAL REGULATION IN MOUSE MACROPHAGES

By

Michael McAndrew

A DISSERTATION

**Submitted to
Michigan State University
in partial fulfillment of the requirements
for the degree of**

Genetics-Doctor of Philosophy

2017

ABSTRACT

CHROMATIN AND TRANSCRIPTIONAL REGULATION IN MOUSE MACROPHAGES

By

Michael McAndrew

Eukaryotic genomes must be extensively packaged into a DNA-protein complex called chromatin due to their large sizes and the spatial restrictions of the nucleus.

Nucleosomes, the basic repeating unit of this complex, have long been viewed as a barrier to basic cellular processes including transcription, and recent studies suggest that chromatin architecture plays a critical role in the regulation of gene expression. We have used primary bone marrow-derived macrophages (BMDMs) as a model to investigate chromatin changes associated with inducible and cell-type specific gene expression in response to bacterial lipopolysaccharide (LPS). Macrophages are specialized cells of the innate immune system that arise during differentiation from multipotent hematopoietic stem and progenitor cells (HSPCs) through the coordinated action of lineage-specific transcription factors (TFs). These cells have unique functions in response to foreign threat, and previous genome-wide studies have identified macrophage-specific distal enhancers that play a key role in the pro-inflammatory response to LPS. Using a quantitative nucleosome occupancy assay, we have shown that nucleosomes are stably evicted from these enhancers under inducing conditions in BMDMs, and this depletion correlates with signal-induced TF binding and increased gene expression. Using a knockdown approach targeting BAF/PBAF chromatin remodeling complexes, we have shown that nucleosome remodelers are recruited to regulatory elements early during differentiation by lineage-specific TFs, and that

disruption of this process results in increased nucleosome occupancy at these elements and prevents nucleosome eviction and gene induction in response to LPS. In order to more precisely determine how and when enhancers might be rendered accessible during differentiation, we further investigated chromatin structure in HSPCs. This led to the surprising finding that nucleosome occupancy may be universally low in these cells. We are now using a genome-wide extension of the quantitative nucleosome occupancy (GNO-seq, Global Nucleosome Occupancy-sequencing) to analyze changes in nucleosome occupancy associated with macrophage differentiation from HSPCs genome-wide. This research will provide crucial insights into the regulation of inducible gene expression, the role of remodelers in maintaining chromatin accessibility, and may demonstrate global differences in chromatin between cell types.

**Copyright by
MICHAEL MCANDREW
2017**

To Elijah. Stay curious.

ACKNOWLEDGMENTS

I would like to thank my mentor Dr. Monique Floer for the opportunity to pursue these projects. I would like to thank her for her time, insight, and patience. My graduate experience has shaped my understanding of what a scientist does and should do, as well as the questions that should be asked and which of these can be adequately addressed with evidence.

I would like to thank all of the former members of the Floer laboratory for their productive scientific discussions and support: Dr. Mohita Tagore, Alison Gjidoda, Tyler Miksanek, Hunter Piegols, and Alexander Woods.

I would like to thank my committee members for guidance and insight: Dr. David Arnosti, Dr. Jason Knott, and Dr. Min-Hao Kuo.

I would like to thank Dr. Amy Ralston and the members of her laboratory for helpful comments and discussion during our joint lab meetings: Dr. Tristan Frum, Dr. Mike Halbisen, Dr. Alyson Lokken, and Dr. Tony Parenti. I would like to especially thank Dr. Halbisen for his assistance with principles of bioinformatics, and Dr. Parenti for providing embryonic stem cells, as well as teaching me to culture them myself.

I would like to thank Dr. Louis King, Dr. Nara Parameswaran, and Michael Steury for their expertise and assistance with cell staining and flow cytometry.

I would like to thank Dr. Shin-Han Shiu, Dr. Sahra Uygun, and Nicholas Panchy for their assistance with genome-wide techniques and subsequent analyses.

I would like to thank Dr. Erik Martinez-Hackert for the use of his tissue culture hood.

I would like to thank past and present members of the Genetics Graduate Program for their friendship, support, and guidance. I would like to especially thank Dr. Barbara Sears for believing in me; Dr. Cathy Ernst for listening to me; and Jeannine Lee for being a good lunch partner and an even better program secretary.

Finally, I would like to thank my wife Rachel, my mother Sandra, my father Michael, my brother Josh, and my sister-in-law Lora for their unconditional love and support during these last six years. I could not have done it without you.

TABLE OF CONTENTS

LIST OF TABLES	xi
LIST OF FIGURES	xii
KEY TO ABBREVIATIONS	xiv
Chapter 1: Introduction	1
Chromatin is a barrier to transcription	2
Mouse macrophages as a model for the study of transcriptional regulation	3
Open chromatin is a feature of lineage-specific enhancers	4
Pioneer factors in macrophage differentiation	5
Chromatin remodeling complexes and transcription	6
Unique chromatin states in multipotent progenitors and stem cells	8
Clinical Significance	10
REFERENCES	11
Chapter 2: Nucleosomes are stably evicted from enhancers but not promoters upon induction of certain pro-inflammatory genes in mouse macrophages	18
Abstract	19
Introduction	19
Experimental Procedures	23
Cell isolation and culture	23
mRNA determination	24
Chromatin immunoprecipitation	24
Quantitative nucleosome occupancy assay	25
Genomic DNA isolation	26
qRT-PCR	26
Results	26
Nucleosome occupancy at the <i>Il12b</i> enhancer and promoter upon LPS induction	26
Changes in nucleosome occupancy at the transcriptional regulatory regions of <i>Il1a</i>	31
Timing of enhancer nucleosome removal	32
Histone modifications at the promoters and enhancers of <i>Il12b</i> and <i>Il1a</i>	32
Binding of cis-regulatory TFs to the distal enhancers of <i>Il12b</i> and <i>Il1a</i>	36
Binding of the transcriptional machinery to nucleosome-free <i>Il12b</i> and <i>Il1a</i> promoters	41
Discussion	43
Acknowledgements	49
REFERENCES	50
Chapter 3: Chromatin remodeler recruitment during macrophage differentiation facilitates transcription factor binding to enhancers in mature cells	56

Abstract.....	57
Introduction	57
Experimental Procedures	60
Cell isolation and culture.....	60
shRNA mediated knockdown of BRG1 and SNF5.....	61
Quantitative nucleosome occupancy assay.....	61
Chromatin immunoprecipitation	61
mRNA determination.....	62
Chromatin fractionation and Western blotting.....	62
Flow cytometry.....	64
Statistical analysis.....	65
Results.....	65
BAF/PBAF is recruited to the <i>Il12b</i> and <i>Il1a</i> enhancers in BMDMs.....	65
BAF/PBAF recruitment is a consequence of PUER translocation to the nucleus.....	66
BAF/PBAF is required for <i>Il12b</i> and <i>Il1a</i> induction in BMDMs.....	71
BRG1 KD affects nucleosome occupancy and eviction at the <i>Il12b</i> and <i>Il1a</i> enhancers	72
Knockdown of SNF5 abolishes BAF/PBAF binding at the <i>Il12b</i> and <i>Il1a</i> enhancers	78
Nucleosome occupancy at the <i>Il12b</i> and <i>Il1a</i> enhancers increases in the absence of BAF/PBAF recruitment.....	82
FACS analysis reveals effects of SNF5 KD on cytokine expression in single cells	86
Discussion	89
Acknowledgements.....	93
REFERENCES	94

Chapter 4: GNO-seq quantifies nucleosome occupancy at gene promoters and enhancers in LPS stimulated macrophages	99
Abstract.....	100
Introduction	101
Experimental Procedures	104
Cell isolation and sample preparation.....	104
Illumina library preparation and sequencing	105
Data processing	105
Generation of lambda-normalized GNO-seq tracks.....	106
Random genomic sampling	107
GC content.....	107
Heatmaps and average nucleosome occupancy plots	108
Identification of nucleosome depleted regions.....	110
Gene ontology analysis.....	110
<i>De novo</i> motif search	110
Nucleosome occupancy at super-enhancers.....	111
Results.....	111
GNO-seq analysis.....	111

GNO-seq validation.....	114
Nucleosome occupancy surrounding transcriptional start sites	118
Promoter nucleosomes at highly induced genes	123
LPS-induced changes in nucleosome occupancy at enhancers.....	126
Identification of regions partially depleted in rM and further depleted in aM	131
Different enhancer categories show characteristic depletion in rM and aM	133
TF consensus-sites associated with poised-activated and poised-not activated enhancers.....	137
Nucleosome depletion at super-enhancers	139
Discussion	143
Nucleosome removal at promoters	143
Nucleosome depletion at enhancers.....	146
Conclusion	147
Acknowledgements.....	148
APPENDICES.....	149
APPENDIX A: Supplementary Experimental Procedures.....	150
APPENDIX B: Supplementary Figures	153
REFERENCES	163

Chapter 5: Global nucleosome occupancy increases during differentiation of hematopoietic stem and progenitor cells into macrophages	171
Introduction	172
Experimental Procedures	174
Cell isolation and culture.....	174
Quantitative nucleosome occupancy assay.....	175
Quantitation of total cellular chromatin protected against digestion by MNase.....	175
Flow cytometry.....	176
Results.....	176
Nucleosome occupancy at macrophage-specific enhancers increases during differentiation	176
Protection of total cellular chromatin against MNase increases as HSPCs differentiate into macrophages.....	184
Nucleosome occupancy is lower in ESCs than in differentiated cells.....	186
Discussion	187
REFERENCES	191
Chapter 6: Conclusions and future directions	194
REFERENCES	199

LIST OF TABLES

Table 2.1.	Statistical significance of factor binding, CHIP of Fig. 2.3	40
Table 4.1.	Categories of putative enhancers identified by Ostuni et al..	127
Table 4.S1	Threshold conditions defining partially depleted regions in rM and regions of nucleosome eviction in aM.....	162

LIST OF FIGURES

Figure 2.1.	Changes in nucleosome occupancy upon LPS induction at a distal enhancer and the promoter of <i>I12b</i>	29
Figure 2.2.	Changes in nucleosome occupancy upon LPS induction at a putative distal enhancer and promoter of <i>I1a</i> , kinetics of nucleosome removal, and changes in histone modifications .	34
Figure 2.3.	Binding of cis-regulatory TFs and recruitment of the transcriptional machinery to the regulatory regions of <i>I12b</i> and <i>I1a</i> upon LPS induction.....	38
Figure 2.4.	PoIII and TBP binding in the fraction of <i>I12b</i> and <i>I1a</i> promoters in a population of induced BMDMs that is nucleosome-free	42
Figure 3.1.	Recruitment of BAF/PBAF to macrophage-specific enhancers	69
Figure 3.2.	KD of the catalytic BAF/PBAF subunit BRG1.....	73
Figure 3.3.	Nucleosome occupancy in sh <i>Luc</i> treated and untreated control cells.....	77
Figure 3.4.	KD of the shared BAF/PBAF core subunit SNF5	80
Figure 3.5.	Nucleosome occupancy in SNF5 KD cells	84
Figure 3.6.	Cytokine expression in SNF5 KD cells	87
Figure 3.7.	Remodeler assisted competition favors TF over nucleosome binding to sites in enhancers	91
Figure 4.1.	GNO-seq analysis	113
Figure 4.2.	Nucleosome occupancy at promoters	120
Figure 4.3.	Nucleosome occupancy at promoters of LPS-induced genes	124
Figure 4.4.	Nucleosome occupancy at macrophage enhancers	130
Figure 4.5.	Regions of nucleosome depletion and TF-motifs in putative enhancers	136

Figure 4.6	Nucleosome occupancy at super-enhancers	141
Figure 4.S1.	Correlation between fractional nucleosome occupancies obtained as the ratio of MNase over Input-fractions and occupancies obtained by curve-fitting	154
Figure 4.S2.	Fragment sizes of inserts in Illumina libraries	155
Figure 4.S3.	GNO-seq analysis at enhancers and promoters of three pro-inflammatory genes	156
Figure 4.S4.	Nucleosome occupancy at <i>Il12b</i> and <i>Il1a</i> determined by the MNase option of deepTools bamCoverage, DANPOS and GNO-seq, and compared to the qRT-PCR based assay	157
Figure 4.S5.	Nucleosome occupancy in the genome analyzed by GNO-seq and deepTools bamCoverage without dyad alignment.....	158
Figure 4.S6.	Expression of genes highly expressed in the presence of LPS	159
Figure 4.S7.	Nucleosome occupancy at enhancers aligned at their midpoint	160
Figure 4.S8.	Nucleosome occupancy at enhancers aligned at their PU.1 or p300 peaks	161
Figure 5.1.	Isolation of HSPCs	177
Figure 5.2.	Nucleosome occupancy in HSPCs and differentiating BMDMs ..	181
Figure 5.3.	Protection of total cellular chromatin against digestion by MNase in HSPCs and in differentiating BMDMs.....	185
Figure 5.4.	Nucleosome occupancy in ESCs and differentiated MEFs....	187

KEY TO ABBREVIATIONS

AP1	Activator protein 1
APC	Allophycocyanin
BAF	BRG1- or HBRM-associated factors
BAF155	BRG1-associated factor 155
BMDM	Bone marrow derived macrophage
BRG1	Brahma-related gene 1 (see also: SMARCA4)
C/EBP β	CCAAT/enhancer-binding protein beta
CSFR1	Colony stimulating factor 1 receptor
DNA	Deoxyribonucleic acid
DNase I	Deoxyribonuclease I
EDTA	Ethylenediaminetetraacetic acid
ESC	Embryonic stem cell
FACS	Fluorescence-activated cell sorting
FBS	Fetal bovine serum
FITC	Fluorescein isothiocyanate
FPKM	Fragments Per Kilobase of transcript per Million mapped reads
H3K4me1	Histone H3 lysine 4 monomethyl
H3K4me3	Histone H3 lysine 4 trimethyl
H3K27ac	Histone H3 lysine 27 acetyl
H3K27me3	Histone H3 lysine 27 trimethyl
HSPC	Hematopoietic stem and progenitor cell
IFNB1	Interferon B1

IL1A	Interleukin 1 alpha
IL12B	Interleukin 12B
IRF	Interferon regulatory factor
KD	Knockdown
LPS	Lipopolysaccharides
M-CSF	Macrophage colony-stimulating factor
MNase	Micrococcal nuclease
PBAF	Polybromo-associated BAF (see also: BAF)
PCR	Polymerase chain reaction
PEG	Polyethylene glycol
PRC2	Polycomb repressive complex 2
PUER	PU.1-estrogen receptor chimera
RNA	Ribonucleic acid
RPL4	Ribosomal protein L4
shRNA	short hairpin RNA
SMARCA4	SWI/SNF related, matrix associated, actin dependent regulator of chromatin, subfamily A, member 4 (see also: BRG1)
SMARCB1	SWI/SNF related, matrix associated, actin dependent regulator of chromatin, subfamily B, member 1 (see also: SNF5)
SNF5	Sucrose nonfermenting 5 (see also: SMARCB1)
SWI/SNF	SWItch/Sucrose Non-Fermentable
TF	Transcription factor
TLR4	Toll-like receptor 4
TSS	Transcription start site

XBP

X-box binding protein

Chapter 1: Introduction

Chromatin is a barrier to transcription

Eukaryotes have large genomes that must be condensed and extensively packaged into a protein-DNA complex called chromatin due to the spatial restrictions of the nucleus.

The basic repeating element of this complex is the nucleosome, an octamer composed of two subunits each of the core histone proteins (H2A, H2B, H3, and H4). This octamer forms a highly basic globular core around which approximately 147 base pairs of DNA is tightly wound (1). Because of its role in compaction, the nucleosome has long been perceived as a barrier that must be overcome in order for the transcriptional machinery to bind.

This perception was reinforced by early studies that identified “nucleosome free” or “nucleosome depleted” regions at specific transcriptional promoters (2). More recent genome-wide studies in the yeast *S. cerevisiae* have indicated that many promoter regions are indeed relatively depleted of nucleosomes compared to the surrounding regions (3,4,5), and studies at individual genes such as the yeast *PHO5* and *GAL1/10* loci have found that promoter nucleosome removal is required for gene induction. This process is mediated by nucleosome remodelers (e.g. the SWI/SNF complex), which are recruited to these promoters by specific transcription factors (TFs) (6,7). Nucleosomal sites at the *GAL1/10* promoters are lowly occupied even before induction, allowing rapid nucleosome removal when the inducer galactose is added (8). Together, these studies suggest that transcriptional regulatory regions in yeast must be cleared of nucleosomes to allow binding of both cis-regulatory TFs and the transcriptional machinery.

Genome-wide studies have suggested that active promoters are also relatively depleted of nucleosomes in mammalian systems (9,10). In higher order organisms, however,

promoter nucleosome depletion is often cell type-specific and limited to genes that are expressed in a particular lineage. The *cKit* gene promoter, for instance, is nucleosome free in mast cells, where the gene is constitutively expressed, but not in other cell types (11). Changes in nucleosome occupancy—as determined by sensitivity to micrococcal nuclease (MNase)—associated with changes in gene expression have also been detected in differentiating embryonic stem cells (ESCs) (10,12), suggesting that nucleosomes may be placed at or removed from promoters in specific cell types in order to facilitate or silence the expression of the associated gene.

Mouse macrophages as a model for the study of transcriptional regulation

The controlled access of transcription factors to DNA binding sites is particularly important in higher eukaryotes, where gene expression programs are often restricted to specific cell lineages. One such program is the pro-inflammatory response which may be activated in mature macrophages, a form of white blood cell whose development requires expression of the lineage-specific TFs PU.1 and C/EBP β in order to properly differentiate from hematopoietic stem cells (HSCs) (14,15). Macrophages are responsible for the stimulation of other immune cells via the release of pro-inflammatory gene products. When macrophages are exposed to a foreign pathogen—an event which may be simulated *in vitro* via the addition of bacterial lipopolysaccharide (LPS) to culture media—the toll-like receptor 4 (TLR4) pathway is activated to stimulate cytokine production (for review, see (15)). The inflammation program in macrophages is thus a critical component of the healthy immune response to pathogens. Misregulation of inflammation in these cells has, however, been implicated in a number of autoimmune diseases and cancers, as well as diabetes, demonstrating the importance of tightly

controlled expression of pro-inflammatory genes. In addition to its role in human disease, the inducible nature of the inflammatory response makes it an ideal model for studying the role of chromatin architecture in highly regulated gene expression programs.

Open chromatin is a feature of lineage-specific enhancers

In addition to their promoters, mammalian genes are often regulated by more distal elements called enhancers that may be thousands of base pairs away from the associated gene (for review, see (16)). These elements may be marked by regions of “open” chromatin—as determined by their sensitivity to nucleases like DNase I and MNase—in a particular cell type in which the associated genes are active, indicating that regulatory elements may be rendered accessible for transcription factor binding in a lineage-specific manner (10,17,18).

These regions were first identified in detailed studies at particular loci (19), and studies by the Smale laboratory were the first to identify a distal enhancer 10 kilobases (kb) upstream of the *Il12b* gene. This element was shown to be involved in *Il12b* expression upon LPS induction, and reporter assays that mimicked the endogenous nucleosome environment confirmed that this putative regulatory region did indeed enhance *Il12b* expression (20).

The advent of genome-wide techniques such as chromatin immunoprecipitation sequencing (ChIP-seq) has allowed the identification of many thousands of putative enhancers of pro-inflammatory and macrophage-specific gene expression based on the presence of histone modifications (histone H3 lysine 4 monomethylation (H3K4me1) and histone H3 lysine 27 acetylation (H3K27ac)) and transcriptional co-

activators/histone-modifying enzymes (p300) (21,22). These elements often contain binding sites for three of the primary signal-induced TFs required for pro-inflammatory gene expression: NF κ B, AP1 and IRF3/7 (23). Macrophage-specific enhancers are also typically associated with the lineage-specific TFs PU.1 and/or C/EBP β even before induction with LPS (21), and both of these TFs have been shown to be required for pro-inflammatory gene expression (21,22,24).

Although these studies have proven useful in identifying regions that may act as transcriptional enhancers, the data gathered does not provide detailed information about nucleosome occupancy and positioning, nor do they always provide direct evidence for the function of these elements. Therefore, it is still unknown how small differences in chromatin architecture may contribute to large differences in gene expression.

Pioneer factors in macrophage differentiation

In addition to their direct role in gene expression, there is mounting evidence that PU.1 and CEBP are pioneer factors, a subset of lineage-specific TFs expressed early during differentiation that have the unique ability among TFs to bind their sites on chromatinized DNA (for review, see (25)).

PU.1 binding is detected at macrophage-specific enhancers even before induction with LPS, and has been shown to lead to nucleosome depletion at these sites by ourselves and others (26,27), suggesting that PU.1 may “prime” enhancers for subsequent transcription factor binding and activity even in the absence of stimuli. Co-immunoprecipitation studies have also shown that PU.1 may directly interact with members of the BAF complex, the mammalian homolog of the yeast SWI/SNF complex

(28, see also *Chromatin remodeling complexes and transcription* below). The lineage-specific TF CEBP β also binds macrophage-specific enhancers, often in a PU.1 dependent manner (22). It has also been reported that CEBP β contains a SWI/SNF interaction domain, which may allow the recruitment of the Brg1 subunit of BAF/PBAF *in vitro* (29). Elegant transdifferentiation studies by Thomas Graf's laboratory have demonstrated that expression of CEBP β and PU.1 is sufficient to convert both B cells (30) and fibroblasts (14) into macrophage-like cells. These results suggest that forced expression of these TFs may render previously inaccessible regulatory elements accessible in differentiated cells, providing further evidence that both of the TFs required for macrophage differentiation (*i.e.*, PU.1 and CEBP β) may interact directly with chromatin and/or chromatin remodelers.

Chromatin remodeling complexes and transcription

Nucleosome remodelers are large protein complexes capable of sliding or removing nucleosomes from DNA *in vitro*, and there is evidence that the SWI/SNF family of remodelers plays a direct role in facilitating TF binding and subsequent gene expression *in vivo*. This complex has been well studied in yeast, where it removes nucleosomes from the *PHO5* and *GAL1/10* promoters upon induction of those genes (6,7). The related RSC (Remodelling the Structure of Chromatin) complex has been shown to properly position nucleosomes at regulatory regions before induction (31,32) and partially unwrap nucleosomes in order to expose TF binding sites (33).

The mammalian BAF and PBAF complexes are the functional homologs of the yeast SWI/SNF and RSC complexes, respectively. The mammalian complexes share the core subunits Brg1, Baf170, Baf155, and Snf5, all of which are required for full nucleosome

remodeling activity *in vitro* (34). Each complex also contains unique subunits that may contribute to differential binding and/or function *in vivo* (for review, see (35)). Both complexes are capable of incorporating the catalytic subunit Brg1, but BAF may also utilize the alternate catalytic subunit Brm. Knockout studies in mice have shown that Brg1 deletion is early embryonic lethal (36), but Brm^{-/-} embryos develop normally, and it has been suggested that Brm^{-/-} cells may compensate for the loss of Brm through the upregulation of Brg1 (37). Brg1 is also required for the differentiation of a variety of cell types, including lymphoid (38) and myeloid (29) lineages, and Brg1 appears to be recruited to cell type-specific genes during erythroid differentiation (39). Taken together, these studies suggest that Brg1 plays a key role in the differentiation of lineages derived from HSCs.

Because of their role in evicting or sliding nucleosomes, chromatin remodeling complexes have long been of great interest in the study of transcriptional regulation, and studies at numerous genes in different cell types have shown an increased sensitivity to nucleases like DNase I and MNase at both promoters and enhancers upon expression of the associated genes, indicating that nucleosomes may be removed from these sites in order to allow binding of TFs or the transcriptional machinery (see for example (40,41)). At the inducible human interferon β gene, for example, the promoter is cleared of nucleosomes upon viral induction, leaving the TATA box accessible for binding (42).

Genome-wide studies suggest that Brg1 is recruited to many inducible genes (43,44), and a recent study classified pro-inflammatory genes according to Brg1 dependence upon LPS induction (45) in a mouse macrophage cell line. Simultaneous knockdown of

both Brg1 and Brm was sufficient to impair the expression of a subset of pro-inflammatory genes when the cells were exposed to stimuli, while changes in the expression of other genes was minimal or unchanged. These authors suggested a role for Brg1/Brm in altering chromatin structure at non-CpG island promoters, and concluded that the expression of secondary response genes, as well as that of a subset of primary response genes, was dependent on Brg1/Brm. They did not, however, investigate the role of BAF/PBAF at pro-inflammatory enhancers, and the role that chromatin remodelers may play at enhancers therefore remains an area of intense investigation.

Unique chromatin states in multipotent progenitors and stem cells

Although the regulation of pro-inflammatory genes in macrophages has been an active area of study for some time, comparatively little is known about chromatin in the hematopoietic stem and progenitor cells (HSPCs) that the myeloid lineage is derived from. It thus remains unclear how lineage-specific TFs like PU.1 and CEBP β might initially access their binding sites during differentiation. A growing number of recent studies suggest that chromatin of other multipotent stem cells may be more accessible to DNA binding proteins, however. A genome-wide MNase-seq study investigated nucleosome binding in embryonic stem cells (ESCs), mouse embryonic fibroblasts (MEFs), and neural progenitor cells (NPCs) suggested that ESC differentiation to these two lineages was associated with changes in nucleosome positioning at regulatory elements (10). Further, the authors concluded that relative nucleosome occupancy—as determined by sensitivity to MNase digestion—at various TF binding sites differed between cell types, suggesting that TFs that are active in a particular lineage may be

associated with nucleosome free or nucleosome depleted sites. How nucleosomes might be depleted from these sites remains unclear, but a recent study from our laboratory investigating the role of PU.1 in macrophage differentiation suggested that lineage-specific factors may bind regulatory elements early during differentiation in order to prevent heterochromatin formation, keeping these loci accessible to TF binding in mature cells (27).

Total chromatin of ESCs has been shown to be more accessible to digestion by either DNase I or MNase than that of differentiated cells (46), and the number of DNase I hypersensitive sites present in ESCs decreases as cells differentiate (47). ChIP-seq studies have also shown that more of the genome is associated with “active” histone modifications (H3/H4 acetylation) in ESCs when compared to differentiated cells (48). Furthermore, less of the genome is associated with repressive histone modifications that may be associated with heterochromatin (histone H3 lysine 9 trimethylation, H3K9me3), and modest levels of transcription were detected from much of the genome in an RNA-seq study (49), suggesting that most ESC DNA may be accessible to the transcriptional machinery. This global transcription is not detected in differentiated cells, and a recent study utilizing super-resolution nanoscopy determined that chromatin becomes more compacted as ESCs differentiate (50), suggesting that increased compaction may silence much of the genome in differentiated cells.

These studies suggest that chromatin of ESCs is qualitatively different from that of differentiated cells. Although chromatin of HSPCs has not been rigorously characterized, changes in chromatin compaction have long been observed in hematopoietic cells as well, and these changes have been used as a measure of a

cell's differentiation state (51). This suggests that there may be analogous differences between chromatin of HSPCs and that of mature cells of the hematopoietic lineage, but this hypothesis remains to be investigated.

Clinical significance

Chronic inflammation is characterized by the prolonged release of pro-inflammatory gene products and repeated activation of the innate immune system, and a number of diseases, including rheumatoid arthritis, are the direct result of this aberrant inflammation. The prevalence of these diseases—classified as immune-mediated inflammatory diseases (IMIDs)—is estimated to be 5-7% in Western society (52). Furthermore, chronic or prolonged inflammation has been implicated in the onset and progression of a number of other diseases including type 2 diabetes (53), Alzheimer's disease (54), and cancer (55). It is therefore crucial to further dissect the underlying mechanism regulating the expression of pro-inflammatory genes, and extensive characterization of the regulatory elements associated with these genes may provide insight into novel therapeutic targets.

REFERENCES

REFERENCES

1. Luger, K., Mader, A. W., Richmond, R. K., Sargent, D. F., and Richmond, T. J. (1997) Crystal structure of the nucleosome core particle at 2.8 Å resolution. *Nature* 389, 251-260.
2. Almer, A., and Horz, W. (1986) Nuclease hypersensitive regions with adjacent positioned nucleosomes mark the gene boundaries of the PHO5/PHO3 locus in yeast. *The EMBO journal* 5, 2681-2687.
3. Yuan GC, Liu YJ, Dion MF, Slack MD, Wu LF, et al. (2005) Genome-scale identification of nucleosome positions in *S. cerevisiae*. *Science* 309: 626–630.
4. Bernstein BE, Liu CL, Humphrey EL, Perlstein EO, Schreiber SL (2004) Global nucleosome occupancy in yeast. *Genome biology* 5: R62.
5. Sekinger EA, Moqtaderi Z, Struhl K (2005) Intrinsic histone-DNA interactions and low nucleosome density are important for preferential accessibility of promoter regions in yeast. *Molecular cell* 18: 735–748.
6. Bryant GO, Prabhu V, Floer M, Wang X, Spagna D, et al. (2008) Activator control of nucleosome occupancy in activation and repression of transcription. *PLoS biology* 6: 2928–2939.
7. Reinke H, Horz W (2003) Histones are first hyperacetylated and then lose contact with the activated PHO5 promoter. *Molecular cell* 11: 1599–1607.
8. Wang X, Bryant GO, Floer M, Spagna D, Ptashne M (2011) An effect of DNA sequence on nucleosome occupancy and removal. *Nature structural & molecular biology* 18: 507–509.
9. Schones DE, Cui K, Cuddapah S, Roh TY, Barski A, et al. (2008) Dynamic regulation of nucleosome positioning in the human genome. *Cell* 132: 887–898.
10. Teif VB, Vainshtein Y, Caudron-Herger M, Mallm JP, Marth C, Hofer T, Rippe K (2012) Genome-wide nucleosome positioning during embryonic stem cell development. *Nature structural & molecular biology* 19: 1185-1192.
11. Berrozpe G, Bryant GO, Warpinski K, Ptashne M (2013) Regulation of a mammalian gene bearing a CpG island promoter and a distal enhancer. *Cell reports* 4: 445–453.
12. Carey, T. S., Choi, I., Wilson, C. A., Floer, M., and Knott, J. G. (2014) Transcriptional reprogramming and chromatin remodeling accompanies Oct4 and

- Nanog silencing in mouse trophoblast lineage. *Stem cells and development* 23, 219-229.
13. Rosenbauer, F., and Tenen, D. G. (2007) Transcription factors in myeloid development: balancing differentiation with transformation. *Nature reviews immunology* 7, 105-117.
 14. Feng, R., Desbordes, S. C., Xie, H., Tillo, E. S., Pixley, F., Stanley, E. R., and Graf, T. (2008) PU.1 and C/EBPalpha/beta convert fibroblasts into macrophage-like cells. *Proceedings of the National Academy of Sciences of the United States of America* 105, 6057-6062.
 15. Medzhitov R (2007) Recognition of microorganisms and activation of the immune response. *Nature* 449: 819–826.
 16. Levine M (2010) Transcriptional enhancers in animal development and evolution. *Current biology: CB* 20: R754–763.
 17. Song, L., Zhang, Z., Grasfeder, L. L., Boyle, A. P., Giresi, P. G., Lee, B. K., Sheffield, N. C., Graf, S., Huss, M., Keefe, D., Liu, Z., London, D., McDaniel, R. M., Shibata, Y., Showers, K. A., Simon, J. M., Vales, T., Wang, T., Winter, D., Zhang, Z., Clarke, N. D., Birney, E., Iyer, V. R., Crawford, G. E., Lieb, J. D., and Furey, T. S. (2011) Open chromatin defined by DNaseI and FAIRE identifies regulatory elements that shape cell-type identity. *Genome research* 21, 1757-1767.
 18. Stamatoyannopoulos, J. A., Snyder, M., Hardison, R., Ren, B., Gingeras, T., Gilbert, D. M., Groudine, M., Bender, M., Kaul, R., Canfield, T., Giste, E., Johnson, A., Zhang, M., Balasundaram, G., Byron, R., Roach, V., Sabo, P. J., Sandstrom, R., Stehling, A. S., Thurman, R. E., Weissman, S. M., Cayting, P., Hariharan, M., Lian, J., Cheng, Y., Landt, S. G., Ma, Z., Wold, B. J., Dekker, J., Crawford, G. E., Keller, C. A., Wu, W., Morrissey, C., Kumar, S. A., Mishra, T., Jain, D., Byrsk-Bishop, M., Blankenberg, D., Lajoie, B. R., Jain, G., Sanyal, A., Chen, K. B., Denas, O., Taylor, J., Blobel, G. A., Weiss, M. J., Pimkin, M., Deng, W., Marinov, G. K., Williams, B. A., Fisher-Aylor, K. I., Desalvo, G., Kiralusha, A., Trout, D., Amrhein, H., Mortazavi, A., Edsall, L., McCleary, D., Kuan, S., Shen, Y., Yue, F., Ye, Z., Davis, C. A., Zaleski, C., Jha, S., Xue, C., Dobin, A., Lin, W., Fastuca, M., Wang, H., Guigo, R., Djebali, S., Lagarde, J., Ryba, T., Sasaki, T., Malladi, V. S., Cline, M. S., Kirkup, V. M., Learned, K., Rosenbloom, K. R., Kent, W. J., Feingold, E. A., Good, P. J., Pazin, M., Lowdon, R. F., and Adams, L. B. (2012) An encyclopedia of mouse DNA elements (Mouse ENCODE). *Genome biology* 13, 418.
 19. McGhee, J. D., Wood, W. I., Dolan, M., Engel, J. D., and Felsenfeld, G. (1981) A 200 base pair region at the 5' end of the chicken adult beta-globin gene is accessible to nuclease digestion. *Cell* 27, 45-55.

20. Zhou L, Nazarian AA, Xu J, Tantin D, Corcoran LM, et al. (2007) An inducible enhancer required for Il12b promoter activity in an insulated chromatin environment. *Molecular and cellular biology* 27: 2698–2712.
21. Ghisletti S, Barozzi I, Mietton F, Polletti S, De Santa F, et al. (2010) Identification and characterization of enhancers controlling the inflammatory gene expression program in macrophages. *Immunity* 32: 317–328.
22. Heinz S, Benner C, Spann N, Bertolino E, Lin YC, et al. (2010) Simple combinations of lineage-determining transcription factors prime cis-regulatory elements required for macrophage and B cell identities. *Molecular cell* 38: 576–589.
23. Kawai T, Akira S (2006) TLR signaling. *Cell death and differentiation* 13: 816– 825.
24. Grove M, Plumb M (1993) C/EBP, NF-kappa B, and c-Ets family members and transcriptional regulation of the cell-specific and inducible macrophage inflammatory protein 1 alpha immediate-early gene. *Molecular and cellular biology* 13: 5276–5289.
25. Zaret, K. S., and Carroll, J. S. (2011) Pioneer transcription factors: establishing competence for gene expression. *Genes & development* 25, 2227-2241.
26. Barozzi, I., Simonatto, M., Bonifacio, S., Yang, L., Rohs, R., Ghisletti, S., and Natoli, G. (2014) Coregulation of transcription factor binding and nucleosome occupancy through DNA features of mammalian enhancers. *Molecular cell* 54, 844-857.
27. Tagore, M., McAndrew, M. J., Gjidoda, A., and Floer, M. (2015) The lineage-specific transcription factor PU.1 prevents polycomb-mediated heterochromatin formation at macrophage-specific genes. *Molecular and cellular biology* 35, 2610-2625.
28. Gu, X., Hu, Z., Ebrahim, Q., Crabb, J. S., Mahfouz, R. Z., Radivoyevitch, T., Crabb, J. W., and Sauntharajah, Y. (2014) Runx1 regulation of Pu.1 corepressor/coactivator exchange identifies specific molecular targets for leukemia differentiation therapy. *The Journal of biological chemistry* 289, 14881-14895.
29. Kowenz-Leutz, E., and Leutz, A. (1999) A C/EBP beta isoform recruits the SWI/SNF complex to activate myeloid genes. *Molecular cell* 4, 735-743.
30. Xie H, Ye M, Feng R, Graf T, York N. (2004) Stepwise reprogramming of B cells into macrophages. *Cell* 117:663-676.
31. Badis, G., Chan, E. T., van Bakel, H., Pena-Castillo, L., Tillo, D., Tsui, K., Carlson, C. D., Gossett, A. J., Hasinoff, M. J., Warren, C. L., Gebbia, M., Talukder, S.,

- Yang, A., Mnaimneh, S., Terterov, D., Coburn, D., Li Yeo, A., Yeo, Z. X., Clarke, N. D., Lieb, J. D., Ansari, A. Z., Nislow, C., and Hughes, T. R. (2008) A library of yeast transcription factor motifs reveals a widespread function for Rsc3 in targeting nucleosome exclusion at promoters. *Molecular cell* 32, 878-887.
32. Hartley, P. D., and Madhani, H. D. (2009) Mechanisms that specify promoter nucleosome location and identity. *Cell* 137, 445-458
 33. Floer, M., Wang, X., Prabhu, V., Berrozpe, G., Narayan, S., Spagna, D., Alvarez, D., Kendall, J., Krasnitz, A., Stepansky, A., Hicks, J., Bryant, G. O., and Ptashne, M. (2010) A RSC/nucleosome complex determines chromatin architecture and facilitates activator binding. *Cell* 141, 407-418.
 34. Phelan ML, Sif S, Narlikar GJ, Kingston RE (1999) Reconstitution of a core chromatin remodeling complex from SWI/SNF subunits. *Molecular cell* 3: 247-253.
 35. Tang, L., Nogales, E., and Ciferri, C. (2010) Structure and function of SWI/SNF chromatin remodeling complexes and mechanistic implications for transcription. *Progress in biophysics and molecular biology* 102, 122-128.
 36. Bultman, S., Gebuhr, T., Yee, D., La Mantia, C., Nicholson, J., Gilliam, A., Randazzo, F., Metzger, D., Chambon, P., Crabtree, G., and Magnuson, T. (2000) A Brg1 null mutation in the mouse reveals functional differences among mammalian SWI/SNF complexes. *Molecular cell* 6, 1287-1295.
 37. Reyes, J. C., Barra, J., Muchardt, C., Camus, A., Babinet, C., and Yaniv, M. (1998) Altered control of cellular proliferation in the absence of mammalian brahma (SNF2alpha). *The EMBO journal* 17, 6979-6991.
 38. Choi, J., Ko, M., Jeon, S., Jeon, Y., Park, K., Lee, C., Lee, H., and Seong, R. H. (2012) The SWI/SNF-like BAF complex is essential for early B cell development. *Journal of immunology* 188, 3791-3803.
 39. Hu, G., Schones, D. E., Cui, K., Ybarra, R., Northrup, D., Tang, Q., Gattinoni, L., Restifo, N. P., Huang, S., and Zhao, K. (2011) Regulation of nucleosome landscape and transcription factor targeting at tissue-specific enhancers by BRG1. *Genome research* 21, 1650-1658.
 40. Lefevre P, Lacroix C, Tagoh H, Hoogenkamp M, Melnik S, et al. (2005) Differentiation-dependent alterations in histone methylation and chromatin architecture at the inducible chicken lysozyme gene. *The Journal of biological chemistry* 280: 27552-27560.
 41. Bert AG, Johnson BV, Baxter EW, Cockerill PN (2007) A modular enhancer is differentially regulated by GATA and NFAT elements that direct different tissue-

specific patterns of nucleosome positioning and inducible chromatin remodeling. *Molecular and cellular biology* 27: 2870–2885.

42. Agalioti T, Lomvardas S, Parekh B, Yie J, Maniatis T, et al. (2000) Ordered recruitment of chromatin modifying and general transcription factors to the IFN-beta promoter. *Cell* 103: 667–678.
43. Burd, C. J., and Archer, T. K. (2013) Chromatin architecture defines the glucocorticoid response. *Molecular and cellular endocrinology* 380, 25-31.
44. Sena JA, Wang L, Hu CJ (2013) BRG1 and BRM chromatin-remodeling complexes regulate the hypoxia response by acting as coactivators for a subset of hypoxia-inducible transcription factor target genes. *Molecular and cellular biology* 33: 3849-3863.
45. Ramirez-Carrozzi, V. R., Braas, D., Bhatt, D. M., Cheng, C. S., Hong, C., Doty, K. R., Black, J. C., Hoffmann, A., Carey, M., and Smale, S. T. (2009) A unifying model for the selective regulation of inducible transcription by CpG islands and nucleosome remodeling. *Cell* 138, 114-128.
46. Schaniel C, Ang YS, Ratnakumar K, Cormier C, James T, Bernstein E, Lemischka IR, Paddison PJ (2009) Smarcc1/Baf155 couples self-renewal gene repression with changes in chromatin structure in mouse embryonic stem cells. *Stem cells* 27: 2979-2991.
47. Stergachis AB, Neph S, Reynolds A, Humbert R, Miller B, Paige SL, Vernot B, Cheng JB, Thurman RE, Sandstrom R, Haugen E, Heimfeld S, Murry CE, Akey JM, Stamatoyannopoulos JA (2013) Developmental fate and cellular maturity encoded in human regulatory DNA landscapes. *Cell* 154: 888-903.
48. Meshorer E, Yellajoshula D, George E, Scambler PJ, Brown DT, Misteli T (2006) Hyperdynamic plasticity of chromatin proteins in pluripotent embryonic stem cells. *Developmental cell* 10: 105-116.
49. Efroni S, Duttagupta R, Cheng J, Dehghani H, Hoepfner DJ, Dash C, Bazett-Jones DP, Le Grice S, McKay RD, Buetow KH, Gingeras TR, Misteli T, Meshorer E (2008) Global transcription in pluripotent embryonic stem cells. *Cell stem cell* 2: 437-447.
50. Ricci MA, Manzo C, Garcia-Parajo MF, Lakadamyali M, Cosma MP (2015) Chromatin fibers are formed by heterogeneous groups of nucleosomes in vivo. *Cell* 160: 1145-1158.
51. Kernell AM, Bolund L, Ringertz NR (1971) Chromatin changes during erythropoiesis. *Experimental cell research* 65: 1-6.

52. Kuek, A., Hazleman, B. L., & Östör, A. J. (2007). Immune-mediated inflammatory diseases (IMIDs) and biologic therapy: a medical revolution. *Postgraduate medical journal*, 83(978), 251-260.
53. Shoelson, S. E., Lee, J., and Goldfine, A. B. (2006) Inflammation and insulin resistance. *The Journal of clinical investigation* 116, 1793-1801.
54. Heppner, F. L., Ransohoff, R. M., and Becher, B. (2015) Immune attack: the role of inflammation in Alzheimer disease. *Nature Reviews Neuroscience* 16, 358-372.
55. Crusz, S. M., and Balkwill, F. R. (2015) Inflammation and cancer: advances and new agents. *Nature Reviews Clinical Oncology* 12, 584-596.

Chapter 2: Nucleosomes are stably evicted from enhancers but not promoters upon induction of certain pro-inflammatory genes in mouse macrophages

This chapter represents a manuscript that was published in *PLoS One* (2014) **9**: e93971. Portions of this manuscript describing results at the IFNB1 locus have been removed.

Authors who contributed to this study were: Alison Gjidoda, Mohita Tagore, Michael McAndrew, Alexander Woods, and Monique Floer.

Abstract

Chromatin is thought to act as a barrier for binding of cis-regulatory transcription factors (TFs) to their sites on DNA and recruitment of the transcriptional machinery. Here we have analyzed changes in nucleosome occupancy at the enhancers as well as at the promoters of three pro-inflammatory genes when they are induced by bacterial lipopolysaccharides (LPS) in primary mouse macrophages. We find that nucleosomes are removed from the distal enhancers of *Il12b* and *Il1a*, as well as from the distal and proximal enhancers of *Ifnb1*, and that clearance of enhancers correlates with binding of various cis-regulatory TFs. We further show that for *Ifnb1* the degree of nucleosome removal correlates well with the level of induction of the gene under different conditions. Surprisingly, we find that nucleosome occupancy at the promoters of *Il12b* and *Il1a* does not change significantly when the genes are induced, and that a considerably fraction of the cells is occupied by nucleosomes at any given time. We hypothesize that competing nucleosomes at the promoters of *Il12b* and *Il1a* may play a role in limiting the size of transcriptional bursts in individual cells, which may be important for controlling cytokine production in a population of immune cells.

Introduction

Genome-wide studies in *S. cerevisiae* have indicated that promoter regions are relatively depleted of nucleosomes compared to the surrounding regions (1,2,3). Where it has been analyzed, for example at the *PHO5* and *GAL1/10* genes of yeast, it was found that removal of promoter nucleosomes is required for gene induction and is mediated by nucleosome remodelers (e.g. the SWI/SNF complex) that are recruited to these regions by specific TFs (4,5). At the *GAL1/10* promoters these nucleosomal sites

are only lowly occupied prior to induction and low promoter nucleosome occupancy is at least partly determined by the underlying DNA-sequence and facilitates rapid nucleosome removal when the inducer galactose is added (6). These studies have suggested that transcriptional regulatory regions have to be nucleosome-free to allow binding of cis-regulatory TFs and the transcriptional machinery. However, at least at one site of binding of a transcriptional activator, the UASg of the *GAL1/10* locus, it was shown that the consensus site-containing piece of DNA is part of an, albeit unusual, nucleosome that apparently accommodates activator binding on its surface (7). Genome-wide studies in mammalian systems have similarly suggested that promoters are relatively depleted of nucleosomes (8,9) and a recent study that analyzed the constitutively expressed *cKIT* gene in mast cells showed that the promoter was nucleosome-free in this cell-type but not in others (10). In addition, studies at many different genes in various cell-types that used changes in sensitivity of chromatin to the enzyme micrococcal nuclease (MNase), to Dnase I or to restriction enzymes, found that chromatin architecture was altered at promoters and enhancers when these genes were expressed indicating that nucleosomes are remodeled at these sites (see for example (11,12)). In one well-studied example of an inducible gene, human interferon β , it was found that the promoter was cleared of nucleosomes upon viral induction, which led to clearing of the TATA-box (13). The interferon β gene contains a promoter proximal enhancer, which forms an enhanceosome (14), and this close proximity of TF-binding sites to the transcriptional start site (TSS) resembles the typical gene architecture in yeast where TF-binding sites are usually within 500 bp of the TSS. However, other mammalian genes are often regulated by distal enhancer elements that can be

thousands of base pairs away (for a recent review see (15)), and are thought to be brought in contact with the promoter by DNA-looping (for an example see (16)). This separation of enhancers and promoters at many mammalian genes prompted us to investigate the changes in nucleosome binding associated with either transcriptional regulatory element upon gene induction. We have used a quantitative assay to analyze changes in nucleosome occupancy at enhancers and promoters of three pro-inflammatory cytokines – *Il1a*, *Il12b* and *Ifnb1* - upon their induction by LPS in primary mouse macrophages. The assay uses a wide range of MNase concentrations and detects the distinct digestion rates of the same segment of DNA, when it is naked or associated with a nucleosome, which allows us to derive the fractional occupancy of a genomic region by a nucleosome (4).

Pro-inflammatory cytokines are expressed by macrophages as part of the innate immune response to various pathogens (for review see (17)) and requires the action of three main TFs, NFκB, AP1 and IRF3/7 (18). Binding sites for these TFs are found in the regulatory elements of many pro-inflammatory genes (19,20). In addition to these signal-induced TFs at least two lineage-specific TFs, PU.1 and C/EBPβ, are required for macrophage differentiation and expression of certain pro-inflammatory genes (21,22,23,24). Both of these TFs have been found to be associated with regulatory elements of many genes even prior to their induction in macrophages (19,20,25). The promoter proximal enhancer of *Ifnb1* is conserved in mice (26), but mouse *Ifnb1* was recently shown to also be regulated by a distal enhancer located 6 kb downstream of its TSS (27). This region was found to also bind the cis-regulatory TF XBP when *Ifnb1* was induced by LPS and thapsigargin (TPG), an inducer of ER-stress that enhances

expression of certain pro-inflammatory cytokines through the action of XBP.

Furthermore, a minimal region of 305 bp that encompasses consensus-sites for XBP and IRF3 was shown to enhance transcription of a reporter gene confirming this region as a bona fide enhancer. Similar studies of the *Il12b* gene performed mostly by Stephen Smale's laboratory identified a distal enhancer located 10 kb upstream of its TSS (28). This distal enhancer was shown to play a role in LPS induction of *Il12b* and was further found to strongly enhance *Il12b* expression in reporter assays that mimic the nucleosome environment found at the endogenous gene (28). The distal enhancers of *Il12b* and *Ifnb1* were also classified as enhancers in two recent genome-wide studies (19,20) that identified thousands of putative enhancers including a region located 10 kb upstream of the *Il1a* gene, which we have included in our studies as a putative enhancer for *Il1a*.

We find that nucleosomes in the distal enhancers of *Il12b*, *Il1a* and *Ifnb1* are rapidly evicted when the genes are induced. Nucleosomes are also removed from the proximal enhancer of *Ifnb1*, which leads to clearance of the adjacent TATA-box and TSS as had been described for the human gene (13). In addition, we show that nucleosome-depletion correlates with binding of cis-regulatory TFs and the co-activator p300 to the distal enhancers of all three genes as well as to the proximal enhancer of *Ifnb1*.

Surprisingly, we find nucleosomes at the *Il12b* and *Il1a* promoters in a large fraction of the population of cells under inducing conditions. Furthermore, we find that promoter nucleosomes around the TSSs of these genes become associated with histone modifications found at active promoters (H3K4me3 and H3K27ac). Our results indicate that promoter nucleosomes are not stably evicted but instead are bound to a fraction of

promoters in the population of cells at any given time. Furthermore, we find that PolII and TBP are only associated with nucleosome-free promoters and we discuss the potential role of competing nucleosomes at the promoters of these cytokine genes in limiting their expression in a population of immune cells.

Experimental Procedures

Cell isolation and culture

Primary cells were isolated from 8–12 week old C57BL/6 mice (NCI). Bone marrow derived macrophages (BMDMs) were generated as described [29] and grown in BMDM medium (60% IMDM medium (Gibco), 30% conditioned medium from L-929 fibroblasts, 10% FBS, 0.1 mM non-essential amino acids, 1 mM sodium pyruvate and 1X penicillin-streptomycin. LPS induction was performed by adding 1 µg/ml LPS from E. coli strain EH100 (Ra mutant)(Sigma) to serum-starved BMDMs for the indicated times. Serum starvation was done by growth of cells in incomplete IMDM medium for 1 h. Other inducers were ISD (interferon stimulatory DNA) derived from *Listeria monocytogenes*; poly(I:C), synthetic dsRNA that acts as a TLR3 agonist; and poly(dA:dT), a synthetic analog of B-DNA (all obtained from Invivogen). 1 µg/ml of either of these inducers was given to BMDMs by transfection with Lipofectamine 2000 (Invitrogen) in an equal volume mixture [30]. Where indicated thapsigargin (Sigma) was added at 1 µM for 1 h to serum-starved cells prior to LPS addition [27]. Splenic B-cells were isolated by negative selection with CD43 antibody-coupled Dynabeads according to the instructions of the manufacturer (Life Technologies), with an additional red blood lysis step using lysis buffer (Sigma). For LPS induction B-cells were grown in B-IMDM medium (IMDM medium (Gibco), containing 55 µM 2-Mercaptoethanol and 2 mM L-glutamine) for 1.5 h

prior to LPS addition for the indicated times. RAW264.7 cells were grown in DMEM medium (Gibco) containing 10% FBS and 1X penicillin-streptomycin.

mRNA determination

Total RNA was isolated from BMDMs or B-cells using Trizol (Invitrogen/Lifetech). In brief, Trizol was added to cells growing in culture, and Trizol lysates were collected. 400 μ l of chloroform was added per 1 ml Trizol lysate, the aqueous phase was extracted, 170 μ l isopropanol was added and the mixture was further purified on ReliaPrep RNA Cell Miniprep System columns according to the manufacturer's protocol (Promega). RNA was converted into cDNA according to the protocol described [31] except that High Capacity Reverse Transcriptase was used (Invitrogen/Lifetech) and analyzed by qRT-PCR with specific primer pairs. Primers used can be given upon request.

Chromatin immunoprecipitation

Chromatin from 5×10^6 cells per antibody that had been cross-linked with 0.5% formaldehyde for 10 min was isolated by sonication with a Branson sonifier (10 pulses of 10" at setting 4) in Lysis buffer (50 mM Hepes-KOH, pH 7.5, 1% TritonX-100, 0.1% SDS) and centrifugation for 10' at 21,000 \times g. To increase the resolution of ChIP experiments when detecting histones or histone modifications, and to differentiate nucleosome binding from PolII and TBP binding, the isolated chromatin was digested with 0.5 or 1 U MNase (NEB) for 1 h 30' in the presence of 0.15 mM CaCl₂, and the digestion reaction was stopped by addition of 20 mM EDTA. Digested chromatin was diluted 3-fold with High Salt ChIP buffer (10 mM Tris-HCl, pH 8, 400 mM NaCl, 1% TritonX-100, 2 mM EDTA, Complete protease inhibitors w/o EDTA (Roche)) to yield 600 μ l total volume and incubated overnight at 4°C with either 5 μ l of anti-H3 (39163, Active

Motif, concentration is not known), 4 µg of anti-H2A.Z (ab4174; Abcam), 1 µg of anti-H3K4me1 (ab8895; Abcam), 1 µg of anti-H3K4me3 (ab8580; Abcam) or 1 µg of H3K27ac (ab4729; Abcam). For all other ChIP experiments isolated chromatin was directly diluted with High Salt ChIP buffer and incubated with either 1 µg of anti-Poll antibody (sc-56767), 6 µg anti-TBP (sc-204), 4 µg anti-PU.1 (sc-352), 4 µg anti-C/EBPβ (sc-150), 6 µg anti-NFκB (sc-372), 5 µg anti-c-Jun (sc-45), 6 µg anti-p300 (sc-585) or 10 µg anti-IRF3 (sc-9082) all from Santa Cruz Biotechnologies. 20 µl of Protein A/G magnetic beads (Pierce) were added to the reaction and incubated at 4°C for 2 h. Beads were washed with 280 µl each of TSE buffer (20 mM Tris pH 8.0, 0.1% SDS, 1% TritonX-100, 2 mM EDTA), TSE250 (TSE buffer, 250 mM NaCl) and TSE500 (TSE buffer, 500 mM NaCl), Wash buffer III (10 mM Tris pH 8.5, 0.25 M LiCl, 1% NP-40/Igepal, 1% deoxycholate, 1 mM EDTA) and TE (10 mM Tris-HCl pH 8.0, 1 mM EDTA) all containing Complete protease inhibitors. Antibody complexes were eluted from the beads with 2×100 µl Elution buffer (0.1 M NaHCO₃, 1% SDS) by incubation for 30' (and 10') at 55°C. Eluates were combined and the cross-link was reversed by incubation at 65°C for 4 h. DNA was purified using a Qiagen PCR purification kit, and analyzed on a Lightcycler 480 (Roche) using primer pairs in the regions indicated. Sequences of the primers used can be given upon request.

Quantitative nucleosome occupancy assay

The assay was performed essentially as described in [4] with certain modifications. Cross-linked chromatin from 1 to 3×10⁷ cells isolated as described for ChIP experiments was incubated in Lysis buffer containing 140 mM sodium chloride with 22 increasing concentrations of MNase (0.001179 U to 20 U, NEB) in the presence of 0.15

mM CaCl₂ for 1 h 30'. DNA was purified as described and quantified using a Roche Lightcycler 480. Digestion data was analyzed using two-state exponential curve-fitting as described [4]. Data was normalized to several genomic locations, including a region in the promoter of *cKIT* [10] that was highly protected and a region in the ORF of *Rpl4*. The data was displayed in the IGV genome browser v2.3 [32] and overlays of nucleosome occupancy during a timecourse of LPS induction were created from IGV tracks using Adobe Photoshop.

Genomic DNA isolation

Genomic DNA was isolated from RAW264.7 macrophages as described [33] and DNA standard curves were created using a 1/3 fold dilution series with the highest concentration yielding qRT-PCR amplification at around cycle 20 for the majority of primer pairs.

qRT-PCR

DNA and cDNA was quantified on a Lightcycler 480 (Roche) as described [4] with the following modifications. Primers were designed using the program PCRTiler [34]. To verify that only a single amplicon was produced by each primer pair and no primer dimers were formed a T_m-curve was performed as a quality control for each primer pair at the end of each qRT-PCR run. We also found that addition of 1.5% PEG400 (Fluka) to the qRT-PCR reaction greatly enhanced performance for many primer pairs and led to a greater linear range of the qRT-PCR measurements.

Results

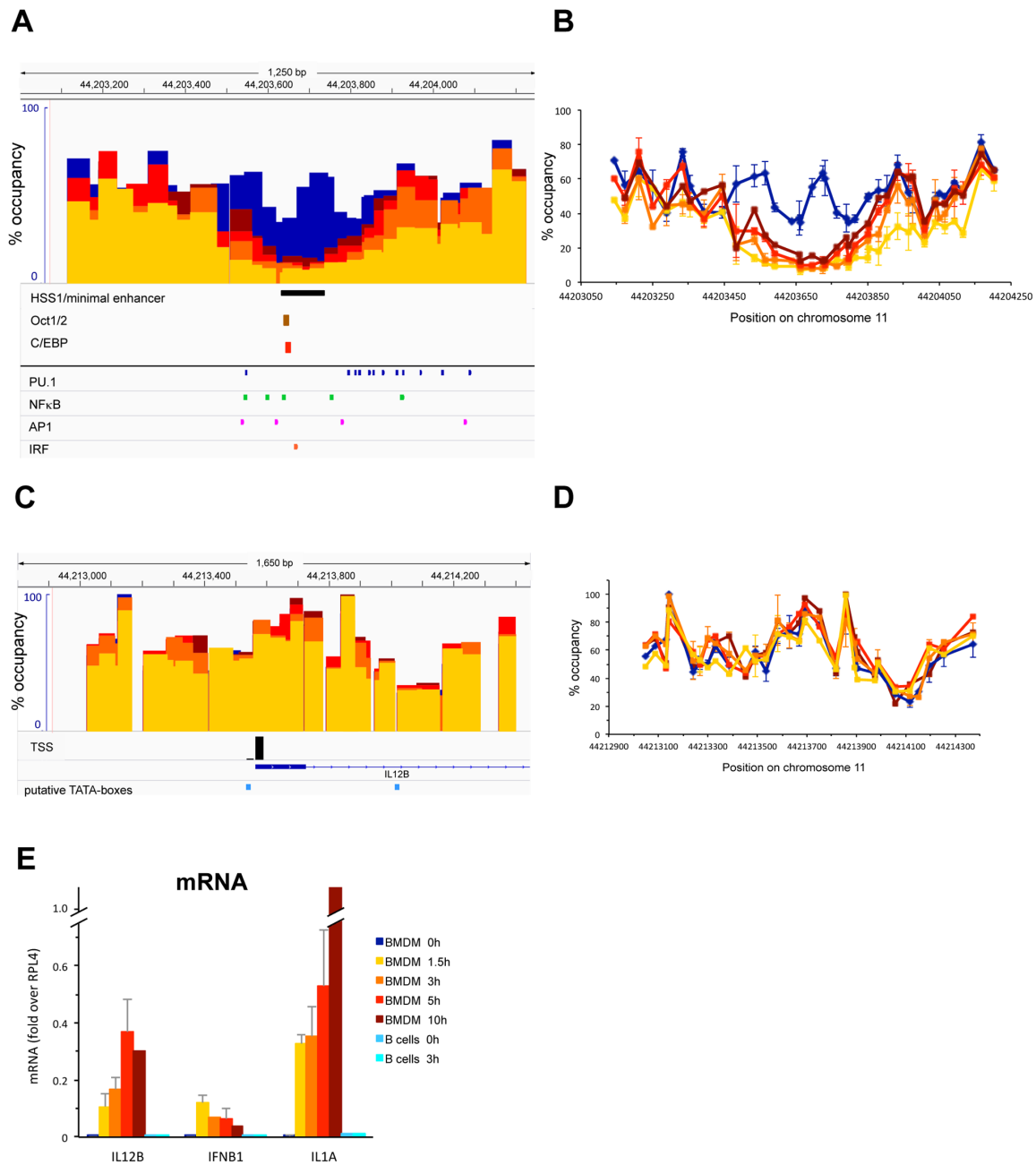
Nucleosome occupancy at the *I12b* enhancer and promoter upon LPS induction

Figure 2.1A and B shows an analysis of nucleosome occupancy in a 1.2 kb region

encompassing the 10 kb upstream enhancer of *Il12b* (28) at different timepoints during LPS induction of primary bone-marrow derived macrophages (BMDMs) using the assay described (4). Prior to induction (blue bars and lines) nucleosomes in the *Il12b* enhancer were relatively well positioned and occupied their sites in around 60% of the population of cells. 1.5 h after LPS addition (yellow) two nucleosomes in the center of the enhancer had been removed. The 5–10% occupancy we detected upon clearance of these nucleosomes is within the accuracy of our assay and we conclude that this region was largely nucleosome-free after 1.5 h. The central nucleosomal position, which remained cleared upon prolonged incubation with LPS up to 10 h (dark red), coincides with a region that was shown by Zhou et al. to become hypersensitive to Dnase I upon LPS induction (see the black bar underneath panel A (28)). We found that the flanking nucleosomes were partially re-formed as induction progressed and after 5 h of induction the nucleosome to the left was again occupied in 30% of the population (light red). The nucleosome to the right was partially removed after 1.5 h (30–40%) and regained 60% occupancy after 5 h (light red). We monitored expression of the associated *Il12b* gene by measuring mRNA levels during the 10 h timecourse (Figure 2.1E). *Il12b* mRNA was detected as early as 1.5 h after LPS addition, and levels increased for up to 5 h, after which *Il12b* mRNA production reached steady-state levels. Figure 2.1E also shows mRNA levels upon LPS induction of *Ifnb1* and *Il1a*. Figure 2.1C and D shows nucleosome occupancy at the *Il12b* promoter including a region 600 bp upstream and 800 bp downstream of the TSS. Surprisingly, we did not find any changes in nucleosome occupancy upon LPS induction over the 10 h timecourse of LPS induction (compare blue bars and lines to increasing shades of red). The region surrounding the

TSS was more highly occupied by nucleosomes than the enhancer prior to induction and nucleosomes were less well positioned than in the *I12b* enhancer. We found that the region directly upstream of the TSS was occupied in about 60% of the population and this region was flanked by more highly occupied nucleosomes (around 90%). A TATAA-sequence that we identified 28 bp upstream of the TSS (light blue box in C) as well as the TSS itself was found at the edge of the highly occupied nucleosome. We found that a region 400 bp downstream of the TSS that contains a TATAT-sequence was relatively lowly occupied by nucleosomes prior to induction (20–30%), which had initially suggested to us that this downstream region might function to assemble a pre-initiation complex. However, a previous search for TSSs that used CAGE-analysis to detect capped mRNAs had not found any transcription starting from this downstream region, but had instead confirmed the annotated TSS for *I12b* (35). We therefore conclude that the upstream TATAA-sequence is used to assemble a PIC. This conclusion was confirmed by our subsequent ChIP analysis, which detected PolII and TBP binding at this site (see Figure 2.3).

Figure 2.1. Changes in nucleosome occupancy upon LPS induction at a distal enhancer and the promoter of *Il12b*.



(A) and **(B)** Nucleosome occupancy at an enhancer 10 kb upstream of the TSS of *Il12b* in BMDMs was analyzed before induction (blue bars and lines), and after 1.5 h (yellow), 3 h (orange), 5 h (light red) and 10 h (dark red) of growth of cells in the presence of 1

Figure 2.1. (cont'd)

$\mu\text{g/ml}$ LPS, using the assay described in (4) with modifications detailed in the Experimental Procedures. In brief, occupancy was measured by determining the sensitivity of cross-linked chromatin to a wide range of MNase. Digestion data for each genomic location analyzed by qRT-PCR with specific primer pairs was fitted to two-state exponential decay functions and the percentage of DNA in the population of cells found to be protected against MNase by binding of a nucleosome is indicated on the y-axis. In panel (A) each overlapping colored bar represents the length of the amplicon measured. The minimal enhancer that was shown by Zhou et al. to contain the LPS-inducible DNaseI hypersensitive site HSS1 as well as consensus-sites for Oct1/2 and C/EBP β is indicated by the black bar (28). Consensus-sites for PU.1, NF κ B, AP1 and IRF identified using ConSite are indicated. In panel (B) nucleosome occupancy at the midpoint of each amplicon measured by the experiment performed in panel (A) is indicated by a dot, with error bars showing the SEM of at least two independent measurements (10 h was measured only once).

(C) and **(D)** BMDMs were induced as described in (A) and nucleosome occupancy in a region surrounding the TSS of *Il12b* was determined. The data is displayed as in panels (A) and (B) respectively. The black bar below the data in (C) indicates the TSS [35] and the light blue bars indicate putative TATA-boxes predicted by ConSite.

(E) Expression of *Il12b*, *Ifnb1* and *Il1a* in response to LPS. mRNA from BMDMs induced with LPS as in panel A as well as from splenic B-cells was isolated as described in the Experimental Procedures, reverse transcribed and cDNA quantified by qRT-PCR. Data was normalized to a location in the ORF of the constitutively expressed *Rpl4* gene. The

Figure 2.1. (cont'd)

SEM of at least two independent measurements is indicated (10 h timepoint was measured only once).

Changes in nucleosome occupancy at the transcriptional regulatory regions of *I11a*

Figure 2.2 shows an analysis of nucleosome occupancy at a putative enhancer 10 kb upstream (panel A and B) and around the TSS (panel C and D) of the *I11a* gene before (blue bars and lines) and upon induction of macrophages with LPS for 1.5 h (yellow) and 3 h (red). Similar to our findings at the *I112b* enhancer we found that the putative *I11a* enhancer was depleted of nucleosomes 1.5 h after LPS addition. This region encompasses 3–4 nucleosomes, which were occupied in 40–60% of the population prior to induction. The center of this region became essentially nucleosome free (5–10%) and remained so even after prolonged LPS induction (3 h, red bars and lines in panels A and B). The three nucleosomes flanking this region became partially depleted upon LPS induction (20–30% occupancy after 1.5h) and occupancy of these flanking nucleosomes increased slightly upon prolonged LPS induction similar to what we had found at the *I112b* enhancer (compare yellow and red bars and lines in Figure 2.2A–D). Panels C and D of Figure 2.2 show that the promoter of *I11a* was not cleared of nucleosomes upon induction. We found that prior to LPS induction the *I11a* promoter was less occupied by nucleosomes than the *I112b* promoter. Thus, a nucleosome that incorporates the TSS and TATAA-sequence of *I11a* was occupied in about 55% of the population of cells before induction. Upon LPS induction nucleosome occupancy at the TSS decreased somewhat (35% after 1.5 h, yellow bars and lines) and then increased

again as LPS induction progressed (45% at 3 h, red). As for *//12b*, the annotated TSS was confirmed as the major TSS for *//1a* by Carninci and colleagues (35) and is indicated by the black bar underneath panel C. As shown in Figure 2.1E we found that *//1a* mRNA levels increased during a 10 h course of LPS induction, suggesting that *//1a* transcription is sustained over this time period. We were not able to determine nucleosome occupancy in a region 100–400 bp downstream of the TSS of *//1a*, since this region consists almost entirely of CTT or CCT repeats and is resistant to qPCR.

Timing of enhancer nucleosome removal

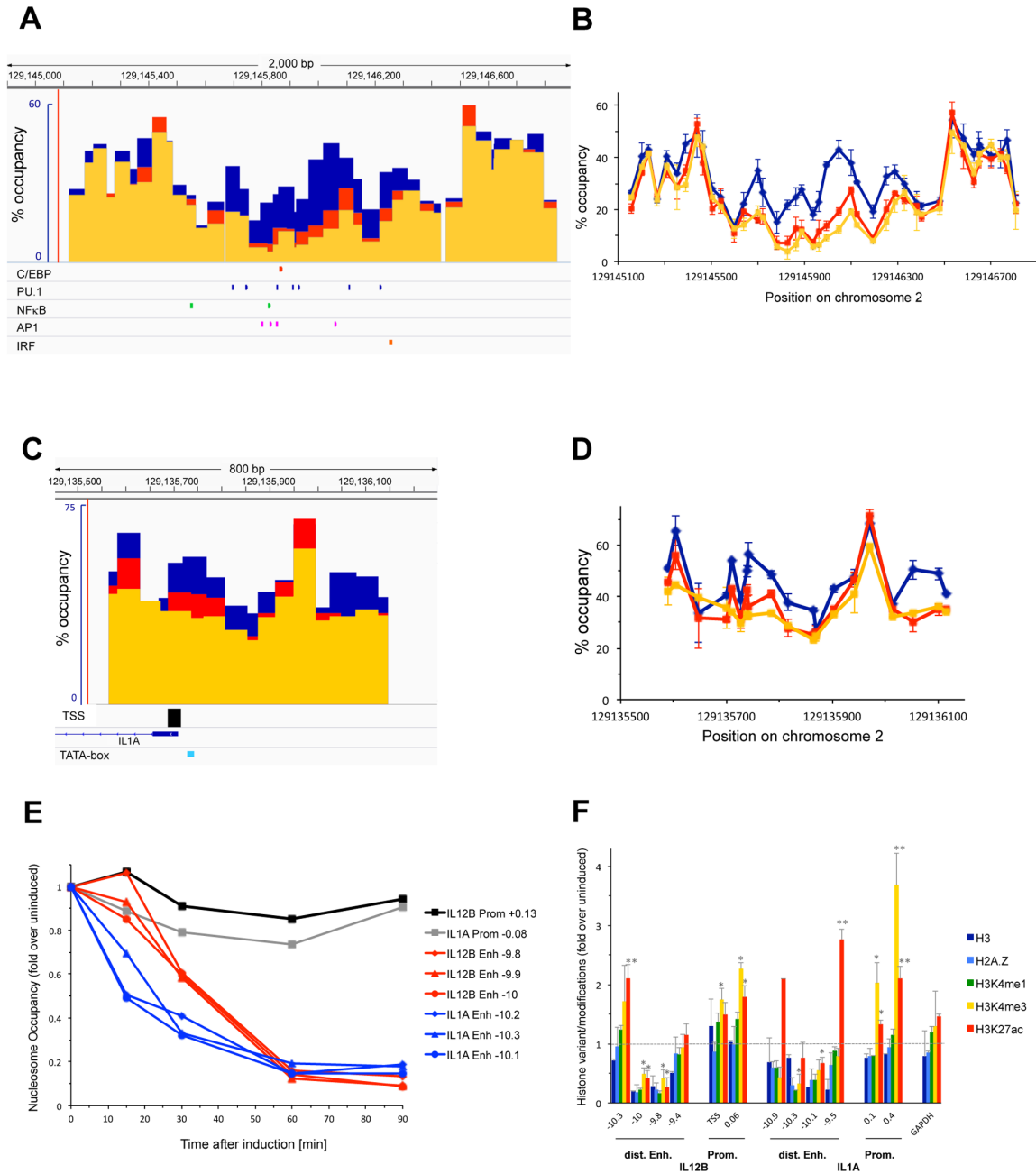
To determine the earliest timepoint of nucleosome removal at the distal enhancers of *//12b* and *//1a* we analyzed nucleosome occupancy in the centers of the two enhancers 15', 30', 60' and 90' after LPS induction. Figure 2.2E shows that the *//1a* enhancer was significantly depleted 15' after LPS induction (blue lines), whereas no nucleosomes had been removed at the *//12b* enhancer at this early timepoint (red lines). Figure 2.2E indicates the fold change of nucleosome removal over the levels found before induction and nucleosome occupancy before induction was similar at the three representative locations in each enhancer. Nucleosome depletion at the *//1a* enhancer was close to completion after 30', while depletion at the *//12b* enhancer had only reached 50%. After 1 h both enhancers had reached their maximal levels of nucleosome depletion. Our results show that nucleosome removal at the *//1a* enhancer occurs with faster kinetics than at the *//12b* enhancer.

Histone modifications at the promoters and enhancers of *//12b* and *//1a*

Figure 2.2F shows the results of ChIP experiments performed with various antibodies that detect histone H3, the histone variant H2A.Z as well as different modifications of

residues in H3 upon induction of BMDMs with LPS. We first confirmed that nucleosomes are evicted from the enhancers of *I12b* and *I1a* but not the promoters using an antibody against H3. Figure 2.2F shows that the H3 signal decreased upon LPS induction only in the regions in the enhancers where nucleosomes were evicted (compare to Figure 2.1A and 2.2A). We found similar results using an antibody against H2A.Z at the enhancers and promoters of both genes, or with an antibody detecting H3K4me1, which was previously shown to be present at the enhancers prior to and upon LPS induction (19,20). Most importantly, we detected an increase in H3K4me3 and H3K27ac at the promoters of *I12b* and *I1a* upon induction. Both modifications have previously been shown to be associated with actively transcribed genes (36,37) and to increase at the two genes we have investigated upon their induction (38).

Figure 2.2. Changes in nucleosome occupancy upon LPS induction at a putative distal enhancer and promoter of *Il1a*, kinetics of nucleosome removal, and changes in histone modifications.



(A) and **(B)** Nucleosome occupancy at a putative enhancer 10 kb upstream of the TSS of *Il1a* was determined in BMDMs prior to (blue bars and lines) and upon 1.5 h (yellow)

Figure 2.2. (cont'd)

or 3 h (red) induction with 1 $\mu\text{g/ml}$ LPS as described in the legend of Figure 2.1. ConSite predicted consensus sites for PU.1, C/EBP, IRF, AP1 and NF κ B are indicated.

(C) and **(D)** Nucleosome occupancy at the promoter of *I11a* was determined as described in panel (A) in a region surrounding the TSS of *I11a*. The TSS (black bar) (35) and a putative TATA-box (blue bar) is indicated in panel (C).

(E) Expression of *I112b*, *I11nb1* and *I11a* in response to LPS. mRNA from BMDMs induced with LPS as in panel A as well as from splenic B-cells was isolated as described in the Experimental Procedures, reverse transcribed and cDNA quantified by qRT-PCR. Data was normalized to a location in the ORF of the constitutively expressed *Rpl4* gene. The SEM of at least two independent measurements is indicated (10 h timepoint was measured only once).

(F) ChIP experiments with antibodies against H3 (dark blue bars), H2A.Z (light blue), H3K4me1 (green), H3K4me3 (yellow) and H3K27ac (red) were performed as described in the Experimental Procedures. For these experiments cross-linked chromatin was lightly digested with MNase before incubation with the respective antibodies to increase resolution of the ChIP signal and the data was normalized to a region in the ORF of *Rpl4*. Changes upon LPS induction in histone binding and histone modifications at the enhancers and promoters of *I112b* and *I11a* as well as at a control region in the *GAPDH* pseudo gene are shown as fold over levels found before induction. For H3K27ac the changes 1.5 h after LPS induction, and for all other histone variants and modifications the changes after 3 h of induction are shown. The error bars show the SEM of at least 3 independent experiments. Statistical significance of the changes in H3K4me3 and

Figure 2.2. (cont'd)

H3K27ac upon LPS induction compared to levels found prior to induction determined by Student's T-tests is indicated (* $P < 0.05$; ** $P < 0.01$).

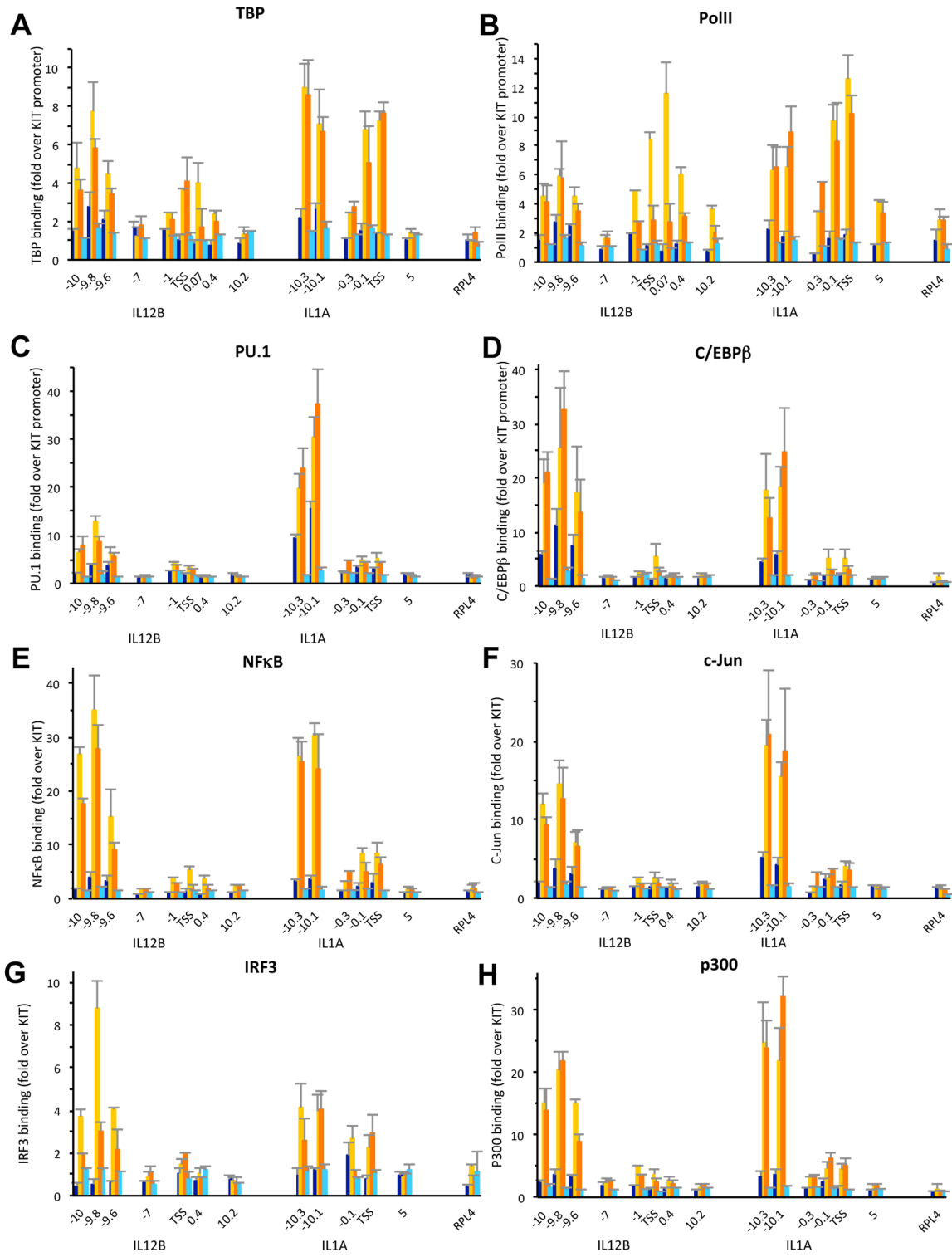
Binding of cis-regulatory TFs to the distal enhancers of *I12b* and *I1a*

The minimal enhancer of *I12b* was previously shown to bind C/EBP β and Oct1/2 upon induction and consensus-sites for these TFs were identified in this region (28). We used the prediction program ConSite (39) to identify consensus-sites for other TFs involved in induction of pro-inflammatory genes in macrophages and found consensus-sites for PU.1, NF κ B, AP1 and IRF3 in the region that becomes depleted upon induction (see Figure 2.1A). A similar survey of the putative enhancer of *I1a* also detected consensus sites for PU.1, C/EBP, IRF3, AP1 and NF κ B in the region that is depleted of nucleosomes upon LPS induction (see Figure 2.2A).

To analyze binding of these TFs to the distal enhancers of *I12b* and *I1a* as well as recruitment of the transcriptional machinery to the enhancers and promoters we performed ChIP experiments in uninduced macrophages and cells induced for 1.5 and 3 h with LPS (Figure 2.3). We found that PolII and TBP were recruited to the TSS of both *I12b* and *I1a* upon induction (Figure 2.3A and B). We also found that similar amounts of PolII and TBP were recruited to the distal enhancers of both genes but not to a control region between the *I12b* TSS and the distal enhancer (-7 kb). For these and all other ChIP experiments we used splenic B-cells as a control (light blue bars). The three genes we have investigated were not induced by LPS in B-cells (see Figure 2.1E, cyan bars) and no factor binding was detected (see Figure 2.3). We also determined binding of the macrophage-specific TFs PU.1 and C/EBP β and confirmed their presence at the

two distal enhancers before LPS induction (Figure 2.3C and D, dark blue bars) (19, 20). Upon induction binding of both factors to the two distal enhancers increased significantly (compare yellow and orange to dark blue bars). We found similar results when we performed a ChIP experiment with an antibody for C/EBP α , indicating that both C/EBP isoforms are present (A.G. and M.F., data not shown). Furthermore, we detected binding of NF κ B, c-Jun (a component of AP1) and IRF3 at the enhancers upon LPS induction (Figure 2.3E-G). The coactivator p300 was previously shown to be recruited upon LPS induction to the regions encompassing the *I12b* as well as the putative *I1a* enhancer (19), a finding we confirmed (Figure 2.3H). Each ChIP experiment was performed at least three times and error bars (SEM) are included. We determined the significance of the detected ChIP signals by performing Student's T-tests (Table 2.1). To obtain robust statistics we pooled all the measurements at the different loci in the enhancer or promoter regions of either gene from 3–4 independent experiments. Overall we find that binding of the cis-regulatory TFs and the co-activator p300 is significant in the enhancers, while binding of PolII and TBP is significant at both enhancers and promoters.

Figure 2.3. Binding of cis-regulatory TFs and recruitment of the transcriptional machinery to the regulatory regions of *Il12b* and *Il1a* upon LPS induction.



(A–H) ChIP experiments in BMDMs before (dark blue bars), and upon 1.5 h (yellow)

Figure 2.3. (cont'd)

and 3 h (orange) of LPS induction as well as in splenic B-cells (light blue) were performed as described in Experimental Procedures using antibodies that recognize (A) TBP, (B) PolIII, (C) PU.1, (D) C/EBP β , (E) NF κ B, (F) c-Jun, (G) IRF3 and (H) p300. Binding data was normalized to a location in the promoter of the KIT gene, and genomic locations in relation to the TSS of *I12b* or *I1a* are indicated on the x-axis in each panel. Binding to a control region in the *Rpl4* ORF is shown for comparison. Error bars indicate the SEM of at least three independent experiments. Statistical significance for binding in each region was determined by Student's T-tests performed for each regulatory region (see Table 2.1 for P-values).

Table 2.1. Statistical significance of factor binding, ChIP of Fig. 2.3.

P-values (Student's T -test)		IL12B							
		IL12B distal Enh.	IL12B intervening reg.	IL12B Prom.	IL12B orf	IL1A distal Enh.	IL1A Prom.	IL1A orf	RPL4
TBP	BMDM 0h vs B-cells	4.754E-02	4.948E-01	1.714E-04	5.617E-01	1.086E-02	1.687E-03	6.564E-01	6.564E-01
	BMDM plus LPS 1.5h vs. 0h	9.755E-04	4.693E-01	5.715E-05	6.567E-01	1.392E-02	6.051E-04	6.465E-01	6.465E-01
	BMDM plus LPS 3h vs. 0h	2.472E-03	8.389E-01	8.553E-04	2.101E-01	3.752E-05	5.136E-03	7.262E-01	7.262E-01
PoII	BMDM 0h vs B-cells	1.341E-02	7.065E-01	9.620E-01	1.642E-01	1.022E-01	4.592E-01	8.007E-01	5.466E-01
	BMDM plus LPS 1.5h vs. 0h	7.188E-05	2.170E-02	3.179E-08	7.706E-04	1.038E-03	3.659E-05	1.134E-05	3.216E-01
	BMDM plus LPS 3h vs. 0h	7.829E-03	3.055E-01	2.434E-06	5.105E-02	2.773E-04	1.581E-04	1.123E-02	2.312E-01
PU.1	BMDM 0h vs B-cells	2.279E-04	7.646E-01	9.697E-01	3.561E-01	1.815E-05	1.127E-03	1.885E-01	3.337E-01
	BMDM plus LPS 1.5h vs. 0h	7.141E-07	8.381E-01	4.888E-02	9.313E-01	2.364E-03	1.528E-03	8.295E-01	3.522E-01
	BMDM plus LPS 3h vs. 0h	3.201E-06	2.645E-01	1.009E-01	4.425E-01	9.322E-04	7.070E-03	8.981E-01	8.561E-01
C/EBPβ	BMDM 0h vs B-cells	3.36E-04	2.15E-01	3.86E-01	8.02E-01	6.86E-05	4.73E-01	2.23E-01	7.40E-01
	BMDM plus LPS 1.5h vs. 0h	8.76E-03	4.10E-01	4.52E-02	2.35E-01	2.10E-03	1.23E-02	2.86E-01	3.81E-01
	BMDM plus LPS 3h vs. 0h	1.41E-03	9.52E-01	2.41E-02	6.77E-01	9.42E-03	4.18E-03	6.71E-01	6.67E-01
NFKB	BMDM 0h vs B-cells	1.615E-02	2.231E-01	2.333E-01	3.615E-01	7.989E-03	2.497E-01	3.745E-01	3.043E-01
	BMDM plus LPS 1.5h vs. 0h	2.493E-07	8.283E-03	2.662E-05	5.394E-02	2.946E-09	1.828E-03	3.341E-02	4.699E-01
	BMDM plus LPS 3h vs. 0h	1.418E-05	1.809E-02	2.570E-02	2.953E-02	3.428E-07	7.844E-03	1.086E-01	3.691E-01
c-Jun	BMDM 0h vs B-cells	1.80E-02	5.57E-01	2.09E-01	3.79E-01	3.92E-04	1.97E-01	3.22E-01	6.44E-02
	BMDM plus LPS 1.5h vs. 0h	1.36E-05	5.21E-01	6.54E-02	5.84E-01	2.05E-05	1.41E-01	9.71E-01	8.14E-01
	BMDM plus LPS 3h vs. 0h	3.00E-04	3.43E-01	3.27E-01	8.45E-01	2.11E-03	1.97E-02	4.58E-01	7.55E-01
IRF3	BMDM 0h vs B-cells	8.92E-05	6.42E-01	6.85E-01	4.51E-01	7.42E-01	2.72E-01	3.51E-01	7.56E-01
	BMDM plus LPS 1.5h vs. 0h	3.49E-04	3.04E-01	2.92E-01	7.60E-01	2.43E-03	9.66E-02	8.28E-01	3.88E-01
	BMDM plus LPS 3h vs. 0h	8.45E-05	8.33E-02	2.50E-01	6.02E-01	3.65E-03	1.84E-01	9.07E-01	7.05E-01
p300	BMDM 0h vs B-cells	3.792E-03	2.324E-01	9.401E-01	8.714E-01	1.489E-03	2.329E-02	6.753E-02	6.955E-01
	BMDM plus LPS 1.5h vs. 0h	4.891E-08	4.972E-01	6.666E-04	3.265E-01	2.367E-04	3.268E-03	1.598E-01	8.703E-01
	BMDM plus LPS 3h vs. 0h	3.613E-05	4.994E-01	2.095E-03	1.025E-01	3.056E-06	4.614E-04	2.346E-02	3.765E-01

Student's tests were performed using normalized data from at least 3 (to 6) independent experiments performed with various antibodies as described in the legend of Figure 2.3.

All the measurements at the 2–4 locations in each enhancer or promoter, as well as the

Table 2.1. (cont'd)

measurements at a single location in each ORF or in the *II12b* intervening region were pooled from each experiment and Student's Tests (two-tailed, equal variance) were performed on each dataset. Table 2.1 shows the P-values obtained. We compared the significance of factor binding in resting BMDMs (0 h) versus B-cells, and in BMDMs after 1.5 h or 3 h LPS induction versus binding in resting BMDMs.

Binding of the transcriptional machinery to nucleosome-free *II12b* and *II1a* promoters

To determine whether PolII and TBP might bind to the promoters of *II12b* and *II1a* in the presence of nucleosomes or whether the transcriptional machinery is only associated with the fraction of promoters that is nucleosome-free we performed the experiment shown in Figure 2.4. For this experiment we treated cross-linked chromatin with MNase prior to performing a ChIP experiment with antibodies detecting PolII or TBP. As seen in Figure 2.4 the PolII or TBP ChIP-signal was lost when chromatin was treated with MNase (compare solid to hatched bars). In contrast, H3, modified H3K4me3 or H3K27ac was resistant to pretreatment with MNase (see Figure 2.2F). This result indicates that only the fraction of the promoters that is nucleosome-free at any given time is associated with the transcriptional machinery.

Figure 2.4. (cont'd)

upon 1.5 h (yellow) or 3 h (red) LPS induction. Cross-linked chromatin was either untreated (solid bars), or lightly digested with MNase (hatched bars) as described in Experimental Procedures. The data was normalized to a region in the *cKIT* promoter and genomic locations are indicated. The experiment was performed twice and error bars indicating the SEM are shown.

Discussion

Our analysis of nucleosome occupancy at the regulatory regions of three pro-inflammatory genes revealed that the distal enhancers of *Il12b* and *Ifnb1* were rapidly cleared of nucleosomes when the genes were induced. The regions that became nucleosome-free include the respective minimal regions that had been shown to have bona fide enhancer activity by previous studies (see Figure 2.1A) (27,28). We found similar removal of nucleosomes in a region 10 kb upstream of *Il1a*, which has been suggested to be a functional enhancer of *Il1a* (Figure 2.2A)(19). In all three distal enhancers the nucleosome-free regions became associated with the TFs NF κ B, AP1 (c-Jun) and IRF3 upon LPS induction, while binding of the macrophage-specific TFs PU.1 and C/EBP β increased (see Figure 2.3). The presence of consensus-sites for these TFs was confirmed with the prediction program ConSite (39)(Figure 2.1A, 2.2A). Together our data suggest that the enhancers of these pro-inflammatory genes have to be cleared of nucleosomes to allow binding of cis-regulatory TFs, although it remains to be determined whether binding occurs only to sites that become nucleosome-free or also to putative consensus-sites found in the surrounding regions (M.F., data not shown) that remain bound by nucleosomes. Future studies will show whether removal of

nucleosomes from consensus-sites can be used as a criterion to distinguish functional binding-sites for specific cis-regulatory TFs in the genome from sites that remain associated with nucleosomes and may therefore not be accessible.

The most surprising result of our study was the finding that the promoters of *//12b* and *//1a* were not cleared of nucleosomes when the genes were expressed, while nucleosomes were rapidly removed from the associated distal enhancers. Thus, we found that the TSS of *//12b* was occupied in about 70% of the population prior to induction and remained essentially unchanged, while the distal enhancer became nucleosome-free in about 90% of the population (see Figure 2.1). We found similar results at the distal enhancer and promoter of *//1a* (Figure 2.2). The presence of nucleosomes at the promoters before and after LPS induction was further confirmed by our histone ChIP experiments (Figure 2.2F). In these experiments, we also detected an increase in H3K4 tri-methylation and H3K27 acetylation of the highly occupied promoter nucleosomes of *//12b* and *//1a* in agreement with previous lower resolution studies (Figure 2.2F, yellow and red bars)(19,38). Our finding that MNase treatment abolished the PolIII and TBP ChIP-signal at the *//12b* and *//1a* promoters (Figure 2.4) strongly suggests that the transcriptional machinery is only associated with the fraction of promoters that is nucleosome-free at any given time. We speculate that in contrast to the stable eviction of nucleosomes at enhancers, which persisted over the timecourse of our induction experiment, nucleosomes may continuously re-associate with the promoters of *//12b* and *//1a*. This would allow only a fraction of the cells to form a PIC at any given time. This idea is in agreement with previous findings that expression of many inducible genes, including the genes we have analyzed, is highly stochastic

(41,42,43,44). Another finding that supports the idea that a changing fraction of the population of cells expresses these genes at any given time, was the observation made by Smale and co-workers that expression of *Il12b* is not restricted to a clonal fraction of a population in a macrophage cell-line under inducing conditions (41). We hypothesize that the presence of competing nucleosomes at the promoters of these cytokines may play a role in limiting the burst size of transcription from individual cells and thus the production of cytokines in the population. We further speculate that certain histone modifications might play a role in increasing nucleosome turnover at these promoters, a hypothesis that awaits experimental confirmation.

Our findings are in contrast to previous findings by Weinmann et al., which had suggested that a region about 200 to 330 bp upstream of the TSS of *Il12b* is nucleosome-free even prior to activation in macrophages (both in cell-lines and thioglycollate-elicited peritoneal macrophages) using sensitivity of chromatin to MNase followed by indirect end-labeling or ligation-mediated PCR to determine nucleosome binding (41). These authors had also suggested that a region downstream of the putative nucleosome-free region contained a positioned nucleosome, which they proposed to harbor putative binding sites for NF κ B (Rel) and C/EBP. Upon activation they found that this region became more sensitive to various restriction enzymes as well as to Dnase I (41), and they suggested that remodeling of the positioned nucleosome might facilitate binding of cis-regulatory TFs. We did not find significant binding of NF κ B or C/EBP β to this region upon LPS induction compared to the strong binding we found at the 10 kb upstream enhancer (see Figure 2.3). Nor did we find a nucleosome-free region in the *Il12b* promoter prior to induction even when we extended our analysis to

include up to 1.5 kb upstream of the TSS of *I12b* (Figure 2.1 and A.G. and M.F., unpublished data). Our quantitative MNase sensitivity assay showed that upon induction there was no significant change in the level of nucleosome occupancy at the *I12b* promoter in the population of cells (Figure 2.1), which was confirmed by histone ChIP experiments (Figure 2.2F). It is possible that our assay does not detect more subtle changes in nucleosome binding that might be induced by nucleosome remodeling and which may be detected by increased sensitivity of chromatin to certain restriction enzymes or Dnase I (41). Furthermore, it is formally possible that macrophages derived from bone marrow may be different from those derived from the peritoneum or from macrophage cell-lines.

I1a contains additional regions between the 10 kb distal enhancer we have investigated and the TSS that become associated with TFs upon induction in dendritic cells (38). This might suggest that additional enhancers may also control expression of *I1a* in primary macrophages, and it remains to be seen whether nucleosomes are similarly evicted from such sites. The nucleosomes that are evicted from the distal enhancers of all the genes we have analyzed are only occupied in 40–60% of a population of resting macrophages, which is lower than the occupancies we found at, for example, the TSS of *I12b* and *Ifnb1* (see Figure 2.1D). Our findings of moderate nucleosome occupancy at enhancers are in agreement with a previous study of an enhancer upstream of the KIT gene in mouse myeloid cells, where occupancy was found to be around 55% (10). Whether this moderate level of nucleosome occupancy allows rapid induction of these and other genes remains to be determined. We also found significant transcription factor binding at enhancers of these genes, while intervening regions (e.g. a region 7 kb

upstream of the TSS of *Il12b*) showed no binding of these factors (see Figure 2.3A and B). This finding is in agreement with the presence of the transcriptional machinery at the enhancers of other actively transcribed genes (see for example (46,47). It has been shown that DNA looping can bring distal enhancers into close proximity of promoters (16,45), and it is therefore possible that we detected PolII and TBP at the enhancers merely as a result of DNA looping. However, our experiments showed clear enrichment of signal-induced TFs and the co-activator p300 at the distal enhancers of *Il12b* and *Il1a* with very little binding at the promoters (Figure 2.3C–H). These results indicate that our ChIP assay can distinguish between genomic locations that are contacted directly by cis-regulatory TFs and the general machinery, and those that may come into proximity of these factors only indirectly as a result of DNA looping. We therefore believe that PolII and TBP are directly recruited to the distal enhancers. Our results are in agreement with previous findings that many active enhancers are transcribed and produce short eRNAs (48,49), but what the role of transcription initiating from such sites might be remains to be determined.

In contrast to our findings at the *Il1a* and *Il12b* promoters we found that the TATAA-sequence in the *Ifnb1* promoter was cleared of nucleosomes upon induction in primary mouse macrophages as had been described for the *Ifnb1* promoter in human cells (13). *Ifnb1* contains a conserved proximal enhancer, which became associated with all the TFs we tested as well as with the co-activator p300 when the gene was expressed. In HeLa cells the proximal enhancer of *Ifnb1* has been reported to be completely nucleosome-free prior to induction (13), but we found that in primary BMDMs the corresponding region was lowly occupied by nucleosomes prior to gene expression and

became completely nucleosome-free upon induction. Together, the changes in chromatin architecture at all the enhancers we have analyzed, both proximal and distal, were similar: enhancers were only moderately occupied by nucleosomes in resting macrophages and a central region was completely cleared of nucleosomes when the associated genes were induced. The size of the cleared region varied from about 1 nucleosome (at the proximal enhancer of *Ifnb1*) to removal of 2–3 nucleosomes in the distal enhancers of *Il12b*, *Ifnb1* and *Il1a*. The small size of the nucleosome-free region in the proximal enhancer of *Ifnb1* is in agreement with the assembly of an enhanceosome at this site, which forms a highly organized structure with a relatively small DNA-footprint (26). Together, our data suggest that enhancers of pro-inflammatory genes undergo similar changes in nucleosome occupancy regardless of their distance from a TSS, and that clearance of enhancer nucleosomes is required to allow binding of cis-regulatory TFs. Moreover, we hypothesize that removal of nucleosomes at the promoter of *Ifnb1* may occur inadvertently due to its proximity to the proximal enhancer.

Il1a and *Ifnb1* have been classified as primary response genes while *Il12b* is a secondary response gene, and it has been shown that they differ in their induction kinetics as well as in their dependence on newly synthesized factors for efficient induction (50). We find that nucleosome removal at the *Il1a* enhancer occurs with faster kinetics than at the *Il12b* enhancer (see Figure 2.2E) and we hypothesize that the different kinetics may indicate the involvement of different nucleosome remodelers as has been suggested (40). While it is possible that nucleosomes may be removed from these regions by competition of signal-induced TFs for binding to their sites, the rapid

kinetics we have observed strongly suggest that nucleosome remodelers are involved (see Figure 2.2E). Future studies will reveal which remodelers play a role at these and other enhancers of inducible genes.

Acknowledgments

We would like to thank Nara Parameswaran and members of his lab for help with isolation of mouse macrophages, members of Norbert Kaminski's lab for help with isolation of B-cells, David Arnosti, Bill Henry, Rick Schwartz, John LaPres and Jason Knott for discussions.

REFERENCES

REFERENCES

1. Yuan GC, Liu YJ, Dion MF, Slack MD, Wu LF, et al. (2005) Genome-scale identification of nucleosome positions in *S. cerevisiae*. *Science* 309: 626–630.
2. Bernstein BE, Liu CL, Humphrey EL, Perlstein EO, Schreiber SL (2004) Global nucleosome occupancy in yeast. *Genome biology* 5: R62.
3. Sekinger EA, Moqtaderi Z, Struhl K (2005) Intrinsic histone-DNA interactions and low nucleosome density are important for preferential accessibility of promoter regions in yeast. *Molecular cell* 18: 735–748.
4. Bryant GO, Prabhu V, Floer M, Wang X, Spagna D, et al. (2008) Activator control of nucleosome occupancy in activation and repression of transcription. *PLoS biology* 6: 2928–2939.
5. Reinke H, Horz W (2003) Histones are first hyperacetylated and then lose contact with the activated PHO5 promoter. *Molecular cell* 11: 1599–1607.
6. Wang X, Bryant GO, Floer M, Spagna D, Ptashne M (2011) An effect of DNA sequence on nucleosome occupancy and removal. *Nature structural & molecular biology* 18: 507–509.
7. Floer M, Wang X, Prabhu V, Berrozpe G, Narayan S, et al. (2010) A RSC/ nucleosome complex determines chromatin architecture and facilitates activator binding. *Cell* 141: 407–418.
8. Schones DE, Cui K, Cuddapah S, Roh TY, Barski A, et al. (2008) Dynamic regulation of nucleosome positioning in the human genome. *Cell* 132: 887–898.
9. Teif VB, Vainshtein Y, Caudron-Herger M, Mallm JP, Marth C, et al. (2012) Genome-wide nucleosome positioning during embryonic stem cell development. *Nature structural & molecular biology* 19: 1185–1192.
10. Berrozpe G, Bryant GO, Warpinski K, Ptashne M (2013) Regulation of a mammalian gene bearing a CpG island promoter and a distal enhancer. *Cell reports* 4: 445–453.
11. Lefevre P, Lacroix C, Tagoh H, Hoogenkamp M, Melnik S, et al. (2005) Differentiation-dependent alterations in histone methylation and chromatin architecture at the inducible chicken lysozyme gene. *The Journal of biological chemistry* 280: 27552–27560.
12. Bert AG, Johnson BV, Baxter EW, Cockerill PN (2007) A modular enhancer is differentially regulated by GATA and NFAT elements that direct different tissue-

specific patterns of nucleosome positioning and inducible chromatin remodeling. *Molecular and cellular biology* 27: 2870–2885.

13. Agalioti T, Lomvardas S, Parekh B, Yie J, Maniatis T, et al. (2000) Ordered recruitment of chromatin modifying and general transcription factors to the IFN-beta promoter. *Cell* 103: 667–678.
14. Wathelet MG, Lin CH, Parekh BS, Ronco LV, Howley PM, et al. (1998) Virus infection induces the assembly of coordinately activated transcription factors on the IFN-beta enhancer in vivo. *Molecular cell* 1: 507–518.
15. Levine M (2010) Transcriptional enhancers in animal development and evolution. *Current biology: CB* 20: R754–763.
16. Deng W, Lee J, Wang H, Miller J, Reik A, et al. (2012) Controlling long-range genomic interactions at a native locus by targeted tethering of a looping factor. *Cell* 149: 1233–1244.
17. Medzhitov R (2007) Recognition of microorganisms and activation of the immune response. *Nature* 449: 819–826.
18. Kawai T, Akira S (2006) TLR signaling. *Cell death and differentiation* 13: 816– 825.
19. Ghisletti S, Barozzi I, Mietton F, Polletti S, De Santa F, et al. (2010) Identification and characterization of enhancers controlling the inflammatory gene expression program in macrophages. *Immunity* 32: 317–328.
20. Heinz S, Benner C, Spann N, Bertolino E, Lin YC, et al. (2010) Simple combinations of lineage-determining transcription factors prime cis-regulatory elements required for macrophage and B cell identities. *Molecular cell* 38: 576–589.
21. Rahman SM, Janssen RC, Choudhury M, Baquero KC, Aikens RM, et al. (2012) CCAAT/enhancer-binding protein beta (C/EBPbeta) expression regulates dietary-induced inflammation in macrophages and adipose tissue in mice. *The Journal of biological chemistry* 287: 34349–34360.
22. Bretz JD, Williams SC, Baer M, Johnson PF, Schwartz RC (1994) C/EBP-related protein 2 confers lipopolysaccharide-inducible expression of interleukin 6 and monocyte chemoattractant protein 1 to a lymphoblastic cell line. *Proceedings of the national academy of sciences U S A* 91: 7306–7310.
23. Screpanti I, Romani L, Musiani P, Modesti A, Fattori E, et al. (1995) Lymphoproliferative disorder and imbalanced T-helper response in C/EBP beta-deficient mice. *The EMBO journal* 14: 1932–1941.

24. Xie H, Ye M, Feng R, Graf T (2004) Stepwise reprogramming of B cells into macrophages. *Cell* 117: 663–676.
25. Grove M, Plumb M (1993) C/EBP, NF-kappa B, and c-Ets family members and transcriptional regulation of the cell-specific and inducible macrophage inflammatory protein 1 alpha immediate-early gene. *Molecular and cellular biology* 13: 5276–5289.
26. Panne D, Maniatis T, Harrison SC (2004) Crystal structure of ATF-2/c-Jun and IRF-3 bound to the interferon-beta enhancer. *The EMBO journal* 23: 4384– 4393.
27. Zeng L, Liu YP, Sha H, Chen H, Qi L, et al. (2010) XBP-1 couples endoplasmic reticulum stress to augmented IFN-beta induction via a cis-acting enhancer in macrophages. *Journal of immunology* 185: 2324–2330.
28. Zhou L, Nazarian AA, Xu J, Tantin D, Corcoran LM, et al. (2007) An inducible enhancer required for Il12b promoter activity in an insulated chromatin environment. *Molecular and cellular biology* 27: 2698–2712.
29. Nociari M, Ocheretina O, Schoggins JW, Falck-Pedersen E (2007) Sensing infection by adenovirus: Toll-like receptor-independent viral DNA recognition signals activation of the interferon regulatory factor 3 master regulator. *Journal of virology* 81: 4145–4157.
30. Stetson DB, Medzhitov R (2006) Recognition of cytosolic DNA activates an IRF3-dependent innate immune response. *Immunity* 24: 93–103.
31. Floer M, Bryant GO, Ptashne M (2008) HSP90/70 chaperones are required for rapid nucleosome removal upon induction of the GAL genes of yeast. *Proceedings of the National Academy of Sciences of the United States of America* 105: 2975–2980.
32. Robinson JT, Thorvaldsdottir H, Winckler W, Guttman M, Lander ES, et al. (2011) Integrative genomics viewer. *Nature biotechnology* 29: 24–26.
33. Sharma RC, Murphy AJ, DeWald MG, Schimke RT (1993) A rapid procedure for isolation of RNA-free genomic DNA from mammalian cells. *BioTechniques* 14: 176–178.
34. Gervais AL, Marques M, Gaudreau L (2010) PCRTiler: automated design of tiled and specific PCR primer pairs. *Nucleic acids research* 38: W308–312.
35. Carninci P, Sandelin A, Lenhard B, Katayama S, Shimokawa K, et al. (2006) Genome-wide analysis of mammalian promoter architecture and evolution. *Nature genetics* 38: 626–635.

36. Heintzman ND, Stuart RK, Hon G, Fu Y, Ching CW, et al. (2007) Distinct and predictive chromatin signatures of transcriptional promoters and enhancers in the human genome. *Nature genetics* 39: 311–318.
37. Mikkelsen TS, Ku M, Jaffe DB, Issac B, Lieberman E, et al. (2007) Genome-wide maps of chromatin state in pluripotent and lineage-committed cells. *Nature* 448: 553–560.
38. Garber M, Yosef N, Goren A, Raychowdhury R, Thielke A, et al. (2012) A high-throughput chromatin immunoprecipitation approach reveals principles of dynamic gene regulation in mammals. *Molecular cell* 47: 810–822.
39. Sandelin A, Wasserman WW, Lenhard B (2004) ConSite: web-based prediction of regulatory elements using cross-species comparison. *Nucleic acids research* 32: W249–252.
40. Ramirez-Carrozzi VR, Braas D, Bhatt DM, Cheng CS, Hong C, et al. (2009) A unifying model for the selective regulation of inducible transcription by CpG islands and nucleosome remodeling. *Cell* 138: 114–128.
41. Weinmann AS, Plevy SE, Smale ST (1999) Rapid and selective remodeling of a positioned nucleosome during the induction of IL-12 p40 transcription. *Immunity* 11: 665–675.
42. Zhao R, Davey M, Hsu YC, Kaplanek P, Tong A, et al. (2005) Navigating the chaperone network: an integrative map of physical and genetic interactions mediated by the hsp90 chaperone. *Cell* 120: 715–727.
43. Shalek AK, Satija R, Adiconis X, Gertner RS, Gaublomme JT, et al. (2013) Single-cell transcriptomics reveals bimodality in expression and splicing in immune cells. *Nature* 498: 236–240.
44. Zhao M, Zhang J, Phatnani H, Scheu S, Maniatis T (2012) Stochastic expression of the interferon-beta gene. *PLoS biology* 10: e1001249.
45. Kieffer-Kwon KR, Tang Z, Mathe E, Qian J, Sung MH, et al. (2013) Interactome maps of mouse gene regulatory domains reveal basic principles of transcriptional regulation. *Cell* 155: 1507–1520.
46. Kagey MH, Newman JJ, Bilodeau S, Zhan Y, Orlando DA, et al. (2010) Mediator and cohesin connect gene expression and chromatin architecture. *Nature* 467: 430–435.
47. Wang Q, Carroll JS, Brown M (2005) Spatial and temporal recruitment of androgen receptor and its coactivators involves chromosomal looping and polymerase tracking. *Molecular cell* 19: 631–642.

48. De Santa F, Barozzi I, Mietton F, Ghisletti S, Polletti S, et al. (2010) A large fraction of extragenic RNA pol II transcription sites overlap enhancers. *PLoS biology* 8: e1000384.
49. Kim TK, Hemberg M, Gray JM, Costa AM, Bear DM, et al. (2010) Widespread transcription at neuronal activity-regulated enhancers. *Nature* 465: 182–187.
50. Ramirez-Carrozzi VR, Nazarian AA, Li CC, Gore SL, Sridharan R, et al. (2006) Selective and antagonistic functions of SWI/SNF and Mi-2beta nucleosome remodeling complexes during an inflammatory response. *Genes & development* 20: 282–296.

Chapter 3: Chromatin remodeler recruitment during macrophage differentiation facilitates transcription factor binding to enhancers in mature cells

This chapter represents a manuscript that was published in *The Journal of Biological Chemistry* (2016) **291**: 18058-71.

Authors who contributed to this study were: Michael McAndrew, Alison Gjidoda, Mohita Tagore, Tyler Miksanek, and Monique Floer.

Abstract

We show how enhancers of macrophage-specific genes are rendered accessible in differentiating macrophages to allow their induction in mature cells in response to an appropriate stimulus. Using a lentiviral knockdown approach in primary differentiating macrophages from mouse bone marrow we demonstrate that enhancers of *I12b* and *I1a* are kept relatively lowly occupied by nucleosomes and accessible through recruitment of the nucleosome remodeler BAF/PBAF. Our results using an inducible cell-line that expresses an estrogen receptor fusion of the macrophage-specific transcription factor PU.1 (PUER) show that BAF/PBAF recruitment to these enhancers is a consequence of translocation of PUER to the nucleus in the presence of tamoxifen, and we speculate that remodeler recruitment may be directly mediated by PU.1. In the absence of BAF/PBAF recruitment, nucleosome occupancy at the enhancer of *I12b* (and to a lesser extent at *I1a*) reaches high levels in bone marrow derived macrophages (BMDMs), and the enhancers are not fully cleared of nucleosomes upon LPS induction resulting in impaired gene expression. Analysis of *I12b* expression in single cells suggests that recruitment of the remodeler is necessary for high levels of transcription from the same promoter and we propose that remodelers function by increasing nucleosome turnover to facilitate transcription factor over nucleosome binding in a process we have termed *remodeler assisted competition*.

Introduction

Lineage-specific transcription factors (TFs) play a crucial role in cellular differentiation. These TFs are often pioneer TFs that have been suggested to control access to *cis*-regulatory elements — in particular gene enhancers — by other ubiquitously expressed

TFs (1). The idea that access to regulatory elements is controlled in a cell-type specific manner is supported by the finding that sensitivity of enhancers to nucleases like DNase I or MNase is cell-type specific (for recent studies see (2,3)), but how lineage-specific TFs render enhancers accessible during differentiation is unknown. Moreover, what constitutes accessible or “open” chromatin has remained unclear. While regulatory regions of constitutively expressed genes are often completely nucleosome-free, we recently showed that the enhancers of inducible genes are occupied by intermediate levels of nucleosomes in resting macrophages, and these nucleosomes are evicted when the genes are induced (4). Furthermore, before induction these enhancers are already bound by the macrophage-specific pioneer TF PU.1 and primed for activation as indicated by the presence of certain histone marks (*i.e.*, H3K4me1)(5). Binding of PU.1 to enhancers was found to lead to a decrease in nucleosome binding (6,7), and we showed that in the absence of PU.1 binding macrophage-specific enhancers become associated with the polycomb repressive complex (PRC2) and with highly occupied, H3K27me3-marked nucleosomes as cells differentiate (8). These results indicated that the pioneer TF PU.1 keeps enhancers accessible and prevents heterochromatin formation at cell-type specific genes, but the underlying mechanism has remained unclear.

We sought to investigate whether nucleosome remodelers are involved in priming of enhancers. Remodelers of the SWI/SNF family have been shown to facilitate gene expression in many organisms, and SWI/SNF function is best understood in the yeast *S. cerevisiae*, where studies showed that SWI/SNF remodelers remove nucleosomes from promoters or partially unwrap nucleosomes to expose TF binding sites (9-13).

Mammals have two related SWI/SNF complexes, BAF and PBAF, which share certain subunits but also contain unique subunits that are thought to play a role in recruitment of either complex to specific sites. Both BAF and PBAF use the catalytic subunit BRG1, but BAF can also use the alternate catalytic subunit BRM. BRG1 deletion results in early embryonic lethality, but BRM^{-/-} mice develop normally and it has been suggested that upregulation of BRG1 may, in part, compensate for the loss of BRM (14,15). BRG1 is required for differentiation, including that of lymphoid and myeloid cells, and BRG1 is recruited to cell-type specific genes during differentiation of erythrocytes, suggesting that a BRG1-containing BAF/PBAF complex may prime gene regulatory regions during hematopoiesis (16-18). That BAF/PBAF may play a general role in cellular differentiation is further supported by the finding that BRG1 and other BAF/PBAF subunits are frequently mutated in diverse human cancers (19). The core subunit SNF5, for example, is mutated in malignant rhabdoid tumors, a rare aggressive cancer affecting young children, and SNF5 mutation is sufficient to induce such tumors in mice (20,21). Rhabdoid tumor cells are unable to proliferate when BRG1 is inactivated, and it has been suggested that these cells may become dependent on an altered BAF/PBAF complex that still relies on the presence of BRG1 (22). Previous studies showed that BAF/PBAF is required for induction of pro-inflammatory genes in mouse macrophages, since simultaneous knockdown of both BRG1 and BRM impaired induction of a subset of pro-inflammatory genes in a macrophage cell-line by bacterial lipopolysaccharides (LPS)(23). These investigators suggested a role for BAF/PBAF in remodeling non-CpG island promoters but did not investigate whether the remodeler creates accessible chromatin at the enhancers of these genes to prime them for later gene induction.

These investigators also determined whether primary and secondary response genes show differential dependence on the BAF/PBAF remodelers, and concluded that secondary and a subset of primary response genes require the remodeler, while other primary response genes are largely independent.

Here, we show how regulatory regions of two representative macrophage-specific genes (*i.e.*, *I11a*, a primary and *I12b*, a secondary response gene) are rendered accessible during differentiation through recruitment of BAF/PBAF, presumably as a consequence of PU.1 binding. This allows induction of these genes in mature macrophages in response to an appropriate signal. We find that both genes depend on BAF/PBAF for induction and nucleosome eviction at their enhancers, but the effects on *I11a* are less pronounced. Our analysis of gene expression in single cells suggests that remodelers function by *remodeler assisted competition* to facilitate TF binding over nucleosome formation at cell-type specific gene enhancers.

Experimental Procedures

Cell isolation and culture

Bone marrow cells and splenic B-cells were isolated as described from 6-8 week old C57BL/6 female mice (NCI/Charles River) with IACUC oversight (4). To obtain BMDMs, cells were differentiated into macrophages by growth in the presence of M-CSF as described (30). BMDMs were induced with LPS as described (4). The PU.1^{-/-} and PUER cells were grown as described previously (8). HSPCs were isolated using the EasySep™ Mouse Hematopoietic Progenitor Cell Isolation Kit (Stemcell Technologies) per manufacturer's instructions, with an additional red blood lysis step prior to progenitor isolation. Briefly, 2-3 x 10⁷ cells were resuspended in 1 ml red cell lysis buffer (Sigma)

and mixed gently for 2 min. before addition of 9 ml IMDM medium (Gibco) and centrifugation at 400 x g for 5 min. The resulting cell pellet was used for HSPC isolation.

shRNA mediated knockdown of BRG1 and SNF5

Lentiviral transductions were performed essentially as described (8). Briefly, lentiviral particles containing shRNAs targeting either BRG1 (*Smarca4*) or SNF5 (*Smarca1*) selected from a pool that had been pre-validated by the Broad Consortium (TRC collection MISSION shRNA library, Sigma) or control shRNA targeting firefly luciferase were produced in HEK293T cells. For lentiviral transductions, bone marrow cells from the femur and tibia of 6-8 week old C57BL/6 female mice were infected with lentivirus after they had been grown for 48 h in BMDM medium containing L929 cell supernatant as a source of M-CSF. 4 h after viral infection the medium was replaced to remove the virus and cells were grown for 48 h. Transduced cells were then selected by growth in the presence of 5 µg/ml puromycin for 5 days. Cells were harvested for various experiments as described (4).

Quantitative nucleosome occupancy assay

The assay was performed essentially as described in (4) except that cross-linked chromatin from 0.5 to 1 x 10⁷ cells was used per experiment and the MNase (NEB) concentrations were adjusted to a range from 0.0027 U to 13.3 U. Bar graphs and overlays were generated using the IGB genome browser. Primer pairs for the amplicons used can be given upon request.

Chromatin immunoprecipitation

ChIP experiments were performed essentially as described (4) except that sonicated chromatin from 1.5 - 2.5 x 10⁶ cells per antibody was diluted 2.5-fold with Low Salt ChIP

buffer (20 mM Tris-HCl, pH 8, 200 mM NaCl, 0.5% Triton X-100, 2 mM EDTA, Halt™ Protease Inhibitor (Thermo Scientific)) to a total volume of 375 µl and incubated overnight at 4°C with either 5 µl anti-SNF5 (ab126734; Abcam), 5 µl anti-BAF155 (D7F8S; Cell Signaling Technology) or 2 µl anti-PU.1 (sc-352; SCBT).

Immunoprecipitated DNA was quantified on a Lightcycler 480 (Roche). LPS-inducible enhancers measured were identified by Ghisletti et al. (5) and have the following genomic locations: 44 kb upstream of *Pel11*, 64 kb upstream of *IL6* and 3.9 kb upstream of *Ccl5* (5). Intergenic region 1 is located 7 kb upstream of the TSS of *I112b*, intergenic region 2 is located 25 kb upstream of the TSS of *I11a* and intergenic region 3 is located in the HOX cluster between *Hoxd11* and *Hoxd10*. Primer sequences can be given upon request. ChIP data is displayed as the fold binding over average binding at control regions (*i.e.*, the *Kit* promoter, *Rpl4* Orf and intergenic region 1).

mRNA determination

RNA isolation and cDNA synthesis were performed as described (4). cDNA was analyzed by qRT-PCR on a Lightcycler 480 (Roche) using gene-specific primer pairs. Primer sequences can be given upon request.

Chromatin fractionation and Western blotting

Chromatin fractionation was performed essentially as described using the high salt extraction protocol of (31). Briefly, $1.5 - 2 \times 10^6$ cells that had been transduced with lentivirus bearing specific shRNAs or untreated control BMDMs were resuspended in 400 µl extraction buffer (10 mM HEPES pH 7.9, 10 mM KCl, 1.5 mM MgCl₂, 0.34 M sucrose, 10% Glycerol, Halt™ Protease Inhibitor (Thermo Scientific)), which contained 0.2% NP40 but no sodium butyrate. The solution was centrifuged for 5 min. at 6,500 x

g. The nuclear pellet was washed in 400 μ l of extraction buffer without NP40 or sodium butyrate and then centrifuged again for 5 min. at 6,500 x *g*. Nuclei were resuspended by vortexing in 400 μ l no-salt buffer (10 mM HEPES pH 7.9, 3 mM EDTA, 0.2 mM EGTA). The solution was placed on a rotator at 4°C for 30 min. and then spun at 6,500 x *g* for 5 min. The pellet containing chromatin was resuspended in 160 μ l high salt solubilization buffer (50 mM Tris-Cl pH 8.0, 2.5 M NaCl, 0.05% NP40), vortexed, and incubated on a rotator at 4°C for 30 min. The samples were then centrifuged for 10 min. at 16,000 x *g*. The supernatant containing solubilized proteins was collected as the chromatin-associated fraction. TCA was added at a final concentration of 10%, samples were incubated for 15 min. and then centrifuged at 21,000 x *g* for 15 min. The resulting pellet was washed with 500 μ l acetone and resuspended in 40 μ l of LDS Sample Buffer (106 mM Tris HCl, 141 mM Tris Base, 2% LDS, Glycerol 10%, 0.51 mM EDTA, pH 8.5). To 30 ml of each sample 3 μ l 0.1% Coomassie blue, 2 μ l 1 M DTT and 5 μ l of 2 x LDS Sample Buffer were added, samples were incubated at 75°C for 10 min and each fraction was analyzed by SDS-PAGE on a 4-12% Bis-Tris Plus gel (Novex, Life Technologies). Western analysis was performed after protein transfer for 2 h at 90 V onto a nitrocellulose membrane and quantification of total protein by Ponceau Red staining, using antibodies against POLII (sc-56767; SCBT), BRG1 (sc-10768; SCBT), SNF5 (ab12167; Abcam), and histone H3 (ab1791; Abcam). Chemiluminescent signal after incubation with appropriate secondary antibodies was quantified on a ChemiDoc MP Imaging system (BioRad) or using ImageJ.

Flow cytometry

Analysis was performed on a BD Biosciences LSR II flow cytometer. 1×10^5 cells were used per antibody. To determine IL12B production, Golgi inhibitor GolgiPlug™ (BD Biosciences) was added to prevent cytokine secretion as described (27). Briefly, 1 ml/ml GolgiPlug™ was added in medium without FBS and cells were incubated for 1 h at 37°C. Then 1 mg/ml LPS from *E. coli* strain EH100 (Ra mutant)(Sigma) was added and cells were grown for 3 h. Cells were collected using Versene (Lifetech) treatment and washed with PBS once. Cells were fixed with 1% formaldehyde for 10 min. and washed with PBS once. To block nonspecific Fc receptor binding, cells were incubated with 2.42G supernatant for 10 min., followed by a wash with PBS. Staining was performed in permeabilization buffer (PBS, 5% FBS, 0.1% sodium azide, 0.5% Triton X-100) for 30 min. in the dark with anti-IL12B-APC (554480; BD Pharmingen) and anti-SNF5-AlexaFluor488 (bs-6109R; Bioss), and cells were subsequently washed twice in flow wash buffer (PBS, 5% FBS, 0.1% sodium azide). Due to differences in total count after size gating, fluorescence histograms were normalized and unit areas are shown in overlays instead of absolute cell counts.

Isolation of Lin⁻ cells was confirmed by flow cytometry using the lineage antibody cocktail provided in the EasySep™ Hematopoietic Progenitor Cell Isolation Kit probing for CD5, CD11b, CD19, CD45R/B220, Ly6G/C(Gr-1), TER119, 7-4 (19856; Stemcell Technologies) followed by secondary incubation with Streptavidin-PE (Lifetech), as well as for anti-CD117/KIT (60025; Stemcell Technologies) and anti-SCA1 (60032; Stemcell Technologies) followed by secondary incubation with anti-mouse-FITC (55499; MP

Biomedicals). BMDMs were also analyzed using anti-F4/80-APC (eBioscience 17-4801) and anti-CD11b-FITC (eBioscience 10-0112) antibodies.

Statistical Analysis

Knockdown experiments were performed at least four times for each shRNA, and mRNA results for target genes and cytokine induction are shown as the average of all experiments. Statistical significance of differences was determined by one-way ANOVA analysis and confirmed by a post-hoc Tukey HSD test. BAF155, SNF5, and PU.1 CHIP experiments were performed at least twice. Statistical significance of the observed differences was determined by one-way ANOVA and confirmed by post-hoc Tukey HSD or Fisher LSD tests. To determine binding to the enhancers, all the data from the different enhancer amplicons tested was analyzed together for statistical significance and compared to all the control amplicons. Nucleosome occupancy experiments were performed twice for each knockdown, and a full analysis including all the amplicons in each enhancer was performed once for the BRG1 KD and twice for the SNF5 KD. The error bars represent the confidence intervals of the curve-fitting analysis for a representative experiment. P-values in the figures indicate the statistical significance of differences between different conditions as determined by paired, two-tailed Student's t-tests.

Results

BAF/PBAF is recruited to the *II12b* and *II1a* enhancers in BMDMs

To investigate how the enhancers of *II12b* and *II1a* are kept accessible and occupied only by intermediate levels of nucleosomes in BMDMs we investigated whether the BAF/PBAF complex is involved in the process. We determined binding of BAF/PBAF to

I12b and *I1a* by ChIP and detected the core subunits BAF155 and SNF5 at both enhancers in resting macrophages (Fig. 3.1A and B, dark blue bars). Recruitment of the remodeler to the *I12b* enhancer further increased upon LPS induction (yellow bars), but the levels of remodeler at *I1a* were already high in resting BMDMs and did not increase significantly upon induction. We found little binding of BAF/PBAF to the enhancers in hematopoietic stem and progenitor cells (HSPCs; isolated by Lin⁻ selection from bone marrow) or B-cells (cyan and green bars, respectively), demonstrating that recruitment of the remodeler to these genes is macrophage-specific. Together our results indicate that BAF/PBAF is recruited to the enhancers of *I12b* and *I1a* at some time during macrophage differentiation, and that gene induction leads to further remodeler recruitment to *I12b*. Binding of SNF5 and BAF155 to the promoters of both genes was low suggesting that the nucleosome remodeler functions predominantly at the enhancers of these genes.

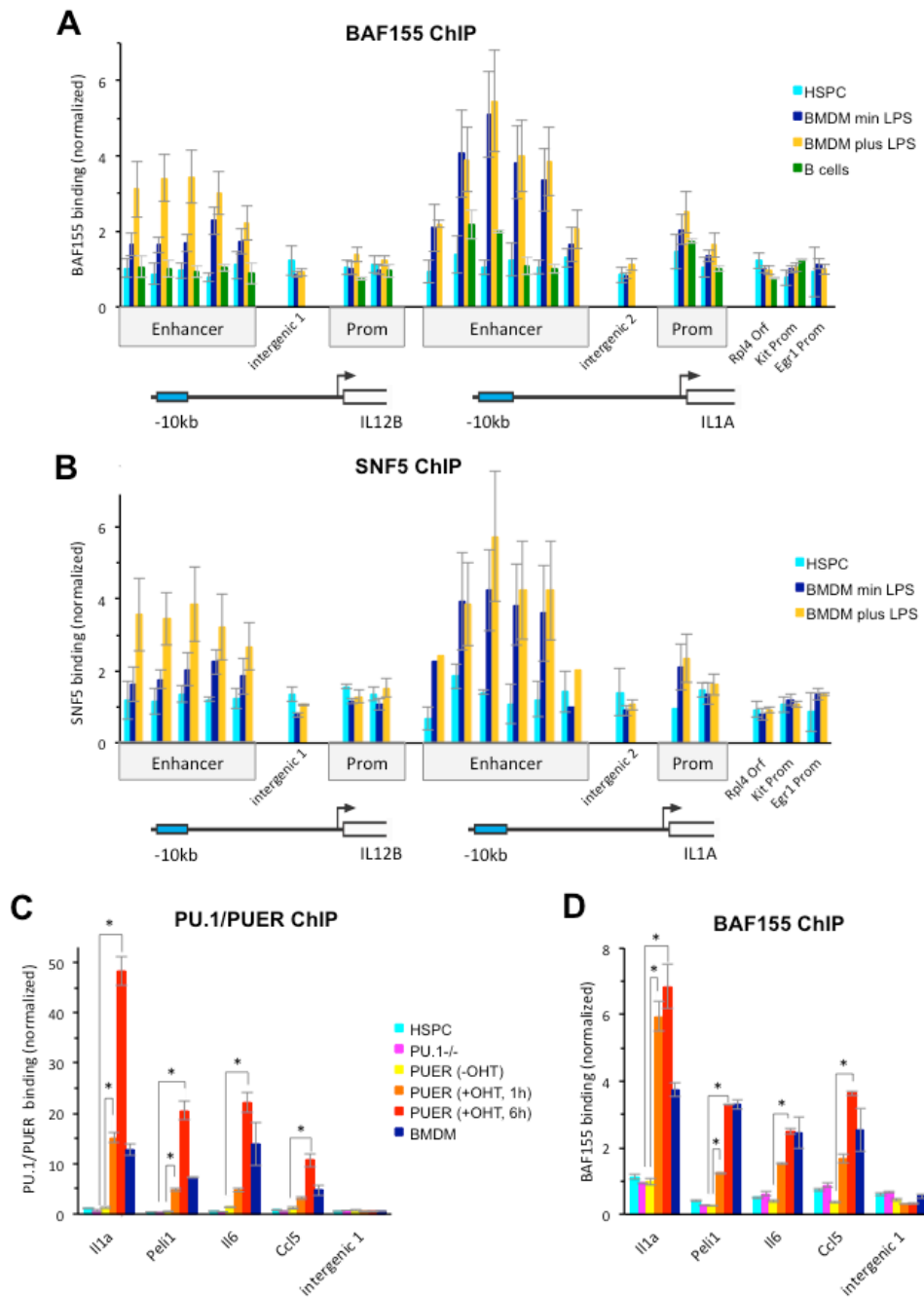
BAF/PBAF recruitment is a consequence of PUER translocation to the nucleus

To determine how BAF/PBAF is recruited to macrophage-specific enhancers we turned to the PUER expressing cell-line that we had previously used to determine the effects of PU.1 binding on nucleosome occupancy (8). This cell-line was derived from hematopoietic progenitors of the fetal liver of a PU.1^{-/-} mouse and expresses the pioneer TF PU.1 as an estrogen receptor fusion (PUER). Growth for prolonged times (*i.e.*, 4 d) in the presence of tamoxifen leads to differentiation of these cells into macrophage-like cells (24). Alternatively, they can be differentiated into mast cells or erythrocyte precursors, indicating that they are multipotent progenitors. We and others previously showed that when these cells were grown in the presence of tamoxifen, PUER bound to

the enhancer of *Il1a* and other inducible genes, which led to reduced nucleosome binding at these sites (6,8). We had also shown that PUER did not bind to the enhancer of *Il12b* and several other inducible macrophage-specific enhancers that are bound by PU.1 in BMDMs, consistent with published results (6). Instead this subset of inducible genes became associated with the polycomb repressive complex PRC2 (*i.e.*, Suz12) and acquired repressive histone marks (*i.e.*, H3K27me3) when the cells were differentiated into macrophage-like cells, indicating that facultative heterochromatin was formed at these sites in the absence of PU.1 binding. To determine if PUER recruited BAF/PBAF to macrophage-specific enhancers that could bind the pioneer TF in this system, we performed a ChIP experiment probing for the BAF155 subunit and for PU.1 and found that recruitment of BAF/PBAF indeed correlated with PUER binding to the enhancers of *Il1a*, *Peli1*, *Il6* and *Ccl5*. Statistically significant BAF155 recruitment and PUER binding was detected as early as 1 h after addition of tamoxifen at *Il1a* and *Peli1* (Fig. 3.1C and D, orange bars) and further increased with prolonged growth in the presence of tamoxifen to reach significant levels at all four enhancers after 6 h (red bars). We had shown previously that at this time the cells still resemble progenitors and that the associated genes are not induced and signal-induced TFs are not bound (8). The rapid appearance of BAF155 binding after tamoxifen addition suggests that remodeler recruitment is a direct consequence of PUER translocation to the nucleus. We speculate that PU.1 may directly recruit BAF/PBAF to these enhancers, although further experiments will have to be performed to confirm this conclusion. We also demonstrated that in primary HSPCs from bone marrow, where BAF/PBAF was not recruited to the enhancers (Fig. 3.1A, B and D, cyan bars), PU.1 was absent as well

(Fig. 3.1C, cyan bars) further supporting the idea that BAF/PBAF recruitment is a consequence of PU.1 binding in primary macrophages. Together, our results suggest that upregulation of PU.1 expression during macrophage differentiation (25) induces PU.1 binding and concomitant recruitment of BAF/PBAF to enhancers of macrophage-specific genes, which primes these genes for induction in mature macrophages.

Figure 3.1. Recruitment of BAF/PBAF to macrophage-specific enhancers.



(A) A ChIP experiment probing for BAF155 was performed in HSPCs (cyan), in BMDMs grown without (dark blue) and with LPS for 1.5 h (yellow), and in splenic B-cells (green). BAF155 binding to the enhancers, promoters and intervening sequences of *Il12b* and

Figure 3.1. (cont'd)

Il1a, and at control regions is shown. ChIP experiments were performed three times and error bars indicate the SEM. One-way ANOVA shows that differences at the enhancers are statistically significant (at the $p < 0.05$ level) between different cell-types, while differences at control locations, the promoters and the intervening regions are not statistically significant. A post-hoc Tukey HSD test confirmed that differences between uninduced BMDMs and HSPCs or B-cells at the enhancers were statistically significant. At the *Il12b* enhancer differences between uninduced and induced BMDMs were also statistically significant while those at the *Il1a* enhancer were not.

(B) A SNF5 ChIP was performed in HSPCs and in BMDMs grown with and without LPS and a statistical analysis confirmed the significance of differences as for the BAF155 ChIP shown in (A).

(C) A ChIP experiment using an antibody that recognizes both PU.1 and PUER was performed in HSPCs (cyan), in the PU.1^{-/-} cell-line (magenta), and in PUER cells grown in the absence of tamoxifen (yellow), and for 1 h (orange) and 6 h (red) in the presence of tamoxifen. All cells were grown in the absence of LPS and resting BMDMs are shown as controls (blue). PU.1/PUER binding at LPS-inducible enhancers of *Il1a*, *Peli1*, *Il6* and *Ccl5* are shown (for genomic coordinates of the enhancers see *Experimental Procedures*). ChIP experiments were performed twice and error bars indicate the SEM. A one-way ANOVA shows statistically significant differences ($p < 0.05$) between different cell-types and growth conditions. Post-hoc comparisons using a Tukey HSD test indicate that at all four enhancers growth in the presence of tamoxifen for 6 h resulted in

Figure 3.1. (cont'd)

statistically significant binding of PUER compared to no tamoxifen, and at *Ii1a* and *Peli1* differences were already statistically significant after 1 h.

(D) A BAF155 ChIP was performed with cells as in (C) and a statistical analysis confirmed significance of the differences in BAF155 recruitment as described for PU.1/PUER binding in (C).

BAF/PBAF is required for *Ii12b* and *Ii1a* induction in BMDMs

To determine whether recruitment of the BAF/PBAF complex rendered the enhancers of *Ii12b* and *Ii1a* accessible during macrophage differentiation we used a lentiviral shRNA-mediated knockdown approach. For these experiments bone marrow cells were transduced with lentivirus containing shRNAs targeting BRG1, encoded by the *Smarca4* gene, or with control shRNA targeting firefly luciferase (*shLuc*). The effect of BRG1 KD was then analyzed in transduced cells that had been differentiated into macrophages in the presence of M-CSF for 9 days. We identified two shRNAs from a pool of shRNAs pre-validated by the Broad Consortium (*shSmarca4-3* and *shSmarca4-4*) that yielded 50-60% knockdown of *Smarca4* as determined by mRNA analysis (Fig. 3.2A) and resulted in reduction of chromatin-associated BRG1 protein by 50% (Fig. 3.2B). This level of knockdown reduced *Ii12b* and *Ii1a* expression 1.5 h after LPS addition by 50% (Fig. 3.2C). Previous studies in the macrophage cell-line J774 had shown that *Ii12b* expression was dependent on BRG1, but these investigators had classified *Ii1a* as a BAF/PBAF-independent gene, although a small decrease in *Ii1a* expression was reported (23). We believe that the more pronounced effect of our BRG1 KD on *Ii1a* induction may be due to differences between the macrophage cell-line J774 and

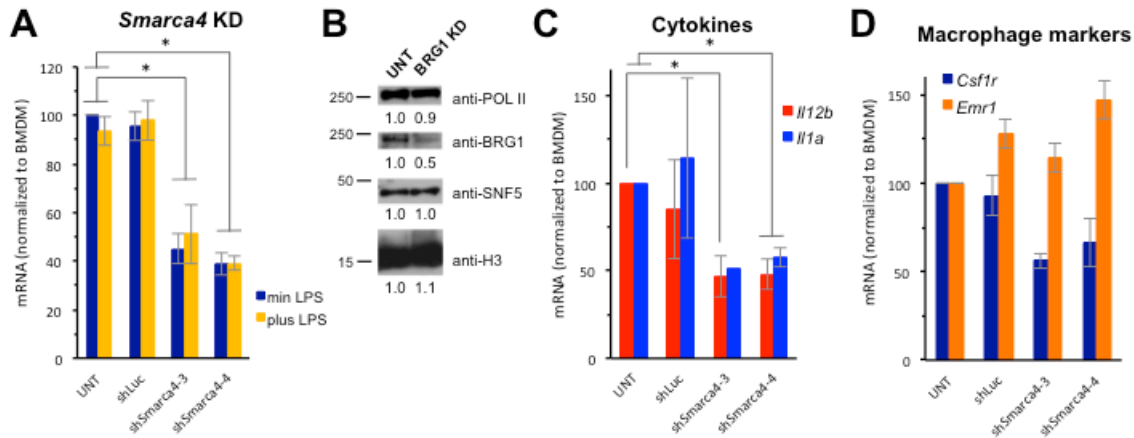
primary BMDMs. The cells differentiated under these conditions still resembled macrophages and expressed the macrophage marker F4/80 (*i.e.*, *Emr1*, orange bars in Fig. 3.2D). However, we found that other macrophage-specific, constitutively expressed genes were expressed at lower levels in BRG1 KD cells (*e.g.*, *Csf1r*, blue bars in Fig. 3.2D).

BRG1 KD affects nucleosome occupancy and eviction at the *I12b* and *I1a* enhancers

To analyze the effect of knocking down BRG1 on nucleosome occupancy at enhancers we pooled cells transduced with lentivirus containing either of the two BRG1-specific shRNAs we had identified, and performed the quantitative nucleosome occupancy assay. We found that nucleosome occupancy over the whole *I12b* enhancer was higher in BRG1 KD compared to untreated control cells (Fig. 3.2E). Nucleosome occupancy at preferred positions increased by 10-25% resulting in peak occupancies of 75-90%. Positioning of nucleosomes was largely unaffected, suggesting that other factors determine nucleosome positioning in the *I12b* enhancer. Knockdown of BRG1 in hematopoietic progenitors also led to increased nucleosome occupancy at the *I1a* enhancer, although the effect was less pronounced than at *I12b* (Fig. 3.2F). P-values of Student's t-tests showed that the differences found over the whole enhancer regions between BRG1 KD and control cells were statistically significant. Control regions were not affected by BRG1 KD (Fig. 3.2G). Analysis of nucleosome occupancy 1.5 h after LPS addition showed less nucleosome eviction at both enhancers in BRG1 KD compared to untreated cells (Fig. 3.2H and I). For example, occupancy at positions in the *I12b* enhancer that are completely cleared of nucleosomes in response to LPS in

untreated cells (< 5%), remained associated with nucleosomes in 15-20% of the population when BRG1 was knocked down.

Figure 3.2. KD of the catalytic BAF/PBAF subunit BRG1.



(A) BRG1 was knocked down in hematopoietic progenitors using two shRNAs (sh*Smarca4-3* and sh*Smarca4-4*) and cells were differentiated into BMDMs as described in *Experimental Procedures*. Cells transduced with control sh*Luc* are also shown. mRNA levels of the *Smarca4* gene were analyzed in untreated BMDMs, and in cells transduced with control and specific shRNAs as indicated. Cells were either grown without (blue) or with (yellow) LPS for 1.5 h. Data was normalized to mRNA levels found in untreated BMDMs grown in the absence of LPS; experiments were performed at least four times and SEMs are indicated by the error bars. One-Way ANOVA shows statistical significance between differently treated cells ($p < 0.05$), and a post-hoc Tukey HSD test confirms statistical significance between untreated (or sh*Luc* treated) and sh*Smarca4* treated cells.

(B) BRG1 protein abundance was determined by Western analysis in the chromatin fraction of untreated BMDMs, and in that of cells transduced with either of the BRG1-specific shRNAs identified in (A) and pooled before fractionation. SNF5, POLII and

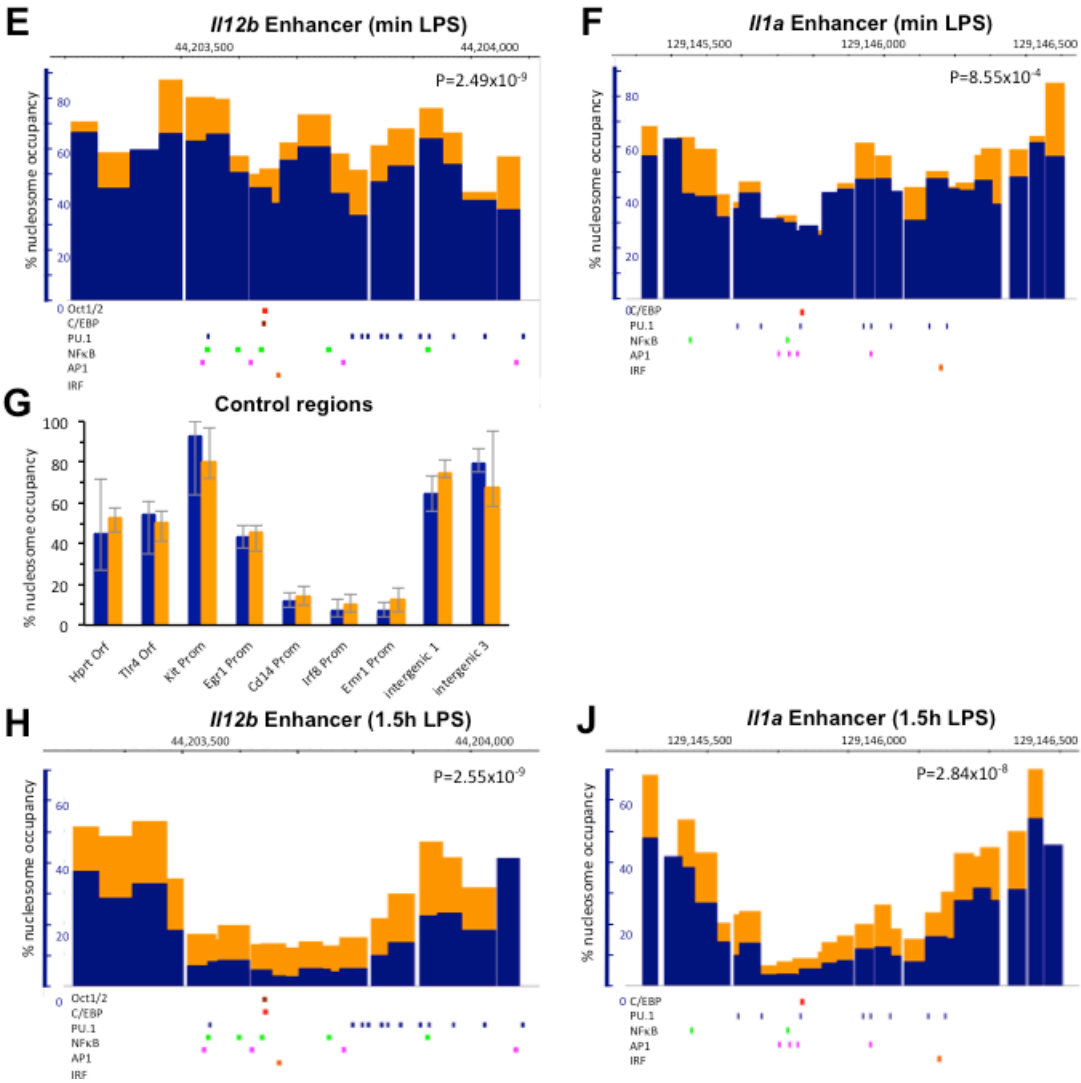
Figure 3.2. (cont'd)

histone H3 levels are shown as controls. Relative abundance of proteins compared to untreated BMDMs is indicated.

(C) mRNA of *Ii12b* (red) and *Ii1a* (blue) in cells as described in (A) and grown in the presence of LPS for 1.5 h. One-Way ANOVA shows statistical significance between differently treated cells ($p < 0.05$), and a post-hoc Tukey HSD test confirms statistical significance between untreated and sh*Smarca4-3* or *4* treated cells for *Ii12b*, and sh*Smarca4-4* treated cells for *Ii1a* induction. Induction data for sh*Luc* treated cells showed higher variability, but was not statistically significantly different from untreated cells.

(D) mRNA of the macrophage markers *Csf1r* (blue) and *Emr1* (orange) is shown in cells as in (A) grown in the absence of LPS.

Figure 3.2. (cont'd)



(E) Untreated BMDMs (blue) and BRG1 KD cells (orange) were obtained as described in (B). Nucleosome occupancy at the *Il12b* enhancer in cells grown without LPS is shown as a bar graph with the width of each bar corresponding to the size of each amplicon. P-value of a Student's t-test shows significance of the differences between untreated and BRG1 KD cells.

(F) Untreated BMDMs (blue) and BRG1 KD cells (orange) were obtained as described in (B). Nucleosome occupancy at the *Il1a* enhancer in cells grown without LPS.

Figure 3.2. (cont'd)

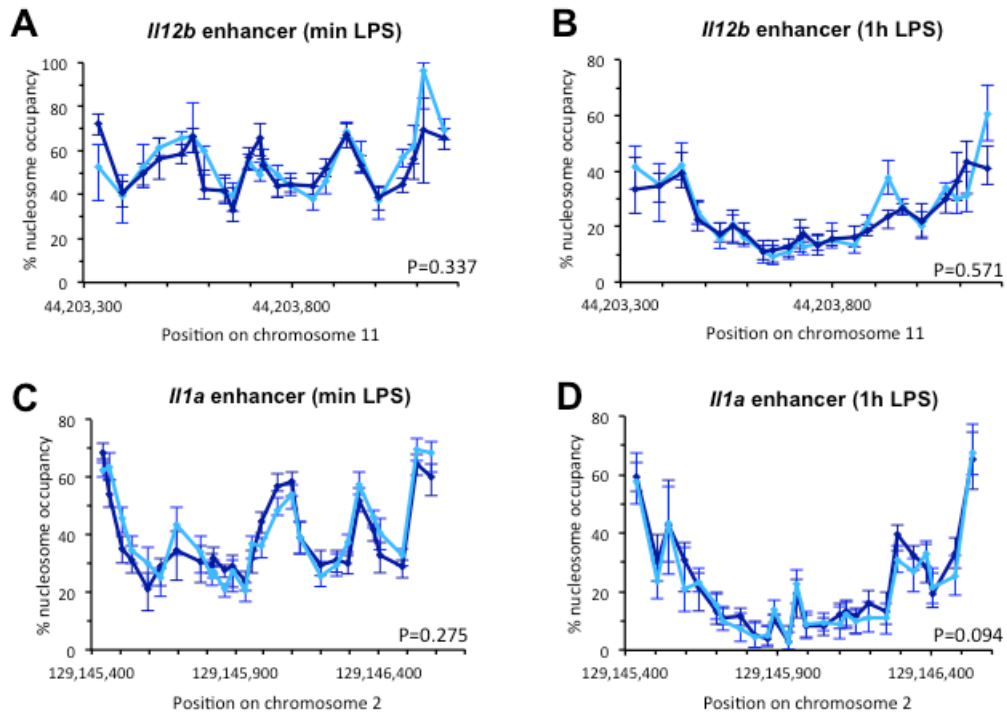
(G) Untreated BMDMs (blue) and BRG1 KD cells (orange) were obtained as described in (B). Nucleosome occupancy at control regions in cells grown in the absence of LPS.

(H) Untreated BMDMs (blue) and BRG1 KD cells (orange) were obtained as described in (B). Nucleosome occupancy at the *I12b* enhancer in cells grown in the presence of LPS for 1.5 h.

(I) Untreated BMDMs (blue) and BRG1 KD cells (orange) were obtained as described in (B). Nucleosome occupancy at the *I1a* enhancer in cells grown in the presence of LPS for 1.5 h.

Control experiments showed that transduction with *shLuc* had no effect on occupancy before or upon LPS induction (Fig. 3.3A-D). Together our results indicate that recruited BAF/PBAF prevents high levels of nucleosome binding at the *I12b* and *I1a* enhancers in resting macrophages and stimulates nucleosome eviction from the enhancers upon LPS induction. However, nucleosomes were still partially evicted in the absence of BRG1, suggesting that a BRM containing BAF complex may partially compensate for the loss of BRG1.

Figure 3.3. Nucleosome occupancy in shLuc treated and untreated control cells.



(A) Nucleosome occupancy at the *Il12b* enhancer in BMDMs (dark blue) and cells transduced with shLuc as described in *Experimental Procedures* (sky blue) grown without LPS. Data is shown as line graphs with each point representing the midpoint of a single amplicon and error bars indicate the confidence interval derived from curve-fitting.

(B) Nucleosome occupancy at the *Il12b* enhancer in cells as in (A) grown with LPS for 1 h.

(C) Nucleosome occupancy at the *Il1a* enhancer in cells grown without LPS.

(D) Nucleosome occupancy at the *Il1a* enhancer grown in the presence of LPS for 1 h.

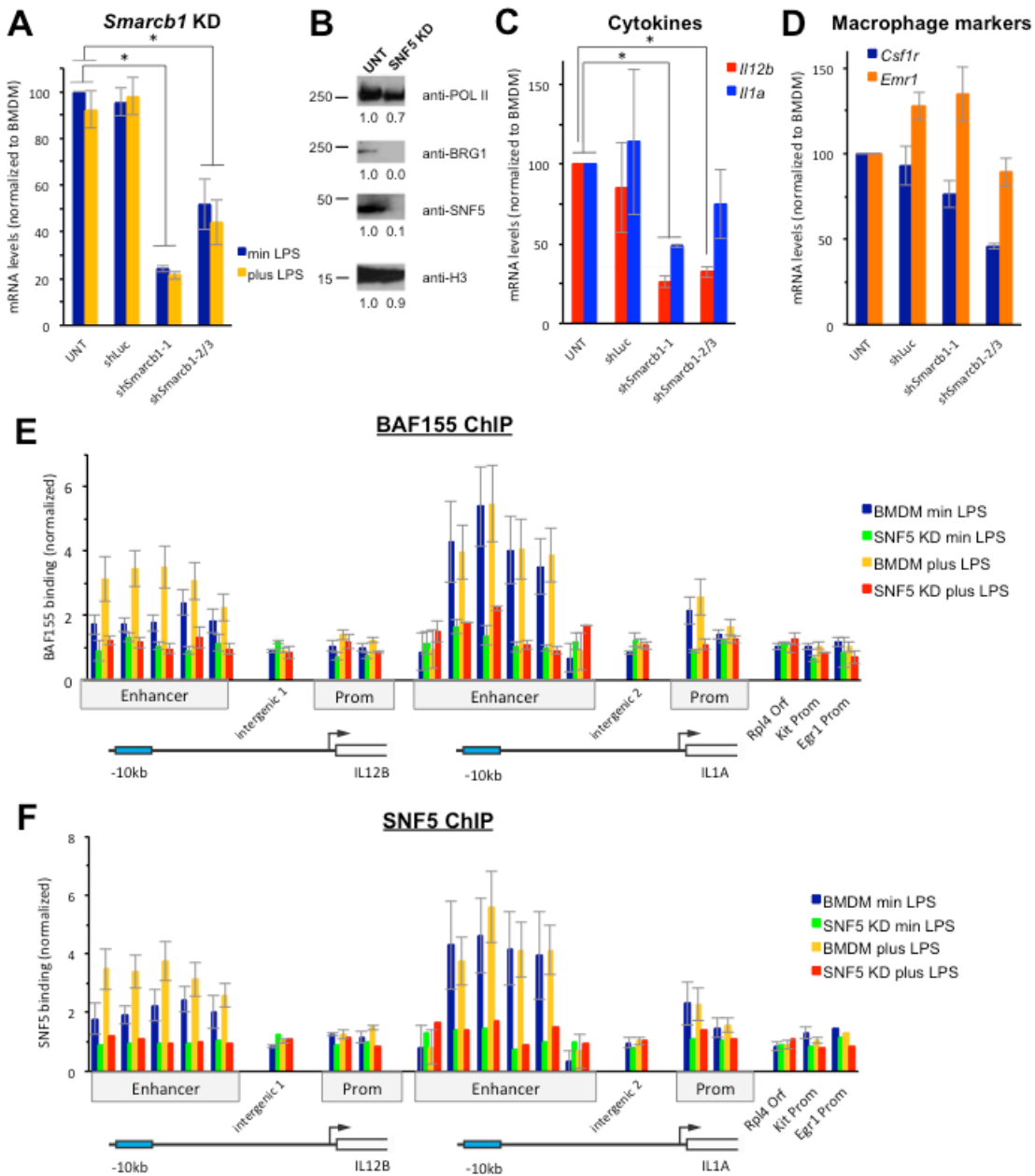
P-values of Student's t-tests indicate that differences between untreated and shLuc transduced cells are not statistically significant.

Knockdown of SNF5 abolishes BAF/PBAF binding at the *I12b* and *I1a* enhancers

To determine whether inactivation of both BAF and PBAF has a stronger effect on nucleosome occupancy at the enhancers, we knocked down the shared core subunit SNF5 in hematopoietic progenitors using the same lentiviral approach. As shown in Fig. 3.4A we identified three shRNAs (sh*Smarca1-1*, 1-2 and 1-3) that knocked down *Smarca1* (the gene encoding SNF5). sh*Smarca1-1* yielded better knockdown (~80%) than either of the other two shRNAs (shown as average) and we therefore selected sh*Smarca1-1* for further analysis. Western blotting confirmed that KD by sh*Smarca1-1* reduced the levels of chromatin-associated SNF5 protein by about 90% (Fig. 3.4B). Moreover, the catalytic subunit BRG1 was no longer detectable in the chromatin-bound fraction when SNF5 was knocked down (Fig. 3.4B). Under these conditions *I12b* induction was reduced by about 75% 1.5 h after LPS addition and *I1a* induction was reduced by about 50% (Fig. 3.4C). Similar to our findings in BRG1 KD cells, we found that SNF5 KD cells still resembled macrophages and expressed macrophage markers (Fig. 3.4D). However, we noted that many cells died during the timecourse of differentiation when we knocked down SNF5, suggesting that loss of SNF5 impairs differentiation and that a minimal amount of SNF5 may be necessary for cells to differentiate into macrophages. Cell survival was also impaired upon BRG1 KD, but to a lesser extent. When we analyzed recruitment of the BAF/PBAF complex to the *I12b* and *I1a* enhancers by ChIP, we found that recruitment of BAF155, both before and upon LPS induction, was strongly reduced in the SNF5 KD (Fig. 3.4E); as expected, SNF5 was no longer detected at the enhancers under these conditions (Fig. 3.4F). This result suggests that the SNF5 subunit is either required for recruitment of BAF/PBAF to

the *112b* and *11a* enhancers or for formation of a stable complex. Previous results indicated that a BAF/PBAF complex is still formed in the absence of SNF5 in rhabdoid tumor cell-lines (26), but our attempts to determine whether BAF/PBAF stability was affected when we knocked down SNF5 in BMDMs were unsuccessful, because low abundance of the complex in whole cell lysates of primary BMDMs made detection of the complex difficult (Floer, M. and Gjidoda, A., unpublished data).

Figure 3.4. KD of the shared BAF/PBAF core subunit SNF5.



(A) mRNA levels of the *Smarcb1* gene were analyzed in untreated BMDMs, and in cells transduced with control and specific shRNAs as indicated. Results in cells transduced with sh*Smarcb1*-2 and 1-3 are shown as an average. Cells were either grown without (blue) or with (yellow) LPS for 1.5 h and data was normalized to uninduced BMDMs.

Figure 3.4. (cont'd)

One-Way ANOVA shows statistical significance between differently treated cells ($p < 0.05$), and a post-hoc Tukey HSD test confirms statistical significance between untreated (or sh*Luc* treated) and sh*Smarca1-1* and sh*Smarca1-2* or 3 treated cells.

(B) SNF5 protein was analyzed in the chromatin fractions of untreated BMDMs and of cells transduced with sh*Smarca1-1*. Western analysis shows loss of SNF5 and BRG1 in the SNF5 KD. POLII and histone H3 are shown as controls. Relative abundance of proteins compared to untreated BMDMs is indicated.

(C) mRNA of *I12b* (red) and *I1a* (blue) in cells as described in (A) and grown in the presence of LPS for 1.5 h. Note that the data shown for cells transduced with sh*Luc* is the same as in Fig. 3.2C. One-Way ANOVA shows statistical significance between differently treated cells ($p < 0.05$), and a post-hoc Tukey HSD test confirms statistical significance between untreated and sh*Smarca1-1* or 2/3 treated cells for *I12b* and for sh*Smarca1-1* treated cells for *I1a*.

(D) mRNA of the macrophage markers *Csf1r* (blue) and *Emr1* (orange) is shown in cells as in (A) grown in the absence of LPS.

(E) A BAF155 ChIP was performed in untreated BMDMs grown in the absence (blue) or presence of LPS for 1.5 h (yellow) or in cells knocked down for SNF5 (sh*Smarca1-1*) and grown in the absence (green) or presence of LPS (red). BAF155 binding to *I12b*, *I1a* and control regions is shown as described in the legend of Fig. 3.1A. One-way ANOVA shows that differences between BMDMs and SNF5 KD cells are statistically significant ($p < 0.05$). A post-hoc Fisher LSD test confirms that differences at the enhancers are statistically significant while differences at control regions are not.

Figure 3.4. (cont'd)

(F) A SNF5 ChIP was performed in untreated BMDMs grown in the absence (blue) or presence of LPS for 1.5 h (yellow) or in cells knocked down for SNF5 (sh*Smarca1-1*) and grown in the absence (green) or presence of LPS (red). BAF155 binding to *I12b*, *I1a* and control regions is shown as described in the legend of Fig. 3.1A. One-way ANOVA shows that differences between BMDMs and SNF5 KD cells are statistically significant ($p < 0.05$). A post-hoc Fisher LSD test confirms that differences at the enhancers are statistically significant while differences at control regions are not.

Nucleosome occupancy at the *I12b* and *I1a* enhancers increases in the absence of BAF/PBAF recruitment

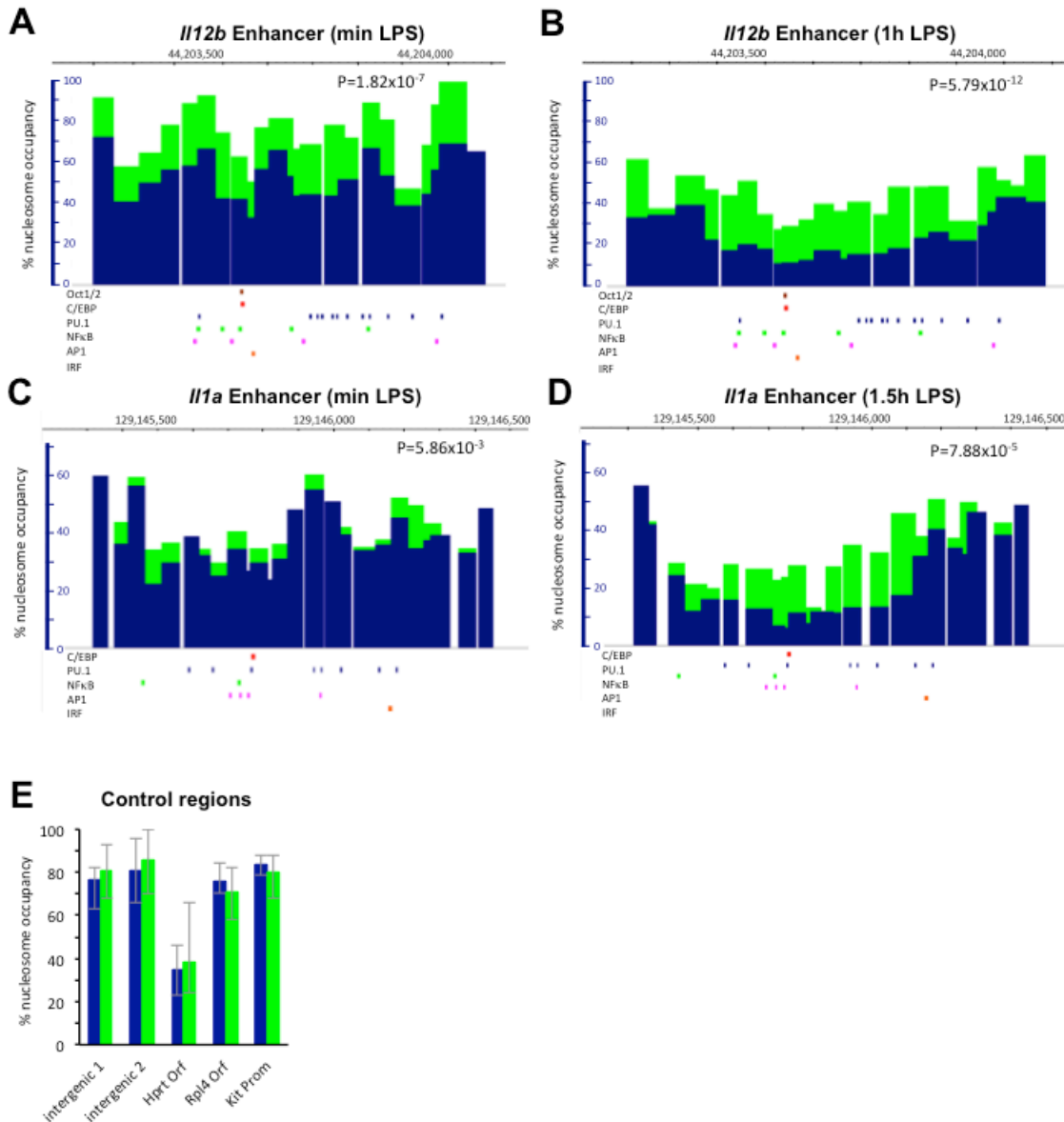
We analyzed nucleosome occupancy in BMDMs that had been transduced with sh*Smarca1-1* expressing lentivirus, and found increased nucleosome occupancy at the *I12b* and *I1a* enhancers, both before and upon LPS induction (Fig. 3.5A-D). The increase in nucleosome occupancy at *I12b* was even more pronounced than in the BRG1 KD and resulted in occupancies at preferred nucleosomal positions around 85-100% before LPS induction (Fig. 3.5A), while control regions were not affected (Fig. 3.5E). 1 h after LPS addition, nucleosomes remained associated with the *I12b* enhancer in 40-50% of the population (Fig. 3.5B) and occupancy did not decrease further with prolonged LPS induction for 1.5 h (see Fig. 3.6C). This result is consistent with the more pronounced effect of SNF5 KD on *I12b* expression compared to KD of BRG1 (compare Fig. 3.2C to 3.4C). We also found increased nucleosome occupancy at the *I1a* enhancer both before and upon LPS induction (Fig. 3.5C and D). The increase in occupancy at the *I1a* enhancer before induction was similar to what we had found in

the BRG1 KD, while nucleosome eviction at *I1a* upon LPS induction was more strongly affected by SNF5 KD. Nevertheless, we note that some level of nucleosome eviction was still seen at both enhancers in the SNF5 KD, and nucleosome occupancy at the *I1a* enhancer before induction was only moderately affected. Whether this is due to the activity of residual SNF5 under the conditions of our KD, or whether other remodelers play a role in addition to BAF/PBAF at these as well as at other enhancers that may regulate these genes remains to be determined.

We also analyzed nucleosome occupancy at the *I12b* and *I1a* promoters in the SNF5 KD, but effects on nucleosome occupancy both before and upon LPS induction at promoters were small compared to those detected at the enhancers (Fig. 3.5F-J).

Together our results indicate that BAF/PBAF regulates nucleosome occupancy at the enhancers of *I12b* and *I1a* and less so at their promoters. This finding is consistent with our previous data showing that nucleosomes at the promoters of *I12b* and *I1a* were not stably evicted under inducing conditions (4), which may contribute to the highly stochastic expression of these genes (27,28).

Figure 3.5. Nucleosome occupancy in SNF5 KD cells.



(A) Nucleosome occupancy at the *//12b* enhancer is shown in untreated BMDMs (blue) and SNF5 KD (green) cells grown in the absence of LPS. P-values of Student's t-tests indicate significance of differences.

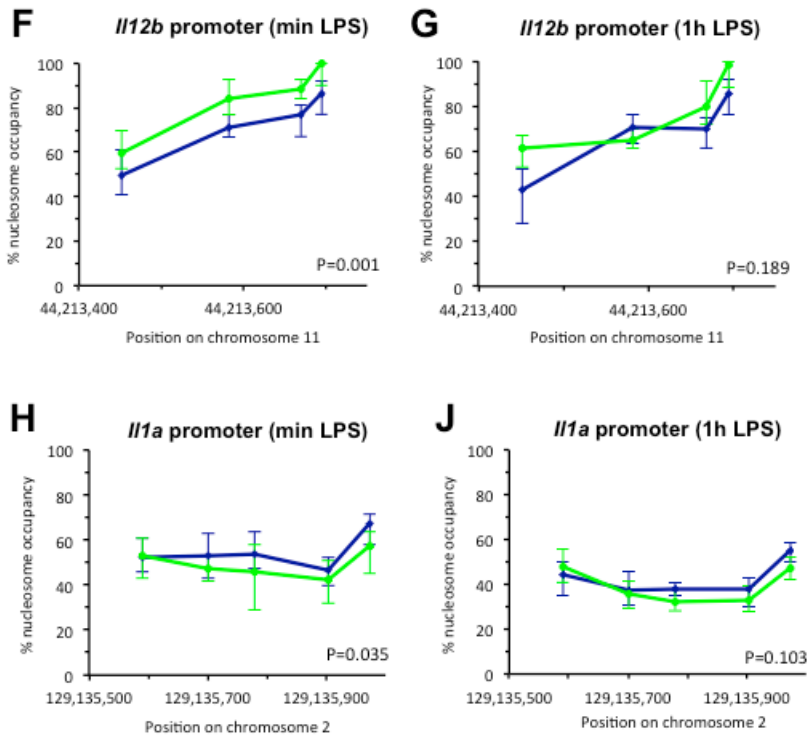
(B) Nucleosome occupancy at the *//12b* enhancer in cells grown for 1 h in the presence of LPS.

(C) Nucleosome occupancy at the *//1a* enhancer in cells grown in the absence of LPS.

Figure 3.5. (cont'd)

(D) Nucleosome occupancy at the *Il1a* enhancer in cells grown for 1.5 h in the presence of LPS.

(E) Nucleosome occupancy at control regions indicated in cells grown in the absence of LPS.



(F) Nucleosome occupancy at the *Il12b* promoter in cells grown in the absence of LPS.

(G) Nucleosome occupancy at the *Il12b* promoter in cells grown in the presence of LPS for 1 h.

(H) Nucleosome occupancy at the *Il1a* promoter in cells grown in the absence of LPS.

(J) Nucleosome occupancy at the *Il1a* promoter in cells grown in the presence of LPS for 1 h.

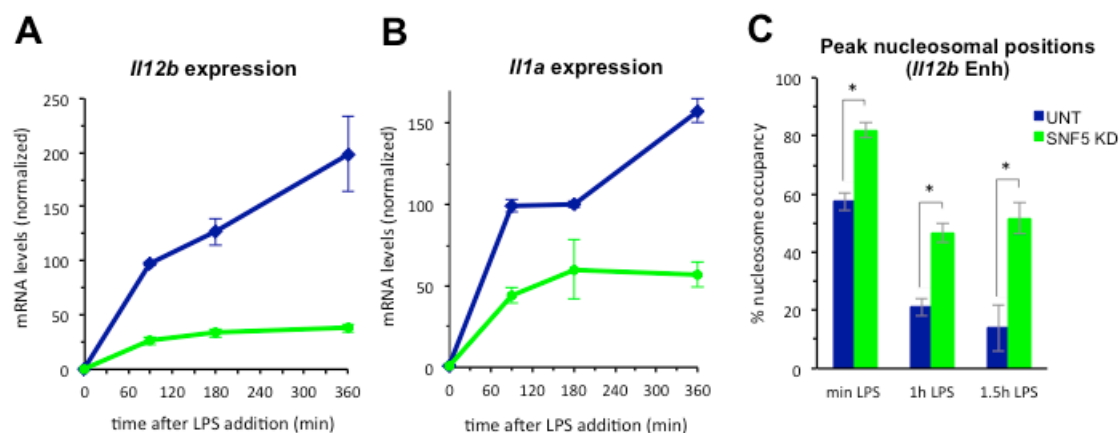
FACS analysis reveals effects of SNF5 KD on cytokine expression in single cells

To determine whether knockdown of SNF5 merely slowed down the rate of mRNA production in the whole macrophage population or also affected the final levels of cytokine expression, we performed a timecourse of LPS induction in SNF5 KD cells. In untreated macrophages *Il12b* and *Il1a* mRNA levels increased during the whole 6 h timecourse of LPS induction as we had shown previously (4)(Fig. 3.6A and B, blue lines). In contrast, when SNF5 was knocked down *Il1a* and *Il12b* mRNA levels reached steady-state after 90-180 min and did not increase further (green lines). Moreover, as mentioned above, we found that nucleosome eviction at the *Il12b* enhancer did not increase further with prolonged LPS induction and nucleosome levels 1.5 h after LPS addition were similar to levels seen after 1 h (Fig. 3.6C). These results suggested that a fraction of cells may not express *Il12b* or *Il1a* when levels of SNF5 are limiting.

To further address this question we analyzed *Il12b* expression in single cells by FACS. We used accumulation of newly synthesized intracellular IL12B protein in cells that had been treated with the Golgi inhibitor brefeldin A to prevent protein secretion to assess *Il12b* expression as described (27). In control macrophages induction of *Il12b* by LPS for 3 h led to accumulation of significant levels of IL12B protein in about 26% of the cells (compare red to blue areas in Fig. 3.6D, and see scatterplot in Fig. 3.6E) consistent with results by others (27). When we knocked down SNF5 and monitored intracellular SNF5 protein levels, we found that KD reduced mean SNF5 levels in the population (indicated by the vertical lines in Fig. 3.6F). More significantly, the fraction of cells with high levels of SNF5 protein was reduced (compare blue to green shoulder areas in Fig. 3.6F). When we analyzed *Il12b* expression in SNF5 KD cells, we found that the fraction of

cells accumulating IL12B protein was dramatically reduced to about 9% (compare green to red area in Fig. 3.6G and see scatterplot in Fig. 3.6H). Furthermore, we found that cells that expressed *I12b* in the SNF5 KD population, expressed only low levels of *I12b* and accumulated less IL12B protein than control macrophages (compare the magnitude of the anti-IL12B-APC fluorescence intensity signal in Fig. 3.6E and H on the y-axis). As shown in Fig. 3.6I we found that IL12B protein accumulation correlated with residual levels of SNF5 protein present in SNF5 KD cells, further demonstrating that the remodeler is required for *I12b* expression.

Figure 3.6. Cytokine expression in SNF5 KD cells.



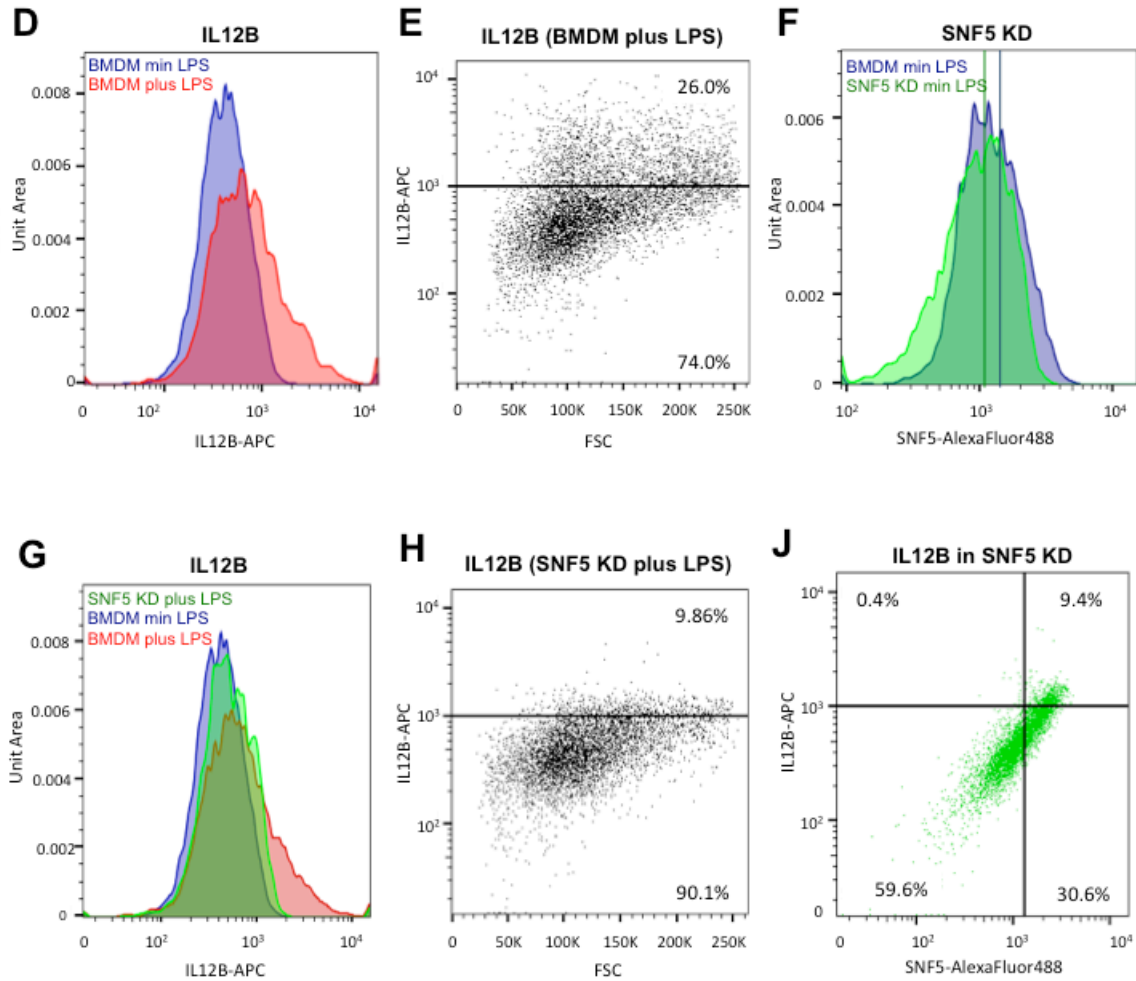
(A) mRNA levels of *I12b* in control BMDMs (blue) and SNF5 KD cells (green). Cells were grown in the absence of LPS, or for increasing times in the presence of LPS as indicated. mRNA levels after 1.5 h were set to 100%. Error bars represent the SEM of at least two measurements.

(B) mRNA levels of *I1a* in cells as in (A).

(C) The average occupancy at the three peak nucleosomal positions in the *I12b* enhancer is shown in cells as in (A) grown without, or with LPS for 1 h and 1.5 h. One-way ANOVA followed by a post-hoc Tukey HSD test ($p < 0.05$) shows that differences

Figure 3.6. (cont'd)

between control and SNF5 KD cells are statistically significant, while occupancy levels in SNF5 KD cells after 1 h and 1.5 h are indistinguishable.



(D) IL12B protein accumulation in control BMDMs grown in the absence (blue) or presence of LPS for 3 h (red) was measured by staining with anti-IL12B-APC. Normalized cell counts are displayed as Unit Areas.

Normalized cell counts are displayed as Unit Areas.

(E) Scatterplot representation of the data from the experiment described in (D). A threshold was set with unstained control BMDMs.

Figure 3.6. (cont'd)

(F) SNF5 protein levels in control BMDMs (blue) and SNF5 KD cells (green) were measured by staining with anti-SNF5-AlexaFluor488. Mean fluorescence intensities of each population are indicated by lines of the respective color.

(G) IL12B accumulation in control BMDMs grown in the absence (blue) or presence of LPS for 3 h (red), and in SNF5 KD cells grown in the presence of LPS for 3 h (green) was measured by staining with anti-IL12B-APC. Note that data for BMDMs is the same as in (D).

(H) Scatterplot representation of the SNF5 KD data from the experiment described in (G).

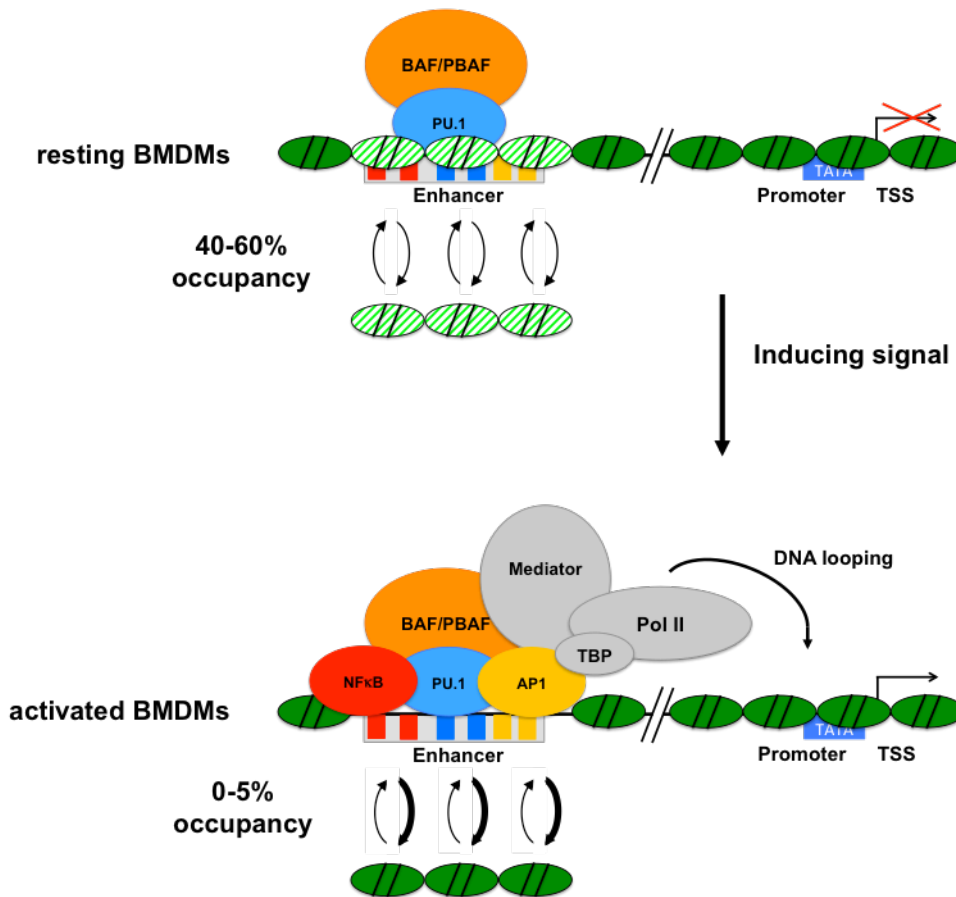
(I) Correlation between IL12B and SNF5 protein levels in SNF5 KD cells grown in the presence of LPS for 3 h was measured by double-staining with anti-IL12B-APC and anti-SNF5-AlexaFluor488. Quartile thresholds were set by analysis of unstained control BMDMs.

Discussion

Our results suggest that BAF/PBAF is recruited to macrophage-specific enhancers in response to PUER translocation to the nucleus (Fig. 3.1), and we speculate that PU.1 recruits the remodeler to these sites. Whether PU.1 directly interacts with BAF/PBAF subunits or whether the interaction is mediated by another factor remains to be determined. We and others showed previously that PU.1 binds to many enhancers together with C/EBP β , the other macrophage-lineage determining pioneer TF, and C/EBP β has been shown to directly interact with BAF/PBAF and to mediate its recruitment in other myeloid cells, suggesting that C/EBP β may recruit BAF/PBAF

together with PU.1 in macrophages (6,8,17). The absence of PU.1 and BAF/PBAF at macrophage-specific enhancers in HSPCs suggests that binding of the pioneer TF and recruitment of the remodeler occurs at some time during macrophage differentiation. Whether the presence of the remodeler in turn stabilizes PU.1 binding to enhancers remains to be determined. If BAF/PBAF is already recruited by PU.1 to some extent prior to gene induction in resting macrophages (Fig. 3.1), how might complete nucleosome eviction be accomplished at enhancers under inducing conditions? We propose that recruited BAF/PBAF increases nucleosome turnover (Fig. 3.7), so that fractional occupancies of enhancer nucleosomes are around 40-60% in a population of resting BMDMs (Fig. 3.2 and 3.5).

Figure 3.7. Remodeler assisted competition favors TF over nucleosome binding to sites in enhancers.



Our model proposes that recruitment of BAF/PBAF to the distal enhancers of *Il12b* and *Il1a* by PU.1 during macrophage differentiation increases turnover of nucleosomes to prevent high occupancy in fully differentiated BMDMs. This results in fractional occupancies of 40-60% for enhancer nucleosomes in the cell population. Under inducing conditions the equilibrium is shifted towards nucleosome removal as signal-induced TFs (e.g., NFκB, AP1) bind to their sites in the enhancers. Note, that increased BAF/PBAF recruitment under inducing conditions (at some enhancers) may further shift the equilibrium towards nucleosome removal. Subsequent steps that result in assembly of a pre-initiation complex at the promoter are not shown.

Upon induction by LPS, signal-induced TFs such as NF κ B and AP1 are activated and compete with nucleosomes for binding to their sites in the enhancers. This shifts the equilibrium towards nucleosome removal (0-5%). We call this model *remodeler assisted competition* between TFs and nucleosomes for binding to enhancers. In the absence of BAF/PBAF, enhancers become more highly occupied by nucleosomes, which impairs gene expression in mature cells in response to an appropriate stimulus (Fig. 3.2 and 3.4). Our model predicts that in the absence of BAF/PBAF, nucleosome turnover is low, and signal induced TFs and the transcriptional machinery are recruited only infrequently, since nucleosome formation is favored over TF binding. This prediction is borne out by our experiments in single cells, where we found that the fraction of cells expressing *Il12b* was reduced in the SNF5 KD (Fig. 3.6G and H). The model further predicts that in the absence of BAF/PBAF, competing nucleosomes reduce the residence times of signal-induced TFs at enhancers, which in turn may decrease the stability of a transcription complex and therefore the transcriptional output from that promoter. Our findings in single cells support this notion, since we found that the levels of IL12B protein that accumulated in individual cells were higher when BAF/PBAF was present at the *Il12b* enhancer than in its absence in the SNF5 KD (compare the magnitude of the IL12B-APC signal in Fig. 3.6E versus H). This finding suggests that in the absence of SNF5 a transcription complex at a promoter may only fire once before it falls apart, while in the presence of SNF5 such a complex may be stable for several rounds of transcription. Previous studies at various genes have suggested that enhancers can function either by increasing the probability that a competent transcription complex is formed at a promoter or by increasing the probability that

another round of transcription is initiated from the same promoter (for a review see (29)). Our results indicate that the distal enhancer of *Il12b* may play a role in both initiation and re-initiation and that *remodeler assisted competition* facilitates TF over nucleosome binding to the enhancer to stimulate both processes.

Acknowledgements

We thank Amy Ralston for helpful discussions; David Arnosti, Jason Knott, Min-Hao Kuo and Erik Martinez-Hackert for careful reading of the manuscript; Louis King, Nara Parameswaran and Michael Steury for help with FACS; Steve Suhr and John LaPres for help with lentiviral transductions.

REFERENCES

REFERENCES

1. Zaret, K. S., and Carroll, J. S. (2011) Pioneer transcription factors: establishing competence for gene expression. *Genes & development* 25, 2227-2241.
2. Stamatoyannopoulos, J. A., Snyder, M., Hardison, R., Ren, B., Gingeras, T., Gilbert, D. M., Groudine, M., Bender, M., Kaul, R., Canfield, T., Giste, E., Johnson, A., Zhang, M., Balasundaram, G., Byron, R., Roach, V., Sabo, P. J., Sandstrom, R., Stehling, A. S., Thurman, R. E., Weissman, S. M., Cayting, P., Hariharan, M., Lian, J., Cheng, Y., Landt, S. G., Ma, Z., Wold, B. J., Dekker, J., Crawford, G. E., Keller, C. A., Wu, W., Morrissey, C., Kumar, S. A., Mishra, T., Jain, D., Byrskabishop, M., Blankenberg, D., Lajoie, B. R., Jain, G., Sanyal, A., Chen, K. B., Denas, O., Taylor, J., Blobel, G. A., Weiss, M. J., Pimkin, M., Deng, W., Marinov, G. K., Williams, B. A., Fisher-Aylor, K. I., Desalvo, G., Kiralusha, A., Trout, D., Amrhein, H., Mortazavi, A., Edsall, L., McCleary, D., Kuan, S., Shen, Y., Yue, F., Ye, Z., Davis, C. A., Zaleski, C., Jha, S., Xue, C., Dobin, A., Lin, W., Fastuca, M., Wang, H., Guigo, R., Djebali, S., Lagarde, J., Ryba, T., Sasaki, T., Malladi, V. S., Cline, M. S., Kirkup, V. M., Learned, K., Rosenbloom, K. R., Kent, W. J., Feingold, E. A., Good, P. J., Pazin, M., Lowdon, R. F., and Adams, L. B. (2012) An encyclopedia of mouse DNA elements (Mouse ENCODE). *Genome biology* 13, 418.
3. Teif, V. B., Vainshtein, Y., Caudron-Herger, M., Mallm, J. P., Marth, C., Hofer, T., and Rippe, K. (2012) Genome-wide nucleosome positioning during embryonic stem cell development. *Nature structural & molecular biology* 19, 1185-1192.
4. Gjidoda, A., Tagore, M., McAndrew, M. J., Woods, A., and Floer, M. (2014) Nucleosomes Are Stably Evicted from Enhancers but Not Promoters upon Induction of Certain Pro-Inflammatory Genes in Mouse Macrophages. *PLoS One* 9, e93971.
5. Ghisletti, S., Barozzi, I., Mietton, F., Polletti, S., De Santa, F., Venturini, E., Gregory, L., Lonie, L., Chew, A., Wei, C. L., Ragoussis, J., and Natoli, G. (2010) Identification and characterization of enhancers controlling the inflammatory gene expression program in macrophages. *Immunity* 32, 317-328.
6. Heinz, S., Benner, C., Spann, N., Bertolino, E., Lin, Y. C., Laslo, P., Cheng, J. X., Murre, C., Singh, H., and Glass, C. K. (2010) Simple combinations of lineage-determining transcription factors prime cis-regulatory elements required for macrophage and B cell identities. *Molecular cell* 38, 576-589.
7. Barozzi, I., Simonatto, M., Bonifacio, S., Yang, L., Rohs, R., Ghisletti, S., and Natoli, G. (2014) Coregulation of transcription factor binding and nucleosome occupancy through DNA features of mammalian enhancers. *Molecular cell* 54, 844-857.

8. Tagore, M., McAndrew, M. J., Gjidoda, A., and Floer, M. (2015) The lineage-specific transcription factor PU.1 prevents polycomb-mediated heterochromatin formation at macrophage-specific genes. *Molecular and cellular biology* 35, 2610-2625.
9. Bryant, G. O., Prabhu, V., Floer, M., Wang, X., Spagna, D., Schreiber, D., and Ptashne, M. (2008) Activator control of nucleosome occupancy in activation and repression of transcription. *PLoS biology* 6, 2928-2939.
10. Reinke, H., and Horz, W. (2003) Histones are first hyperacetylated and then lose contact with the activated PHO5 promoter. *Molecular cell* 11, 1599-1607.
11. Floer, M., Wang, X., Prabhu, V., Berrozpe, G., Narayan, S., Spagna, D., Alvarez, D., Kendall, J., Krasnitz, A., Stepansky, A., Hicks, J., Bryant, G. O., and Ptashne, M. (2010) A RSC/nucleosome complex determines chromatin architecture and facilitates activator binding. *Cell* 141, 407-418.
12. Badis, G., Chan, E. T., van Bakel, H., Pena-Castillo, L., Tillo, D., Tsui, K., Carlson, C. D., Gossett, A. J., Hasinoff, M. J., Warren, C. L., Gebbia, M., Talukder, S., Yang, A., Mnaimneh, S., Terterov, D., Coburn, D., Li Yeo, A., Yeo, Z. X., Clarke, N. D., Lieb, J. D., Ansari, A. Z., Nislow, C., and Hughes, T. R. (2008) A library of yeast transcription factor motifs reveals a widespread function for Rsc3 in targeting nucleosome exclusion at promoters. *Molecular cell* 32, 878-887.
13. Hartley, P. D., and Madhani, H. D. (2009) Mechanisms that specify promoter nucleosome location and identity. *Cell* 137, 445-458.
14. Bultman, S., Gebuhr, T., Yee, D., La Mantia, C., Nicholson, J., Gilliam, A., Randazzo, F., Metzger, D., Chambon, P., Crabtree, G., and Magnuson, T. (2000) A Brg1 null mutation in the mouse reveals functional differences among mammalian SWI/SNF complexes. *Molecular cell* 6, 1287-1295.
15. Reyes, J. C., Barra, J., Muchardt, C., Camus, A., Babinet, C., and Yaniv, M. (1998) Altered control of cellular proliferation in the absence of mammalian brahma (SNF2alpha). *The EMBO journal* 17, 6979-6991.
16. Choi, J., Ko, M., Jeon, S., Jeon, Y., Park, K., Lee, C., Lee, H., and Seong, R. H. (2012) The SWI/SNF-like BAF complex is essential for early B cell development. *Journal of immunology* 188, 3791-3803.
17. Kowenz-Leutz, E., and Leutz, A. (1999) A C/EBP beta isoform recruits the SWI/SNF complex to activate myeloid genes. *Molecular cell* 4, 735-743.
18. Hu, G., Schones, D. E., Cui, K., Ybarra, R., Northrup, D., Tang, Q., Gattinoni, L., Restifo, N. P., Huang, S., and Zhao, K. (2011) Regulation of nucleosome

landscape and transcription factor targeting at tissue-specific enhancers by BRG1. *Genome research* 21, 1650-1658.

19. Shain, A. H., and Pollack, J. R. (2013) The spectrum of SWI/SNF mutations, ubiquitous in human cancers. *PLoS One* 8, e55119.
20. Klochendler-Yeivin, A., Fiette, L., Barra, J., Muchardt, C., Babinet, C., and Yaniv, M. (2000) The murine SNF5/INI1 chromatin remodeling factor is essential for embryonic development and tumor suppression. *EMBO reports* 1, 500-506.
21. Roberts, C. W., Galusha, S. A., McMenamin, M. E., Fletcher, C. D., and Orkin, S. H. (2000) Haploinsufficiency of Snf5 (integrase interactor 1) predisposes to malignant rhabdoid tumors in mice. *Proceedings of the National Academy of Sciences of the United States of America* 97, 13796-13800.
22. Wang, X., Sansam, C. G., Thom, C. S., Metzger, D., Evans, J. A., Nguyen, P. T., and Roberts, C. W. (2009) Oncogenesis caused by loss of the SNF5 tumor suppressor is dependent on activity of BRG1, the ATPase of the SWI/SNF chromatin remodeling complex. *Cancer research* 69, 8094-8101.
23. Ramirez-Carrozzi, V. R., Braas, D., Bhatt, D. M., Cheng, C. S., Hong, C., Doty, K. R., Black, J. C., Hoffmann, A., Carey, M., and Smale, S. T. (2009) A unifying model for the selective regulation of inducible transcription by CpG islands and nucleosome remodeling. *Cell* 138, 114-128.
24. Walsh, J. C., DeKoter, R. P., Lee, H. J., Smith, E. D., Lancki, D. W., Gurish, M. F., Friend, D. S., Stevens, R. L., Anastasi, J., and Singh, H. (2002) Cooperative and antagonistic interplay between PU.1 and GATA-2 in the specification of myeloid cell fates. *Immunity* 17, 665-676.
25. Laiosa, C. V., Stadtfeld, M., and Graf, T. (2006) Determinants of lymphoid-myeloid lineage diversification. *Annual review of immunology* 24, 705-738.
26. Doan, D. N., Veal, T. M., Yan, Z., Wang, W., Jones, S. N., and Imbalzano, A. N. (2004) Loss of the INI1 tumor suppressor does not impair the expression of multiple BRG1-dependent genes or the assembly of SWI/SNF enzymes. *Oncogene* 23, 3462-3473.
27. Weinmann, A. S., Plevy, S. E., and Smale, S. T. (1999) Rapid and selective remodeling of a positioned nucleosome during the induction of IL-12 p40 transcription. *Immunity* 11, 665-675.
28. Shalek, A. K., Satija, R., Adiconis, X., Gertner, R. S., Gaublomme, J. T., Raychowdhury, R., Schwartz, S., Yosef, N., Malboeuf, C., Lu, D., Trombetta, J. J., Gennert, D., Gnirke, A., Goren, A., Hacohen, N., Levin, J. Z., Park, H., and Regev, A.

- A. (2013) Single-cell transcriptomics reveals bimodality in expression and splicing in immune cells. *Nature* 498, 236-240.
29. Blackwood, E. M., and Kadonaga, J. T. (1998) Going the distance: a current view of enhancer action. *Science* 281, 60-63.
30. Nociari, M., Ocheretina, O., Schoggins, J. W., and Falck-Pedersen, E. (2007) Sensing infection by adenovirus: Toll-like receptor-independent viral DNA recognition signals activation of the interferon regulatory factor 3 master regulator. *Journal of virology* 81, 4145-4157.
31. Shechter, D., Dormann, H. L., Allis, C. D., and Hake, S. B. (2007) Extraction, purification and analysis of histones. *Nature protocols* 2, 1445-1457.

Chapter 4: GNO-seq quantifies nucleosome occupancy at gene promoters and enhancers in LPS stimulated macrophages

This chapter represents a manuscript under review in *Genome Research* (2017, manuscript ID: GENOME/2017/227504).

Authors who contributed to this study were: Michael McAndrew, Alison Gjidoda, Wolfgang Resch, Kyong-Rim Kieffer-Kwon, Rafael Casellas, and Monique Floer.

Abstract

The transcriptional response of macrophages to a variety of pathogens has been well studied, and stimulation by bacterial lipopolysaccharides (*i.e.*, LPS) serves as a paradigm for inducible gene expression in mammalian cells. We used GNO-seq (Global Nucleosome Occupancy-sequencing) an extension of conventional MNase-seq, to quantify differences in nucleosome occupancy genome-wide between resting and LPS-induced mouse macrophages. We find that the majority of LPS-induced genes are already expressed to some extent in resting macrophages, and increased expression is associated with further nucleosome depletion at their promoters but also with partial nucleosome depletion in regions upstream of promoters and in the 5' ORFs. In contrast, we show that the promoters of a small group of highly induced genes that are repressed in resting macrophages remain associated with nucleosomes under inducing conditions. This finding is in agreement with our previous findings at two cytokine genes (*i.e.*, *Il12b* and *Il1a*), and we propose that tight control of promoter access by chromatin may limit expression of this group of genes. Our analysis also reveals differences in nucleosome occupancy at different types of enhancers involved in macrophage biology (*i.e.*, constitutive, poised, latent enhancers), and we show that levels of nucleosome occupancy in resting macrophages are indicative of the response to LPS. GNO-seq therefore allows characterization of enhancers beyond histone modifications and TF binding, and we propose that incorporation of quantitative nucleosome occupancy information has the potential to facilitate identification of functional elements in other systems.

Introduction

Nucleosomes, the basic building blocks of chromatin, are generally thought to restrict access of sequence specific transcription factors (TFs) and the transcriptional machinery to DNA. Determining nucleosome binding in the genome has therefore been the focus of intense research in the field of gene regulation. Approaches commonly used in these studies take advantage of enzymes that cut nucleosome-free DNA but leave nucleosomal DNA intact, and micrococcal nuclease (MNase) from *Staphylococcus aureus* has emerged as the enzyme of choice. MNase is an endo/exonuclease that preferentially cuts linker DNA, but can also digest nucleosomal DNA when present in excess or given enough time to complete the reaction. Enzymes such as DNase I and Tn5 transposase on the other hand, are more restricted by chromatin structure, possibly due to their larger sizes and approaches such as DNase-seq and ATAC-seq that use these enzymes, therefore preferentially identify regions highly accessible to sequence-specific TFs and the transcriptional machinery (1-3). In contrast, MNase-seq - performed after limited digestion of chromatin and sometimes in conjunction with histone ChIP - reveals preferred nucleosomal positions anywhere in the genome and has been used to assemble nucleosome position maps for various organisms (4-8). Variations of the assay that utilize low enzyme concentrations or digestion performed in low salt conditions have revealed “fragile” or MNase-sensitive nucleosomes at specific genomic locations that are not observed by standard protocols (9-13). What the function of these fragile nucleosomes may be remains elusive. While MNase-seq reveals preferred nucleosomal positions in the genome, the assay in its current form provides only limited information about quantitative levels of occupancy

of any given nucleosomal position, due to the inherent sequence bias of the enzyme and of Illumina sequencing itself. In other approaches, such as ChIP-seq sequence, bias is typically overcome by normalizing the data to input chromatin and input chromatin has been taken into account in a quantitative MNase assay developed by (14). Fractional nucleosome occupancies in a population of cells are derived in this assay by curve-fitting of digestion data from a large range of MNase concentrations to two-state exponential decay functions, which largely eliminates the underlying sequence bias in MNase digestion. Studies using this approach have provided valuable insights into the role of chromatin in inducible gene expression in different organisms (15-17). However, because this assay quantifies DNA by qRT-PCR, its use has been limited to the focused analysis of specific genomic regions of interest. Two recent studies used MNase digestion with a range of concentrations followed by Illumina sequencing and linear regression to determine differences in chromatin accessibility (11,18). However, because undigested input chromatin was not analyzed, effects of the underlying DNA sequence on MNase digestion could not be separated from differences in nucleosome occupancy in a population of cells. Furthermore, linear regression to fit data that follows exponential digestion curves - as shown by Bryant et al. (14) - is likely to introduce considerable artifacts. Most importantly, because MNase-data from different samples (*i.e.*, different growth conditions) was not normalized to an external reference, any broader changes in nucleosome occupancy that may pertain to larger parts of the genome could not be detected.

LPS induction of macrophages has become a paradigm for inducible gene expression in mammalian cells and previous studies have identified the genes whose expression

changes in response to LPS as well as the putative transcriptional elements involved in their regulation (19-25). LPS induction relies on two classes of transcription factors *i.e.*, the macrophage lineage determining TFs PU.1 and C/EBP β , and the signal-induced TFs NF κ B, AP-1 and IRF. PU.1 and C/EBP β are already bound to enhancers of many inducible genes in resting macrophages and have been shown to play a role in enhancer priming for later induction (17,20,21,26,27). We recently showed that PU.1 recruits the remodeler BAF/PBAF to the enhancers of two example pro-inflammatory genes during macrophage differentiation, which keeps these enhancers accessible and occupied only by intermediate levels of nucleosomes in mature macrophages and facilitates complete nucleosome eviction in response to LPS (28). In the absence of the remodeler the enhancers become associated with highly occupied nucleosomes, and their response to LPS is impaired.

Here we have analyzed the changes in nucleosome occupancy at LPS-responsive genes genome-wide, using a novel method that combines the crucial aspects of the assay of Bryant et al. (14) with Illumina sequencing to determine fractional nucleosome occupancies anywhere in the genome. Significantly, we sequence pooled DNA isolated from chromatin digested with a range of enzyme concentrations, to capture nucleosomal DNA at most genomic regions, and we sequence DNA isolated from input chromatin, which we use for normalization. We have termed the assay GNO-seq for Global Nucleosome Occupancy sequencing and use the approach to measure quantitative changes in nucleosome occupancy upon LPS-induction of bone marrow derived mouse macrophages (BMDMs). While previous studies have compared chromatin in different cell-types, the immediate changes in nucleosome occupancy

upon gene induction at transcriptional regulatory regions genome-wide are less well understood in mammalian systems. Our study identified distinctive changes in nucleosome occupancy at promoters and transcriptional enhancers, and also detected broader genome-wide changes associated with macrophage activation. Our results further indicate that the levels of nucleosome occupancy at transcriptional regulatory regions are indicative of their response to an inducing stimulus. These findings highlight the importance of obtaining quantitative information on nucleosome occupancy when examining functional elements. We propose that GNO-seq has the potential to help identify regulatory elements in other cell-types and systems, and to distinguish functional elements from regions that lack regulatory activity but are nonetheless associated with histone modifications and TF-binding.

Experimental Procedures

Cell isolation and sample preparation

Bone marrow cells were isolated from 6-8 week old female C57BL/6 mice (NCI, Charles River) under Institutional Animal Care and Use Committee oversight and bone marrow derived macrophages (BMDMs) were generated by growth in the presence of M-CSF as described (17). Cells were either grown in the absence or presence of LPS for 1.5 h (*i.e.*, rM and aM for resting and activated macrophages, respectively). Formaldehyde cross-linked chromatin from 1.5×10^7 uninduced or induced cells was split into 24 samples, 2 samples remained undigested and 22 samples were digested with 0.0027-13.3 U of MNase (NEB), respectively. Digestion was analyzed by qRT-PCR and curve-fitting at different locations in the genome as described (17) and primers can be given upon request. For the Input-fractions DNA isolated from the two undigested control

samples and a sample digested with the lowest concentration of MNase (*i.e.*, 00027 U) were pooled. For the MNase-fractions DNA isolated from samples digested with 0.014, 0.020, and 0.030 U MNase respectively were pooled. DNA was isolated using a Qiaquick 96 well DNA purification kit (Qiagen). DNA in the Input-fractions was sonicated using a Covaris sonicator to yield fragments between 130-200 bp. Lambda DNA (Promega) was sonicated using the same conditions and 0.055 µg sonicated lambda DNA was added as a spike-in control to each Input and MNase-fraction so that the amount of lambda DNA as a fraction of total DNA was between 1-4% per sample.

Illumina library preparation and sequencing

DNA isolated from Input and MNase-fractions was blunt-ended with End-It DNA end repair kit (Epicenter) and polyadenylated with Taq DNA polymerase (Invitrogen) in the presence of 200 µM dATP for 40 min at 70°C. Samples were purified by column (DNA clean & concentrator kits, Zymo Research) after each reaction. Illumina compatible adaptors (Bio Scientific) were then ligated using T4 DNA ligase (Enzymatics), and the reaction was purified once with AMPure XP magnetic beads (Beckman Coulter).

Samples were PCR amplified for 4 cycles with KAPA HiFi DNA polymerase mix (KAPA Biosystems) and purified by column. Paired-end sequencing data (*i.e.*, 50 cycles) was acquired on HiSeq 2000 and 2500 sequencers (Illumina). See Suppl. Fig. 4.S2 for insert lengths and read numbers in each sample.

Data processing

Raw FASTA files of paired-end Illumina sequencing reads for either the Input or MNase-fractions of rM and aM were trimmed using Trimmomatic 0.33 (default settings for Truseq3-PE adapters except LEADING = 20, TRAILING = 20, SLIDING WINDOW =

4:30)(29) and mapped to either the *Mus musculus* genome (UCSC mm9) or the *Enterobacteria phage lambda* genome (GenBank: J02459.1) using Bowtie2 2.2.6 (--phred33 --local --sensitive- local -l 0 -X 1000 --no-discordant --no-mixed --fr --no-unal)(30). Merged BAM files containing all reads with MAPQ ≥ 30 for the MNase or Input-fractions from rM and aM respectively, were generated using SAMtools 0.1.19 (31).

Generation of lambda normalized GNO-seq tracks

To obtain GNO-seq tracks for rM and aM (*i.e.*, rMratio_GNOseq and aMratio_GNOseq), we normalized the number of Input and MNase-seq reads to the number of lambda DNA reads per Million in each fraction as described for external reference normalization (32)(see also *Suppl. Experimental Procedures*) and then derived the ratio of reference-normalized MNase over Input RPM. Scaling factors for rM Input and rM MNase-fractions are 2.353 and 1.200, and for aM Input and rM MNase-fractions 2.575 and 0.798, respectively. GNO-seq bigwig files were then generated using deepTools bamCompare (-b1 = MNase, -b2 = input, --ratio = ratio, bin size -bs = 1, --scaleFactors)(33). To distinguish regions without nucleosome occupancy from regions that are undersampled and lack reads in the Input-seq data, pseudocount was set to 0, so that a value of zero was assigned to regions without occupancy and a value of “Infinity” to regions lacking coverage in the Input-data. bwtool was used to remove regions lacking reads in the Input (equal “Infinity”)(34). These are the files used for all subsequent analyses. GNO-seq tracks at individual genomic locations are displayed using IGV (35).

Random genomic sampling

To obtain random genomic regions we first generated a total of 100,000 regions of 6 kb using bedTools random from GNO-seq bigwig files for rM and aM (-l 6000, -n 100,00). These regions were shuffled into regions with sufficient GNO-seq data coverage and excluded from regions with no coverage using bedTools shuffle (-incl covered, -excl not covered). Bigwig files containing occupancy data for only these regions were produced using bwtool remove (mask random -inverse), and the resulting bigwig files were converted to bed format as described and merged using bedtools merge (-d 0, -c 5, -o mean, min, max) to produce 60,749 continuous genomic regions. The resulting regions were used for determination of average nucleosome occupancy and GC content.

GC content

To determine the GC content in regions without Illumina-sequencing coverage and alternatively, in regions without nucleosome occupancy, we first identified such regions in the genome. We generated bigwig coverage tracks from merged BAM files of Input and MNase-fractions from rM and aM using deepTools bamCoverage (bin size -bs = 1, -scaleFactor = 1). These files were converted from bigwig to wig format using UCSC tools bigWigToWig (36), then converted from wig to bed format using BEDOPS convert2bed (--zero-indexed)(37). To generate regions without nucleosome occupancy we used bedtools intersect (-v -a Input -b MNase)(38) to generate bed files containing regions sequenced in the Input, but not in the MNase-fractions (*i.e.*, regions without nucleosome occupancy). To generate regions without Illumina-sequencing coverage we generated intervals that were not present in the Input or MNase-fraction bed files using bedtools complement (-g mm9). We then generated bed files containing regions not

sequenced in either fraction using bedtools intersect (-u -a Input -b MNase)(*i.e.*, regions without Illumina-sequencing coverage). We used bedtools nuc (-fi mm9) to determine the GC content of each region, and the boxplot function in R to calculate the median GC content and create boxplots. We also calculated the average GC content normalized to the size of each category by dividing the number of GC base pairs by the total number of base pairs in each category. GC content was calculated similarly in the random regions generated as described above.

Heatmaps and average nucleosome occupancy plots

To sort genes by levels of expression in aM we used RNA-seq data of uninduced and induced (*i.e.*, 2 h LPS) BMDMs from Mancino et al. (22). We first assigned Refseq IDs and coordinates to genes in this dataset using BioMart (39). To exclude TSSs with less than 90% coverage in the region 3 kb upstream and downstream of the TSSs, bedtools intersect was used to determine sequence coverage of the Input-fraction in these regions (-wo -a TSS +/- 3 kb -b Input). Regions with less than 90% coverage were filtered out using a custom python script available upon request. This resulted in a total of 23,265 unique TSSs, which were used for subsequent analyses. TSSs were separated into groups based on the quartiles of FPKM expression values of the associated genes in the presence of LPS. Genes were aligned at their TSSs and heatmaps and average nucleosome occupancy plots in regions 3 kb upstream and downstream were generated for each quartile using deepTools computeMatrix (--referencePoint = TSS, bin size -bs = 1) and deepTools plotHeatmap (--missingDataColor = yellow, --sortUsingSamples 2 (aM), --colorList red, white, blue, grey, black)(33). Genes in the most highly expressed quartile were further separated

into four clusters based on nucleosome occupancy in aM across the entire region using k-means clustering in deepTools plotHeatmap (settings as above, with --kmeans = 4). To determine nucleosome occupancy around TSSs of genes that are lowly or not expressed in rM but induced by LPS in aM we excluded genes expressed in rM (*i.e.*, FPKM > 1) from the 23,265 Refseq genes and sorted the remaining genes into groups A-D according to levels of expression in rM and aM. Genes in each group were aligned at the TSS, and heatmaps and average plots of nucleosome occupancy were generated as described.

To analyze nucleosome occupancy at enhancers we used the 69,559 macrophage enhancers identified by Ostuni et al. (23). We adhered to the enhancer classification suggested by these authors, but further split the “not steady” category into “not steady-activated” and “not steady-repressed” enhancers based on increases and decreases in the levels of H3K27ac ChIP-seq signals, respectively, in cells grown for 4 h and/or 24 h in the presence of LPS (23)(Table 4.1). For alignment at the site of PU.1 binding we first used bedTools intersect to identify ChIP-seq peaks of PU.1-binding within enhancers in cells treated for 4 h with LPS (23). Subsequently, we aligned enhancers containing a PU.1-peak at the midpoint of each PU.1-peak and generated heatmaps and average plots of nucleosome occupancy in rM and aM in regions 3 kb upstream and downstream as described. For alignment of enhancers at their sites of p300 recruitment we first used bedTools intersect to find overlap between previously identified p300 ChIP-seq peaks in cells treated for 2 h with LPS (20) and putative enhancers of Ostuni et al. We subsequently aligned enhancers containing p300-peaks at the midpoint of the p300-

peaks, and generated heatmaps and average plots of nucleosome occupancy in rM and aM in the surrounding regions.

Identification of nucleosome depleted regions

To identify depleted regions in rM and aM, we first removed regions with occupancy values higher than a threshold (*i.e.*, 70%, 75%, and 80% for rM; 20%, 25%, and 30% for aM) from GNO-seq data using `bwtool remove` (34). The resulting bigwig files contained only regions with nucleosome occupancy below the set threshold and were converted to wig using UCSC tools `bigWigToWig` (36), and then to bed format using `BEDOPS convert2bed (--zero-indexed)`(37). To produce regions of a defined length and allowing for gaps in the occupancy defined by the threshold the files were first merged using `bedTools merge (-d [gap size])`(38) and then filtered by size. The lengths of gaps in occupancy we allowed and the lengths of the depleted regions can be found in Suppl. Table 4.S1. To determine the fraction of the regions of interest (*i.e.*, enhancers, promoters, super- enhancers etc.) that encompass a (partially) depleted region we used `bedTools intersect` (default settings using `-u` to return regions of interest in the `-a` file overlapping regions in the `-b` file). Scatterplots and bargraphs were generated in Microsoft Excel.

Gene ontology analysis

Gene ontology analysis was performed using the Gene Ontology Consortium web browser using the GO Ontology database release 2017-06-29 (40).

***De novo* motif search**

De novo motif search in poised-activated and poised-not activated enhancers was performed using HOMER 4.7.2 `findMotifsGenome.pl` (21) with GC-content matched

genomic regions as the control sequence set (default settings with genome = mm9, size = given, -mask). Motif logos were generated using HOMER 4.7.2 motif2Logo.pl.

Nucleosome occupancy at super-enhancers

To determine nucleosome occupancy at SEs in macrophages and other cell-types we used the super-enhancers identified by (41). We aligned GNO-seq data from rM and aM at the midpoint of each superenhancer specific to ESC, BMDM, Myotubes, Pro-B and T helper cells using deepTools computeMatrix (--referencePoint = center, bin size -bs = 1). Flanking sequence was added according to the average size of SEs from different cell-types and heatmaps and average nucleosome occupancy plots were generated as described.

Results

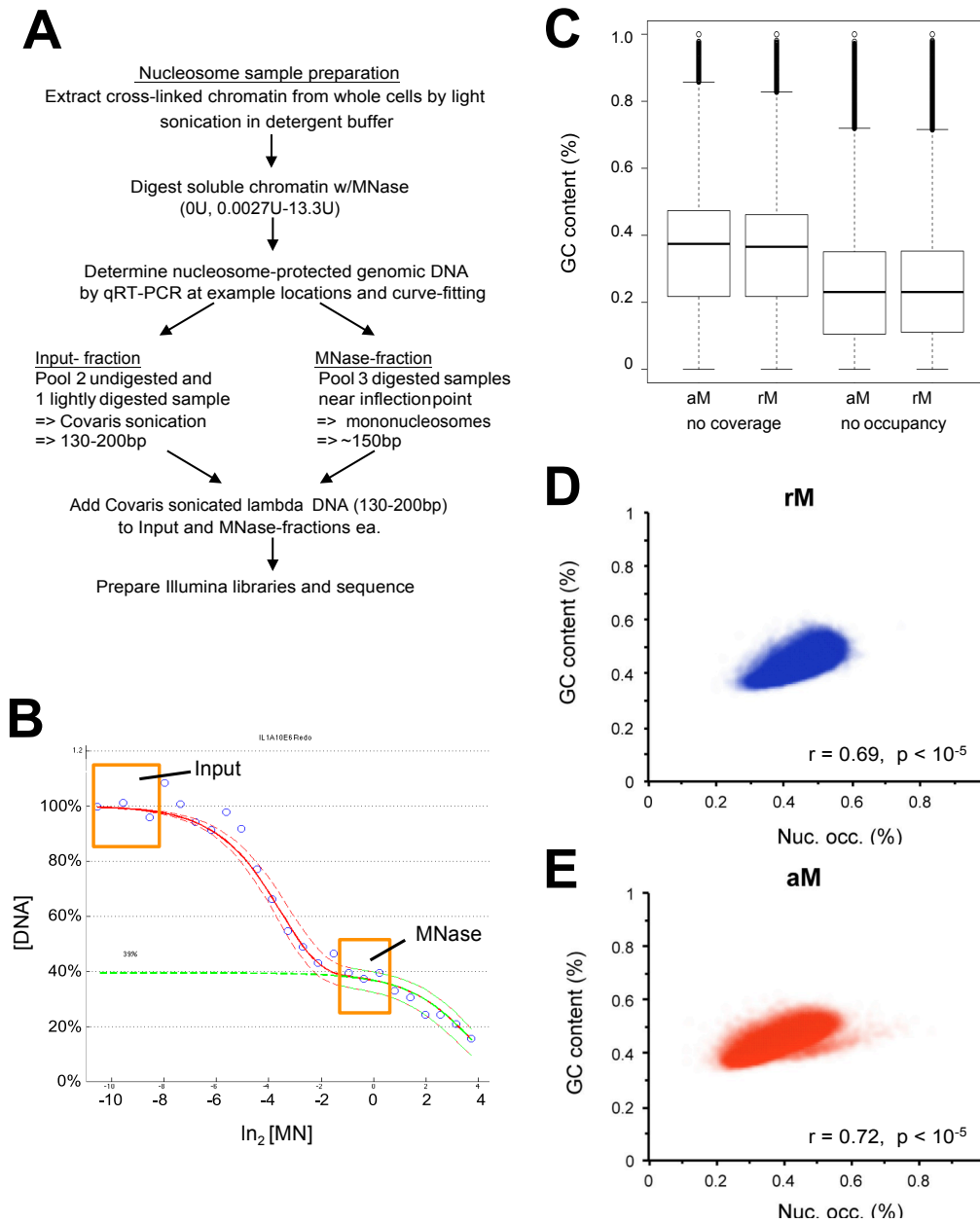
GNO-seq analysis

In GNO-seq we digest cross-linked chromatin with 24 different enzyme concentrations (spanning nearly four orders of magnitude *i.e.*, 0.0027-13.3 U) and then fit the digestion data obtained by qRT-PCR at representative genomic regions to two-state exponential curves to determine the range of enzyme concentrations that captures most nucleosomal fragments in the genome as previously described (Fig. 4.1A)(14, 17).

While sequencing DNA isolated from digestion with the entire range of enzyme concentrations followed by curve-fitting would ideally yield the most accurate quantitative information, such an approach is prohibitive because of the cost of sequencing 24 different samples at sufficient coverage of the mouse genome. Instead, we found in initial MNase digestion experiments using qRT-PCR that pooling DNA from digestion with a limited range of enzyme concentrations, representing the “lip” of the

digestion curves (*i.e.*, MNase-fraction in Fig. 4.1B), largely eliminated the sequence bias of the enzyme and preserved nucleosomal-sized DNA fragments at most sites in the genome (Suppl. Fig. 4.S1). In GNO-seq we therefore pooled three MNase-digested samples, which we sequence as the MNase-fraction. To account for any sequence bias of Illumina-sequencing itself and any bias introduced by our chromatin extraction procedure, we also pooled undigested and lightly digested chromatin as the Input-fraction and sheared the isolated DNA by Covaris sonication to fragment sizes similar to those in the MNase-fraction before Illumina sequencing (*i.e.*, the majority of fragments are 130-200 bp in length, see Suppl. Fig. 4.S2). Furthermore, we spiked in Covaris sonicated lambda DNA into MNase and Input- fractions before Illumina-library preparation, which we used for external reference normalization of sequencing reads obtained from different fractions and growth conditions as previously described (43,44). Specifically, we obtained reference- normalized reads per Million (RPM) from MNase and Input-fractions by multiplying the number of aligned mouse reads with a normalization factor as described (32)(see *Experimental Procedures*), and then calculated the fractional nucleosome occupancy (*i.e.*, the % nucleosome occupancy) as the ratio of MNase over Input reference-normalized RPM. Initial proof-of-principle experiments using qRT-PCR measurements at many different genomic locations showed that occupancies derived as the ratio of MNase over Input correlated well with occupancies obtained by curve-fitting ($R^2=0.90$, Suppl. Fig. 4.S1), indicating that this approach might allow determination of nucleosome occupancies anywhere in the genome at single nucleotide resolution.

Figure 4.1. GNO-seq analysis.



(A) Flowchart illustrating the workflow for GNO-seq sample preparation, Illumina library preparation and sequencing.

Figure 4.1. (cont'd)

(B) Curve-fitting of MNase-digestion data measured by qRT-PCR at a location in the *Il12b* enhancer. Orange boxes indicate the samples pooled for the Input and MNase-fractions, respectively.

(C) GC content in regions without Illumina sequencing coverage and in regions without nucleosome occupancy determined in rM and aM as described in *Experimental Procedures*.

(D) and **(E)** Relationship between GC content and nucleosome occupancy in rM and aM, respectively. Density plots show the GC content of ~60,000 randomly chosen regions of about 6 kb as a function of the average occupancy in these regions. Note that average occupancies include linker DNA and are distinct from occupancies at preferred nucleosomal positions in these regions. Pearson's correlation coefficients and p-values are indicated in the figures.

GNO-seq validation

Our initial survey of GNO-seq data obtained from resting (rM) and activated macrophages (aM), grown for 1.5 h in the presence of LPS, indicated that levels of nucleosome occupancy at regulatory regions of three pro-inflammatory genes (*i.e.*, *Il12b*, *Il1a* and *Ifnb1*) were comparable to our previous results using the qRT-PCR based approach (Suppl. Fig. 4.S3)(17). For example, GNO-seq detected complete nucleosome eviction upon LPS induction at the distal enhancers of *Il12b*, *Il1a* and *Ifnb1*, which were occupied by intermediate levels of nucleosomes before induction in rM. GNO-seq also showed that the promoters of *Il12b* and *Il1a* remained associated with nucleosomes under inducing conditions, while nucleosomes at the promoter of *Ifnb1*

were evicted. Together our data show that GNO-seq faithfully detects changes in nucleosome occupancy associated with LPS induction at representative genomic locations.

To further validate the approach and to compare it to standard MNase-seq protocols that use only one concentration of MNase without input normalization, we also analyzed the MNase-seq fraction of our data alone without considering the input using published methods. We used either the MNase option in deepTools bamCoverage or DANPOS according to published protocols (33,42). Both programs include a dyad alignment step, which centers reads on the nucleosome dyad based on the assumption that certain nucleosome positions are preferred in a population of cells, and DANPOS further adjusts read lengths while the MNase option of bamCoverage only considers reads between 130 and 200 bp. We found that either approach detected loss of nucleosomes at the *I12b* and *I1a* enhancers upon LPS induction, as well as retention of nucleosomes at the *I12b* promoter (Suppl. Fig. 4.S4). However, levels of nucleosome occupancy measured by the qRT-PCR based assay were best reproduced using GNO-seq. We note that inclusion of Input-data in GNO-seq precluded dyad alignment, since it cannot be performed *after* taking the ratio of MNase over Input-data. Furthermore, we found that dyad alignment of both Input-data and MNase-data *before* taking the ratio greatly distorted the resulting nucleosome occupancies (Floer, M and McAndrew, M.J., unpublished results). Nevertheless, we noted that dyad alignment of MNase-data generally overemphasizes occupancy at preferred nucleosomal positions. We therefore find that nucleosome occupancies are best quantified by Input-normalization in GNO-seq without dyad alignment. In addition, we found that Input-normalization in GNO-seq

reduced apparent differences in occupancies seen broadly in MNase-seq data between different regions of the genome that are likely an artifact of chromatin extraction and Illumina sequencing bias (Suppl. Fig. 4.S5). Nevertheless, a small decrease in nucleosome occupancy associated with macrophage activation in large parts of the genome, could be detected by GNO-seq as well as MNase-seq analysis (Suppl. Fig. 4.S5). This result is consistent with previous findings of a general loss of nucleosomes upon LPS induction of macrophages derived from fetal liver- derived monocytes (45), but what the significance of this general loss of nucleosome occupancy might be remains to be determined. We recently found that LPS activation of B-cells resulted in a similar wide-spread loss in nucleosome occupancy, and we showed that this was accompanied by a general decondensation of chromatin (Kieffer-Kwon et al, manuscript accepted). Whether macrophage activation is also associated with chromatin decondensation remains to be determined.

Normalization to the input in GNO-seq also allows us to distinguish regions that are nucleosome-free from regions that are simply under-sampled and therefore lack reads also in the Input-fraction. The ability to unequivocally identify sites of nucleosome depletion is an important advance of GNO-seq over conventional MNase-seq, since transcriptional regulatory activity is usually associated with nucleosome eviction and researchers therefore often focus exclusively on nucleosome-free sites. Because previous MNase-seq analyses lack input normalization we hypothesize that many studies may erroneously have categorized some genomic regions as nucleosome-free that simply lack any sequence coverage. To determine if under-sequenced regions (*i.e.*, no reads in MNase and Input-fractions) generally have a different sequence

composition than other regions in the genome, we determined their GC content. We found that the median GC content in such regions was around 37% and average occupancy after adjustment to the total number of base pairs was around 40%, which is similar to the overall GC content of the mouse genome (*i.e.*, 42% (46))(Fig. 4.1C). This indicates that undersampling of regions in Illumina sequencing is unlikely a direct result of the underlying DNA sequence. We sequenced each sample to 300-400 million paired-end reads (see Suppl. Fig. 4.S2B), and while we found that higher levels of sequence coverage performed for samples in a parallel study using B-cells (~1,000 million paired-end reads (Kieffer-Kwon et al, manuscript accepted) allowed inclusion of a small fraction of additional genomic locations, it did not significantly alter the fractional occupancies measured and we conclude that insufficient sequencing depth is not the reason for missing data in our current study.

In contrast, we found that the GC content in regions that lack nucleosomes in rM or aM (*i.e.*, no reads in MNase, but reads in Input-fractions) was low, around 23% (Fig. 4.1C) or 28% after adjustment for the total number of base pairs. This result suggests that low nucleosome occupancy in mouse macrophages is related to low GC content, consistent with previous results from yeast and other organisms that showed a preference of nucleosome formation at GC-rich sequences (7,47-51). To determine overall correlation between nucleosome occupancy and GC content we analyzed ~60,000 random genomic regions of around 6 kb. We plotted average GC content versus average nucleosome occupancy over each region and found a strong correlation with Pearson coefficients of $r = 0.69$ ($p < 10^{-5}$) for rM and $r = 0.72$ ($p < 10^{-5}$) for aM, respectively (Fig. 4.1D and E).

Nucleosome occupancy surrounding transcriptional start sites

Earlier studies of chromatin changes associated with gene induction in yeast and also in mammalian cells had suggested that nucleosomes may generally occlude promoters of silent genes and have to be removed to allow gene expression (52-54). However, our previous studies at three example genes in macrophages had indicated that some promoters remain associated with nucleosomes even under inducing conditions (17,28). To determine changes at promoters genome-wide upon LPS induction of macrophages we analyzed nucleosome occupancy around the TSSs of 23,265 mouse Refseq genes, for which published gene expression data was available in BMDMs and for which we had sufficient GNO-seq coverage (*i.e.*, >90% coverage in the Input-sequence data) in a 6 kb window including 3 kb upstream and downstream of the TSS. We separated the genes into four groups (*i.e.*, quartiles Q1-4,) with Q1 containing the genes most lowly expressed in aM, as inferred from mRNA levels 2 h after LPS addition (data taken from (22)). We aligned the genes in each quartile by their TSSs and generated average nucleosome occupancy plots and heatmaps of nucleosome occupancy in surrounding regions (Fig. 4.2A and B). Genes within each quartile were sorted by levels of nucleosome occupancy in aM over the whole region in the heatmaps (*i.e.*, low to high from bottom to top). The average occupancy plots and heatmaps show that the promoter nucleosome position just upstream of the TSS was depleted at most of the highly expressed genes (*i.e.*, genes in Q3 and Q4). The nucleosome-depleted region usually corresponded to the size of a single nucleosome and was flanked downstream by a well-positioned +1 nucleosome in the ORF. Such nucleosome arrangements have previously been described at the promoters of genes actively transcribed in yeast and

higher organisms (6,8,10,16,55-57). We did not detect extensive phasing of additional nucleosomes beyond the +1 position, presumably because of our omission of the dyad alignment step as discussed above. We believe that in the absence of dyad alignment nucleosome positions including that of the +1 nucleosome are less emphasized. This is consistent with our finding that peak occupancies at the +1 position were only around 50% when we averaged many different genes (Fig. 4.2A), while +1 occupancies at individual genes reached up to 100% (e.g. Fig. 4.2E).

Significantly, we found that most promoters of the genes highly expressed in aM (in Q3 and Q4 in Fig. 4.2B) were already significantly depleted in rM and often became completely nucleosome-free in aM. This result is consistent with our finding that most of these genes were already expressed at some basal level in rM as shown by our analysis of the gene expression data of Mancino et al. (22). Analysis of genes in Q1-4 showed that most of the genes significantly expressed in response to LPS – setting an arbitrary threshold for significant expression to FPKM > 1 – were already significantly transcribed in rM (Fig. 4.2I Q3 and Q4, see also Suppl. Table S1). Furthermore, we found that the majority of genes that were expressed to a lesser extent in aM – setting the threshold to FPKM > 0 – were nevertheless already transcribed at a low level in rM (Fig. 4.2J, Q2, Q3 and Q4). In contrast, we found that the majority of genes in Q1 and Q2 showed very little nucleosome depletion as expected from the low levels of expression of these genes in rM and aM.

Figure 4.2. Nucleosome occupancy at promoters.

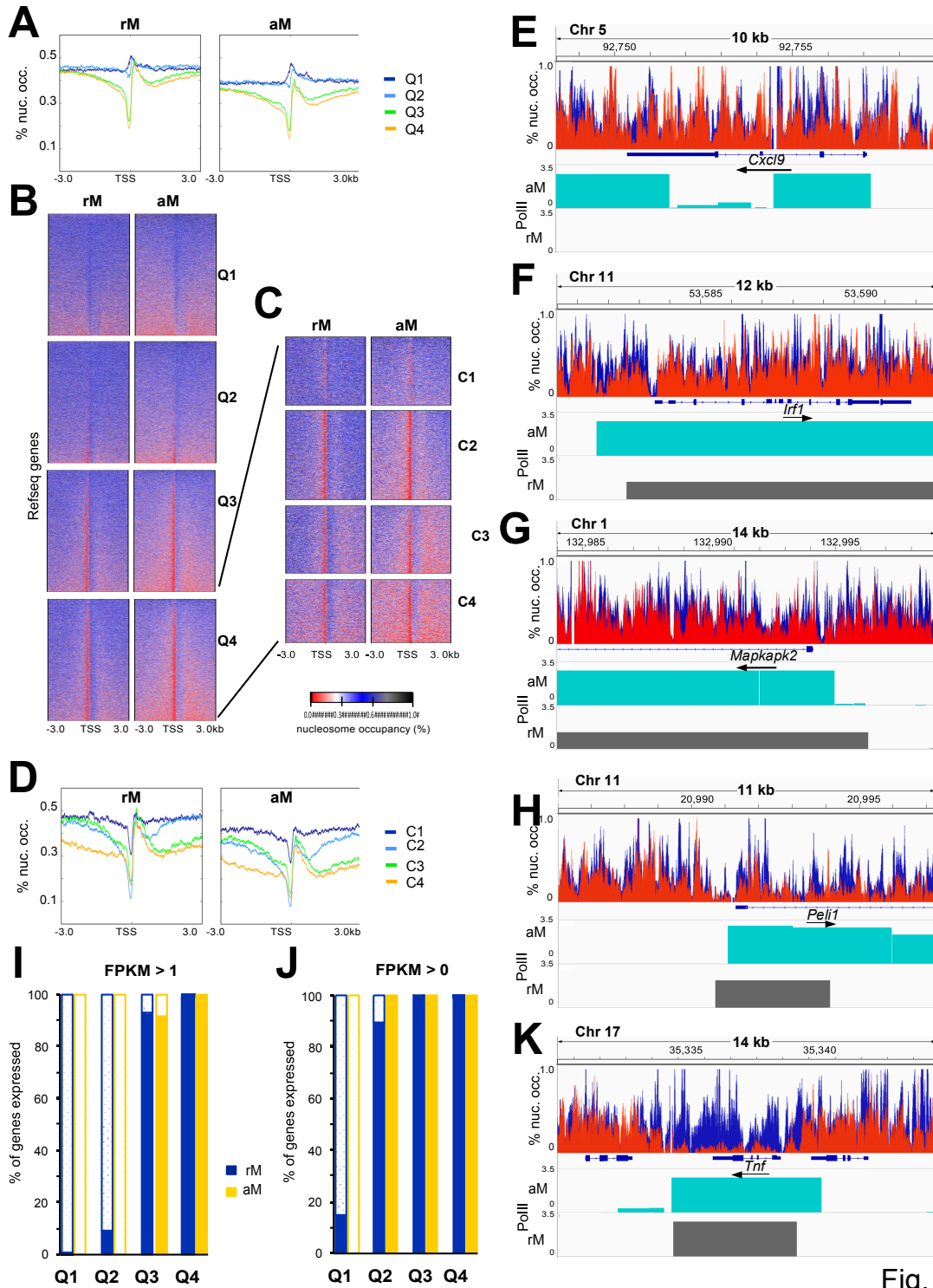


Fig. 2

Nucleosome occupancy was analyzed by GNO-seq in regions 3 kb upstream and downstream of TSSs after aligning 23,265 Refseq genes at their TSSs.

Figure 4.2. (cont'd)

(A) and (B) Genes were separated into quartiles (Q1-4) by gene expression levels in aM (*i.e.*, FPKM at 2 h LPS; taken from (22)) with Q4 containing the most highly expressed genes. Average nucleosome occupancy plots and heatmaps are shown. Within each quartile genes were sorted by levels of nucleosome occupancy in aM over the whole region (*i.e.*, low to high from bottom to top).

(C) and (D) Genes in Q4 were further separated into four clusters (C1-4) by k-means analysis, and heatmaps and average plots of nucleosome occupancy in each cluster are shown.

(E-H) Nucleosome occupancy in rM (blue) and aM (red) at representative genes taken from C1-4, respectively. Pol II ChIP-seq peaks from (23) in resting (grey) and activated (cyan) macrophages 4 h after LPS induction are shown underneath each panel.

(I) and (J) Gene expression data from (22) is shown for Refseq genes in each quartile of (A). Gene expression in rM is shown in blue and in aM in yellow. Solid bars indicate expression using a cut-off of FPKM > 1 (I) or FPKM > 0 (J) in each quartile, and hatched bars indicate genes whose expression falls below this value.

(K) Nucleosome depletion in aM over the whole *Tnf* gene locus is shown as in Fig. 5.2E-H.

Strikingly, we found that in addition to further nucleosome eviction at promoters upon LPS induction, nucleosomes were also partially lost from the 5' ORFs and from regions upstream of promoters of many highly expressed genes (*i.e.*, Q3 and Q4 Fig. 4.2A and B). To further dissect the changes in nucleosome occupancy at the most highly expressed genes we separated genes in Q4 into four clusters using k-means clustering

(Fig. 4.2C and D). Genes in clusters C1-4 showed varying levels of additional depletion upstream and/or downstream of the completely depleted promoter nucleosome and examples of genes from each cluster (*i.e.*, C1-4, respectively) are shown in Figs. 4.2E-H. We found that genes in C1 showed only modest depletion in regions other than their promoters, and a minority of these genes even retained significant levels of promoter nucleosomes when highly expressed (*e.g.*, *Cxcl9*, Fig. 4.2E). This finding is reminiscent of our previous results at the promoters of *Il12b* and *Il1a*, where nucleosomes were present even under inducing conditions (17). In contrast, we found that genes in cluster C2 were mostly associated with additional, partial depletion upstream of the promoter (*e.g.*, *IRF1* in Fig. 4.2F), while genes in cluster C3 were partially depleted in the 5'ORF and also upstream (*e.g.*, *Mapkapk2* in Fig. 4.2G). Genes in cluster C4 were most significantly depleted both upstream and downstream of the promoter (*e.g.*, *Peli1* Fig. 4.2H). However, depletion in these regions was incomplete and fractional nucleosome occupancies remained higher than at the promoters. In contrast, we identified a small group of genes that showed almost complete loss of nucleosomes over a broad region encompassing the whole gene locus (*e.g.*, *Tnf* Fig. 4.2K). Other genes in this group include *Ccl2*, *Ccl3*, *Ccl4* and *Ccl7*. This result is reminiscent of findings at heat shock genes in *Drosophila* and yeast, where nucleosomes are broadly lost from the gene locus (58-59) but such dramatic loss of nucleosomes has not been described for other classes of highly expressed genes. Nevertheless, our data show that complete nucleosome loss is not a prerequisite for high levels of gene expression, since genes in clusters C1-4 showed a similar range of expression in response to LPS (see Suppl. Fig. 4.S6). For the example genes in Fig. 4.2E-H the levels of Pol II binding in the absence

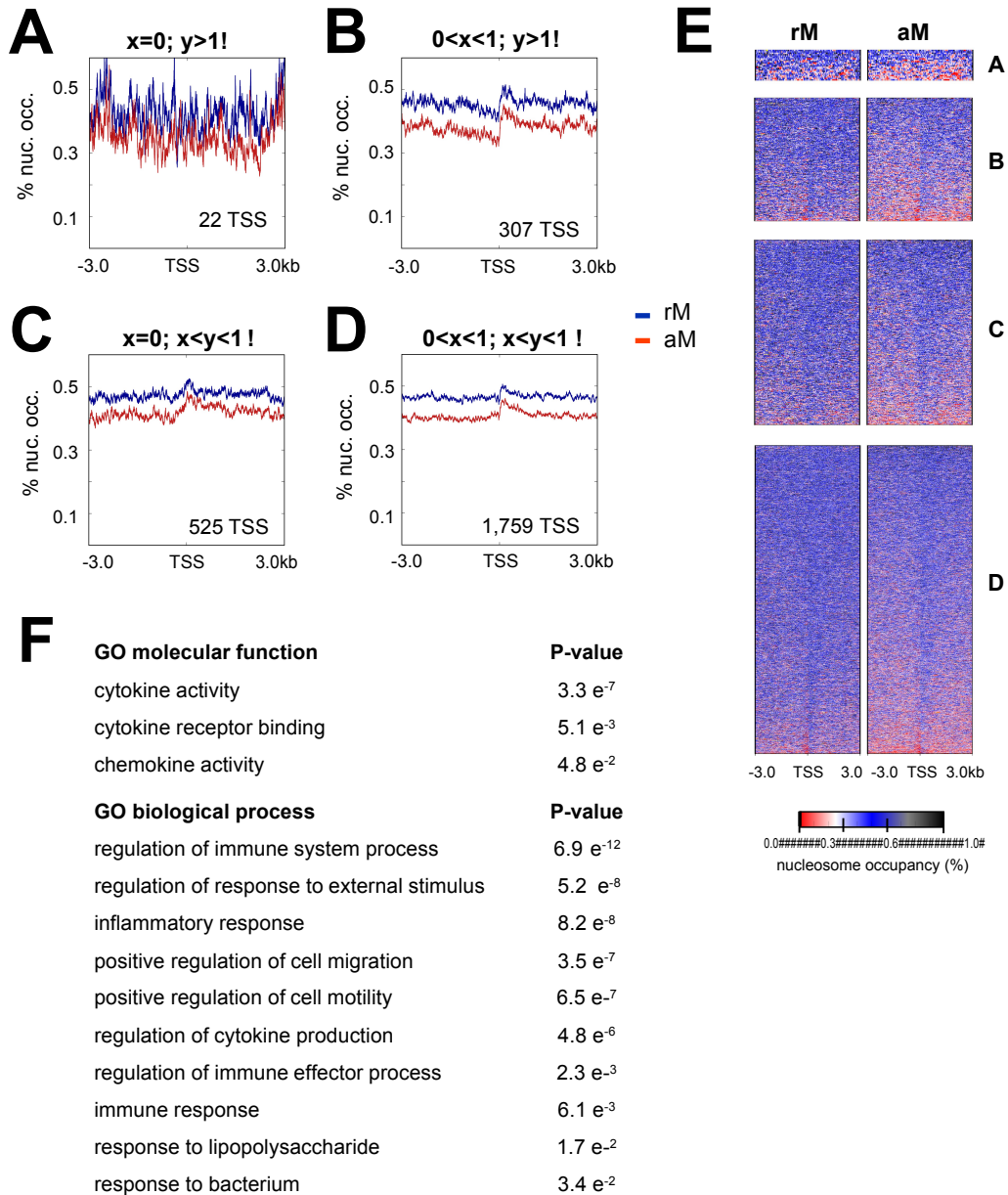
and presence of LPS (*i.e.*, Pol II ChIP-seq peaks before and 4 h after LPS-induction taken from (23)) are indicated underneath each panel in grey and cyan, respectively. Together our data indicate that high levels of gene expression are associated with nucleosome depletion at most promoters and unexpectedly, that increased expression in response to LPS often leads to additional partial nucleosome depletion of regions surrounding promoters and extending into ORFs.

Promoter nucleosomes at highly induced genes

Our finding that a number of highly induced genes (*e.g.*, *Cxcl9*, *Il12b*, *Il1a*) retained nucleosomes at their promoters under inducing conditions prompted us to investigate highly induced genes further. Previous studies in macrophages classified LPS-induced genes based solely on the fold induction of expression, but did not distinguish genes with different absolute levels of expression in the presence of LPS, nor did these studies distinguish genes with significant basal expression from those truly repressed in resting macrophages (19,22,25). To determine whether promoter nucleosome retention was a feature of many genes highly induced in response to LPS, we defined conditions for LPS-induction: We excluded genes that were already significantly expressed in rM (FPKM > 1 from (22)) and then further separated these genes into four groups (Fig. 4.3). Group A contained genes repressed in rM ($x=0$) and expressed significantly in aM ($y>1$). Group B contained genes with some low level of expression in rM ($0<x<1$) and expressed significantly in aM ($y>1$). Groups C and D contained genes repressed or lowly expressed in rM respectively, but only lowly expressed in aM ($x<y<1$). Surprisingly we found that only a minority of genes in Groups A-D showed clear depletion of the promoter nucleosome position directly upstream of the TSS. Group A contained only a

handful of genes and a large fraction of these genes encode small RNAs (*i.e.*, microRNAs or snoRNAs).

Figure 4.3. Nucleosome occupancy at promoters of LPS-induced genes.



Nucleosome occupancy was analyzed in rM (blue) and aM (red) in regions surrounding TSSs of Refseq genes from Fig. 4.2 that are not significantly expressed in rM but show

Figure 4.3. (cont'd)

LPS-induced expression in aM. FPKM from gene expression data of (22) in rM is indicated by x, and FPKM in aM by y.

(A) Alignment at the TSSs of genes not expressed in rM and highly expressed in aM representing Group A.

(B) Alignment at the TSSs of genes lowly expressed in rM and highly expressed in aM representing Group B.

(C) Alignment at the TSSs of genes not expressed in rM and lowly expressed in aM representing Group C.

(D) Alignment at the TSSs of genes lowly expressed in rM and lowly expressed in aM representing Group D.

(E) Heatmaps of nucleosome occupancy around TSSs of genes of Groups A-D.

(F) GO analysis using the Gene Ontology web browser (40) of 179 genes in Group B that retain promoter nucleosomes in aM.

While it is tempting to speculate that these small RNAs may play a role in LPS induction, we found that many of the small RNAs overlapped with the ORFs of other genes expressed in the presence of LPS, and we can therefore not exclude the possibility that the FPKM signals recorded for these genes are generated by transcription of the overlapping genes and not by transcription of the small RNAs themselves. It remains to be seen whether these small RNAs are indeed upregulated in response to LPS and what their function might be. In contrast, we found that Group B contains 307 genes induced by LPS and we identified 179 genes in this group that retained nucleosomes at their promoters under inducing conditions (*i.e.*, average

occupancy above 20% in the 200 bp upstream of the TSSs). This group includes many genes previously classified as induced by LPS and a gene ontology analysis using the GO Consortium web browser (40) revealed that genes in this group were overrepresented for cytokine activity and production, and immune and inflammatory responses among other molecular functions and biological processes (Fig. 4.3F). This result extends our previous findings at *I12b* and *I1a* to a larger group of genes that are associated with promoter nucleosomes under inducing conditions (17). Groups C and D contained genes that were upregulated in response to LPS ($x < y < 1$), but their overall levels of expression in aM remained low. Together our results show that while the majority of highly expressed genes in LPS-induced cells (*i.e.*, in Q3 and Q4) are depleted at their promoters and often also in surrounding regions, these genes are usually already significantly expressed in rM. In contrast, we find that another group of genes, repressed or only lowly expressed in rM but significantly expressed in response to LPS, retain promoter nucleosomes even under inducing conditions. What distinguishes this group of genes from other induced genes and leads to the high levels of nucleosome occupancy at their promoters remains to be determined.

LPS-induced changes in nucleosome occupancy at enhancers

Previous studies have identified the putative enhancer repertoire controlling the pro-inflammatory response of mouse macrophages to LPS (20-21), and a recent study further separated enhancers into different categories (23). Classification relied mostly on the presence or absence of the macrophage master transcription factor PU.1, and histone modifications associated with poised (*i.e.*, H3K4me1) and active enhancers (*i.e.*, H3K27ac), but transcriptional enhancer activity has only been confirmed for a fraction of

these enhancers in functional assays. We had previously shown that distal and proximal enhancers of three example genes, *Il12b*, *Il1a* and *Ifnb1*, are poised and partially nucleosome depleted in resting macrophages and that a subset of nucleosomes within each enhancer is completely evicted upon activation by LPS (17). To determine whether this distinct chromatin architecture is associated with putative enhancers of Ostuni et al. (23), we analyzed nucleosome occupancy from rM and aM at these regions. We used the enhancer classification of these researchers (see Table 4.1), but further separated the “not steady” category into enhancers that were active in rM and became either further activated or repressed upon LPS induction (*i.e.*, not steady-activated and not steady-repressed, respectively).

Table 4.1. Categories of putative enhancers identified by Ostuni et al.

Type	putative enhancers	PU.1-bound (4h LPS)	Definition
all	69,559	38,315	all categories
poised - activated	5,277	3,512	H3K4me1 and PU.1 present before LPS induction, H3K27ac acquired upon LPS induction
poised - not activated	37,629	14,532	H3K4me1 and PU.1 present before induction, no H3K27ac acquired upon LPS induction
constitutive	9,013	6,913	H3K4me1, H3K27ac, and PU.1 present before and after LPS induction
latent	1,351	574	acquire H3K4me1, H3K27ac, and PU.1 only upon LPS induction
not steady - activated	3,082	2,654	H3K4me1, H3K27ac, and PU.1 present before LPS induction, additional H3K27ac upon LPS induction
not steady - repressed	13,207	10,130	H3K4me1, H3K27ac, and PU.1 present before LPS induction, less H3K27ac upon LPS induction

Inspection of individual enhancers belonging to the different classes showed that

nucleosomes were completely evicted only from relatively small regions within the larger enhancer regions, and only from enhancers that became activated in response to LPS (*i.e.*, poised-activated, constitutive, latent, not-steady-activated, Fig. 4.4A and C-E), but not from enhancers that were not activated or became repressed (*i.e.*, poised-not activated, not steady-repressed Fig. 4.4B and F). Poised-not activated enhancers were sometimes also associated with nucleosome-free regions, but these regions were usually of subnucleosomal length (see Fig. 4.4B). When we aligned all the putative enhancers belonging to each class at their enhancer midpoints and analyzed regions 3 kb upstream and downstream, we detected some nucleosome depletion in the center of poised-activated, constitutive, not-steady-activated and not steady-repressed enhancers in rM as well as an overall decrease in occupancy upon LPS induction over the entire regions at all enhancers (Suppl. Fig. 4.S7A and B). However, the average alignments did not reveal the complete nucleosome eviction at specific sites within active enhancers that we could detect at individual enhancers. Furthermore, we found that depletion over the whole length of the enhancer regions was similar to depletion at random genomic regions outside of enhancers (Suppl. Fig. 4.S7C). Such a widespread decrease in occupancy of about 5-10% is consistent with our findings of a loss of occupancy in large parts of the genome (Suppl. Fig. 4.S5). However, alignment at the midpoints did not reveal the distinct changes in occupancy we detected at individual enhancers of different categories and we reasoned that due to the large range of sizes of the putative enhancers identified by Ostuni et al. (*i.e.*, 110 bp to 28,220 bp), alignment by midpoint might obscure changes in occupancy restricted to individual nucleosomal sites within enhancers. We therefore selected only enhancers that were

PU.1-bound in rM and/or aM and aligned them at their PU.1-peaks (PU.1 ChIP-seq peaks at 4 h LPS were taken from (23)). This alignment revealed partial depletion at PU.1-sites in rM at all enhancers except those classified as latent, which lack PU.1 binding in rM (Fig. 4.4G and Suppl. Fig. 4.S8A), and this result is consistent with previous findings that PU.1 binding leads to reduced nucleosome occupancy (21,26-27). Upon LPS induction, the sites of PU.1 binding became more nucleosome depleted at all enhancers, except at enhancers that were repressed by LPS (*i.e.*, not steady-repressed). Nevertheless, the average changes in occupancy at the PU.1-sites were small (5-10%) compared to the changes we observed at individual enhancers or when we aligned a subset of all putative enhancers at their previously identified p300 peaks (*i.e.*, ~1,300 enhancers that overlap with p300 peaks at 2 h LPS taken from (20), Fig. 4.4H and Suppl. Fig. 4.S8B). These results are consistent with our findings at the enhancer of *I12b* where we showed that maximal nucleosome depletion upon LPS induction did not occur at the PU.1 consensus sites but in adjacent regions (17). Furthermore, our findings of only a partial decrease in nucleosome occupancy at PU.1-sites in enhancers support the idea that PU.1 may be able to bind its sites in the presence of nucleosomes as has been suggested for other pioneer TFs (60). In contrast, complete nucleosome eviction upon LPS induction may be required at neighboring sites to allow binding of signal-induced TFs and recruitment of the transcriptional machinery to enhancers (17).

Figure 4.4. Nucleosome occupancy at macrophage enhancers.

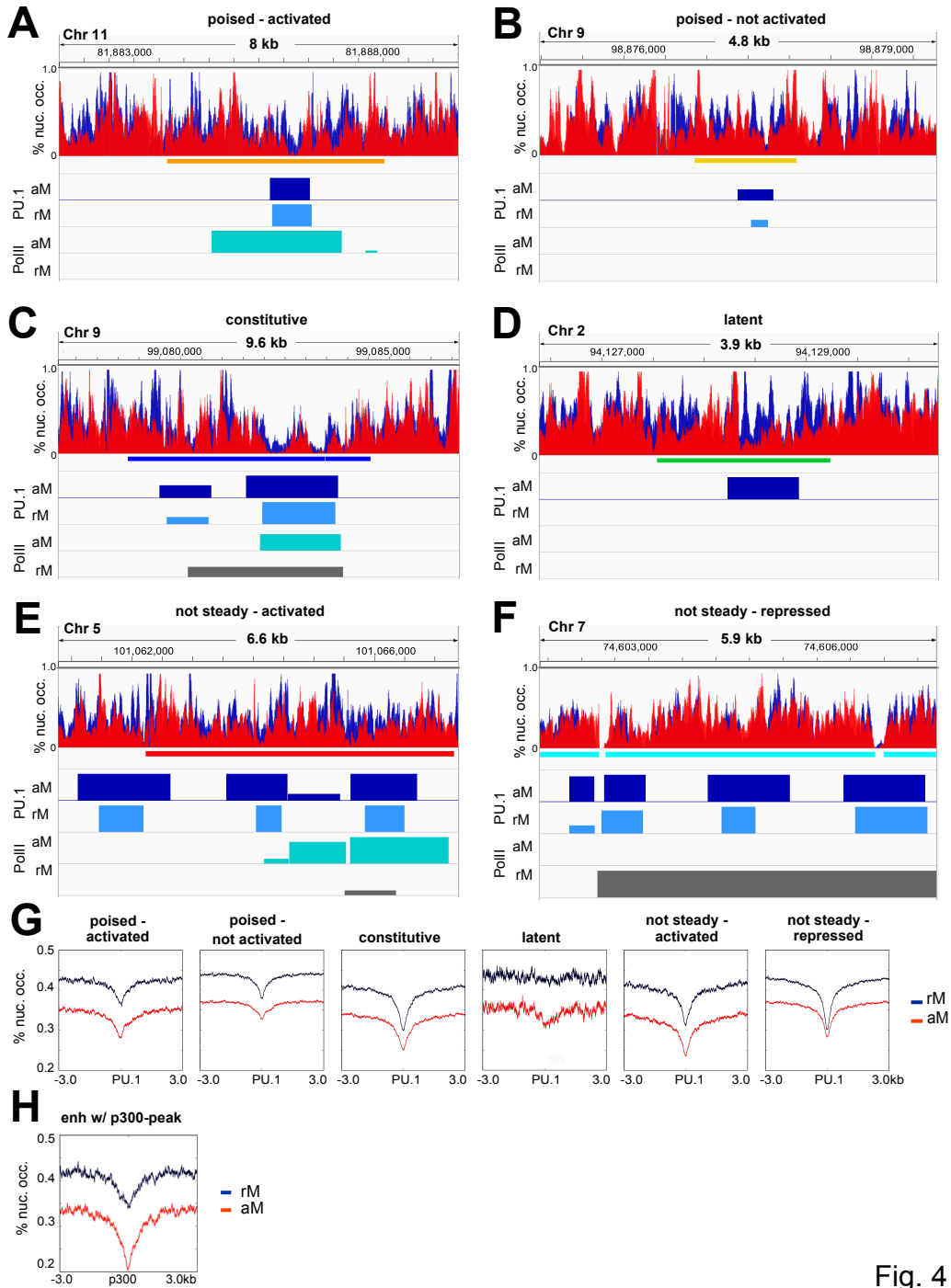


Fig. 4

(A-F) Nucleosome occupancy in rM (blue) and aM (red) at examples of the different enhancer categories are shown. The enhancer regions demarcated by histone modifications are shown as colored bars underneath the nucleosome occupancy tracks,

Figure 4.4. (cont'd)

and PU.1 and Pol II ChIP-seq peaks in rM and aM (*i.e.*, after 4 h LPS, data taken from (23)) are indicated in each figure.

(G) Average nucleosome occupancy plots in rM (blue) and aM (red) of enhancers that contain a PU.1 peak identified as described in *Experimental Procedures* (see Table 4.1). Enhancers were separated into categories as described and aligned at their PU.1 peaks.

(H) Average nucleosome occupancy plot in rM (blue) and aM (red) at the subset of enhancers that contain a p300 peak identified as described in *Experimental Procedures*, after alignment at the p300 peaks.

Identification of regions partially depleted in rM and further depleted in aM

Our analysis suggested that proper alignment of enhancers may be crucial when trying to identify regions of nucleosome depletion within enhancers of different lengths. Ostuni et al. defined putative enhancers broadly by the sizes of histone modification peaks, and our analysis of their data shows that 65% of enhancers are 200-1,500 bp in length, which corresponds to 1-7 nucleosomal positions assuming a precision length of 200 bp (23). However, 35% of their putative enhancers are longer and 10% extend over regions larger than 3 kb. Inspection of examples of such enhancers in IGV indicated that eviction of individual nucleosomes upon LPS induction is not restricted to the center of regions defined by histone modifications, but can occur anywhere in the larger enhancer regions (Fig. 4.4A-E). We therefore sought to take an alternative approach that neither depends on enhancer lengths nor precise information of TF binding, but is based on our previous findings at the enhancers of the three example pro-inflammatory genes that we

had studied in detail (17). Using the qRT-PCR based approach of (14) we had previously shown that the enhancers of *Il12b*, *Il1a* and *Ifnb1* were already partially depleted in rM (*i.e.*, 50-70% occupancy) over regions encompassing 4-6 nucleosomes. We further showed that between 1 and 3 of these partially occupied nucleosomes were evicted upon LPS induction. To determine if such regions also exist in the putative enhancers of Ostuni et al. we used a thresholding approach that first identified all partially depleted regions in rM and all regions of nucleosome eviction in aM in the genome, and then determined overlap of such regions with putative enhancers. For partially depleted regions in rM we chose an upper length limit between 800-1,200 bp, corresponding to 4-6 nucleosomes, and varied the upper limit of nucleosome occupancy between 70-80% (see Suppl. Table 4.S1). We also allowed this occupancy to be discontinuous by permitting a gap in maximal occupancy varying between 1-3 bp. For regions completely depleted in aM we varied the upper length limit between 100-600 bp (*i.e.*, 1-3 nucleosomes), and varied the maximal occupancy allowed between 20-30% over the whole region and we also allowed a gap ranging from 0-20 bp in size. We then plotted the percentage of all putative enhancers that contained a partially depleted region in rM or a region of nucleosome eviction in aM versus all genomic regions identified by each occupancy threshold (Fig. 4.5A and B). As we relaxed threshold conditions for depletion (*i.e.*, shorter regions, higher occupancy and larger gap allowed) we captured a higher fraction of putative enhancers but also greatly increased the total number of regions defined as depleted in the genome. Significantly, the relationship between recall of putative enhancers and detection of additional depleted regions in the genome is not linear and this may indicate that some of the enhancers identified by

Ostuni et al. may be false positives. These enhancers may not be accessible in chromatin although they are associated with histone modifications and PU.1 binding. Our results also indicate that additional genomic regions that lie outside of enhancers become nucleosome depleted upon LPS induction. Such regions presumably include regions surrounding promoters, as we had shown (Fig. 4.2), but may also include as yet unidentified genomic regions that might play a role in gene regulation upon LPS induction.

Different enhancer categories show characteristic depletion in rM and aM

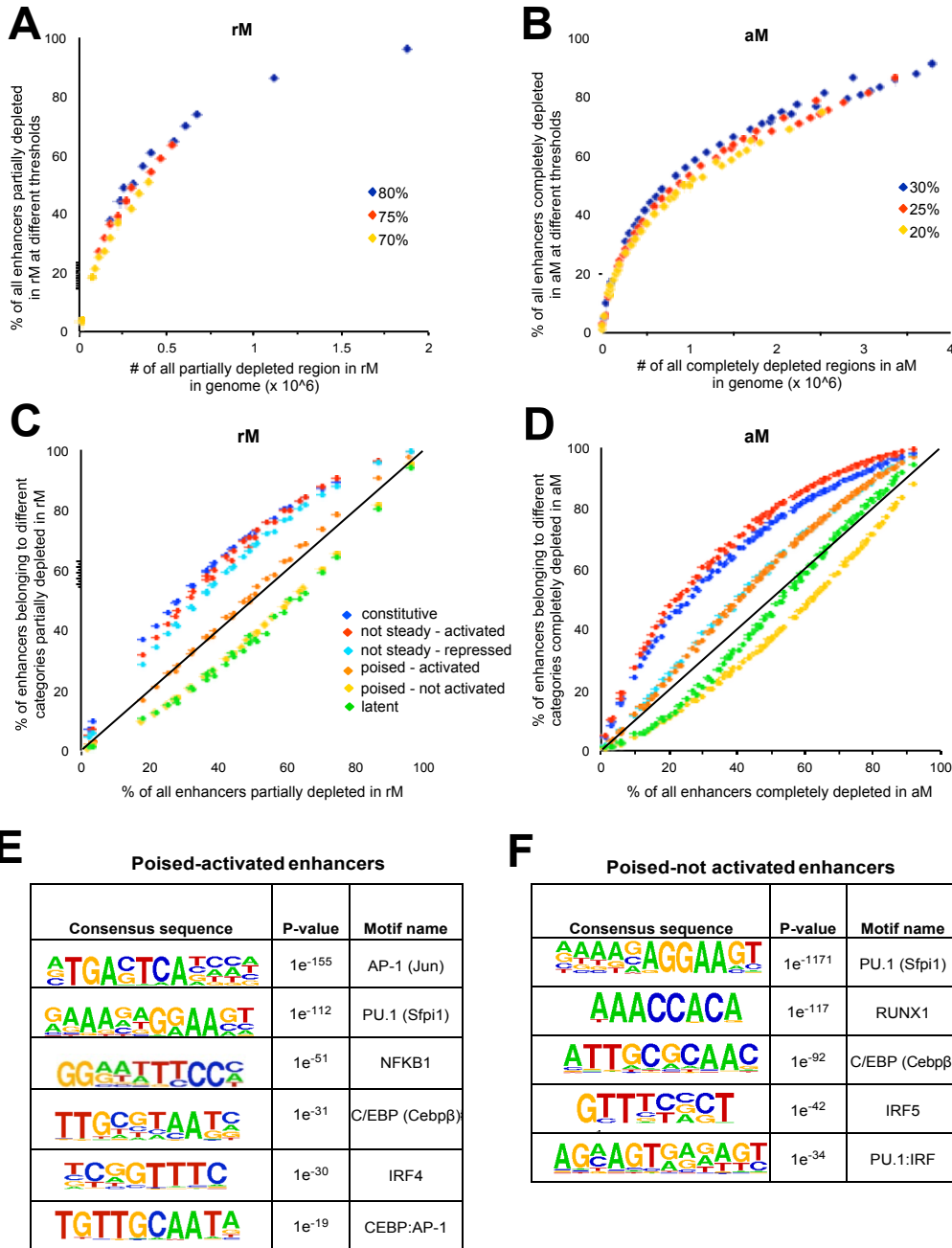
To determine whether our thresholding approach distinguishes different enhancer categories, we plotted the percentage of putative enhancers in each category that encompassed a partially depleted region in rM or region of nucleosome eviction in aM versus the percentage of all enhancers (Fig. 4.5C and D). This analysis revealed that constitutive and not steady enhancers were more likely to already contain a partially depleted region in rM compared to all enhancers (*i.e.*, hatched line), consistent with enhancer activity of these elements in rM. In contrast, we found that latent and poised-not activated enhancers were less likely to have a partially depleted region in rM than all enhancers, and these two classes of enhancers were indistinguishable in rM. The finding that latent and poised-not activated enhancers resemble each other in rM was surprising since it was previously shown that poised-not activated enhancers are associated with PU.1 and H3K4me1 in rM while latent enhancers are not (23). Previous studies had suggested that PU.1 binding leads to partial nucleosome depletion at the PU.1-site (21,26), a result confirmed by our analysis of average nucleosome occupancy after alignment of enhancers at their PU.1-sites (Fig. 4.4G). However, our results

suggest that PU.1 binding may not be sufficient to create larger regions of partial depletion encompassing several nucleosomal sites and extending beyond the PU.1-sites themselves, and we hypothesize that additional factors including nucleosome remodelers may have to be recruited to create such regions. We further hypothesize that such additional factors may be recruited only to poised-activated enhancers but not to poised-not activated enhancers in rM, since we found that poised-activated enhancers were more likely to have a partially depleted region in rM than poised-not activated enhancers (compare orange to yellow dots in Fig. 4.5C). Together our results indicate that GNO-seq analysis in resting cells allows us to distinguish different types of enhancers and most significantly, our thresholding approach allows us to separate poised enhancers that are indeed functional in response to LPS from those that are not responsive by identifying regions of larger partial nucleosome depletion in rM.

When we analyzed regions of nucleosome eviction in aM we found that constitutive and not steady-activated enhancers were more likely to be associated with such regions than not steady-repressed enhancers, consistent with transcriptional activity of these elements in aM. This result also suggests that enhancers that were active but then become repressed, were less likely to further gain depleted regions and might instead reassemble nucleosomes upon LPS induction. This finding was confirmed by inspection of individual repressed enhancers (*e.g.*, Fig. 4.4F). However, enhancers that had never been active in rM and remained inactive in aM (*i.e.*, poised-not active) were even less likely to have completely nucleosome-free regions in aM than enhancers that became repressed, indicating that gain of nucleosomes at repressed enhancers

1.5 h after LPS addition may be incomplete. As expected, regions of nucleosome eviction in aM were found with higher frequencies in poised-activated than in poised-not activated enhancers consistent with their transcriptional activity (Fig. 4.5D). Furthermore, we found that latent enhancers became associated with regions of nucleosome eviction upon LPS induction and could be distinguished from poised-not activated enhancers when we used relaxed threshold conditions, but resembled poised-not activated enhancers under more stringent conditions. Together, our thresholding analysis reveals specific depletion signatures in rM and aM associated with each enhancer category that correlated well with their responses to LPS. Our finding that only a fraction of enhancers in each class were associated with partial nucleosome depletion or nucleosome eviction under all but the least stringent conditions, suggests that some of the putative enhancers identified by Ostuni et al. may not be functional because they may not be accessible in chromatin.

Figure 4.5. Regions of nucleosome depletion and TF-motifs in putative enhancers.



(A) The percentage of all putative enhancers of Ostuni et al. (23) that contain a partially depleted region in rM was determined as described in *Experimental Procedures* and

Figure 4.5. (cont'd)

was plotted against the number of all genomic regions identified as partially depleted in rM. Individual threshold conditions can be found in Suppl. Table 4.S1.

(B) The percentage of all putative enhancers that contain a region of nucleosome eviction in aM was determined as described in *Experimental Procedures* and was plotted as in (A) against the number of all such genomic regions in aM.

(C) and **(D)** The percentage of enhancers, separated by category as described in Table 4.1, that contains a partially depleted region in rM or a region of nucleosome eviction in aM respectively, was determined as described in *Experimental Procedures* and was plotted against the percentage of all putative enhancers. Different enhancer categories are shown in different colors as indicated in (C).

(E) and **(F)** A *de novo* motif search using Homer (21) was performed in poised-activated and poised-not activated enhancers, respectively, and enriched motifs are shown.

TF consensus-sites associated with poised-activated and poised-not activated enhancers

To determine whether the differences between poised-activated and poised-not activated enhancers we detected are the result of differential binding of TFs in rM, we performed a *de novo* motif analysis in these enhancers using Homer (21). We found a composite C/EBP:AP-1 motif amongst the 10 most highly enriched motifs in poised enhancers that became activated, but not in those that were not (Fig. 4.5E and F). Both types of poised enhancers had canonical sites for C/EBP, but it was previously shown

that the composite motif was most strongly associated with C/EBP β binding in macrophages (21,61).

We therefore hypothesized that C/EBP β , presumably together with AP-1, might bind more strongly to poised-activated than poised-not activated enhancers, which might contribute to partial nucleosome depletion in rM. However, our inspection of published ChIP-seq data showed that C/EBP β and JunB were bound only in a small fraction of poised enhancers in rM in these experiments (24) and while the percentage of C/EBP β -bound enhancers was slightly larger in poised-activated than poised-not activated enhancers (*i.e.*, in 1.2% vs. 0.5%) the overall level of C/EBP β and JunB binding was too low to account for the partial depletion we found in a large fraction of these enhancers. We therefore hypothesize that other, as yet unidentified TFs, may bind differentially to poised-activated and poised-not activated enhancers and determine nucleosome occupancy. In addition, we speculate that such additional TFs affect recruitment of the remodeler BAF/PBAF by PU.1. It remains to be determined whether BAF/PBAF is preferentially recruited to poised-activated over poised-not activated enhancers as predicted by our results.

Nevertheless, our motif analysis also revealed motifs for the TLR4 signal-induced TF NF κ B and canonical AP-1 motifs in poised-activated enhancers only, and the absence of such sites in poised-not activated enhancers is consistent with their failure to respond to LPS. In addition, we found different types of IRF motifs associated with poised enhancers - *i.e.*, IRF4- motifs enriched in LPS-responsive enhancers and IRF5 and composite PU.1:IRF-motifs enriched in LPS non-responsive enhancers (Fig. 4.5E and F), which may further distinguish the response of these enhancers to LPS, since IRF4

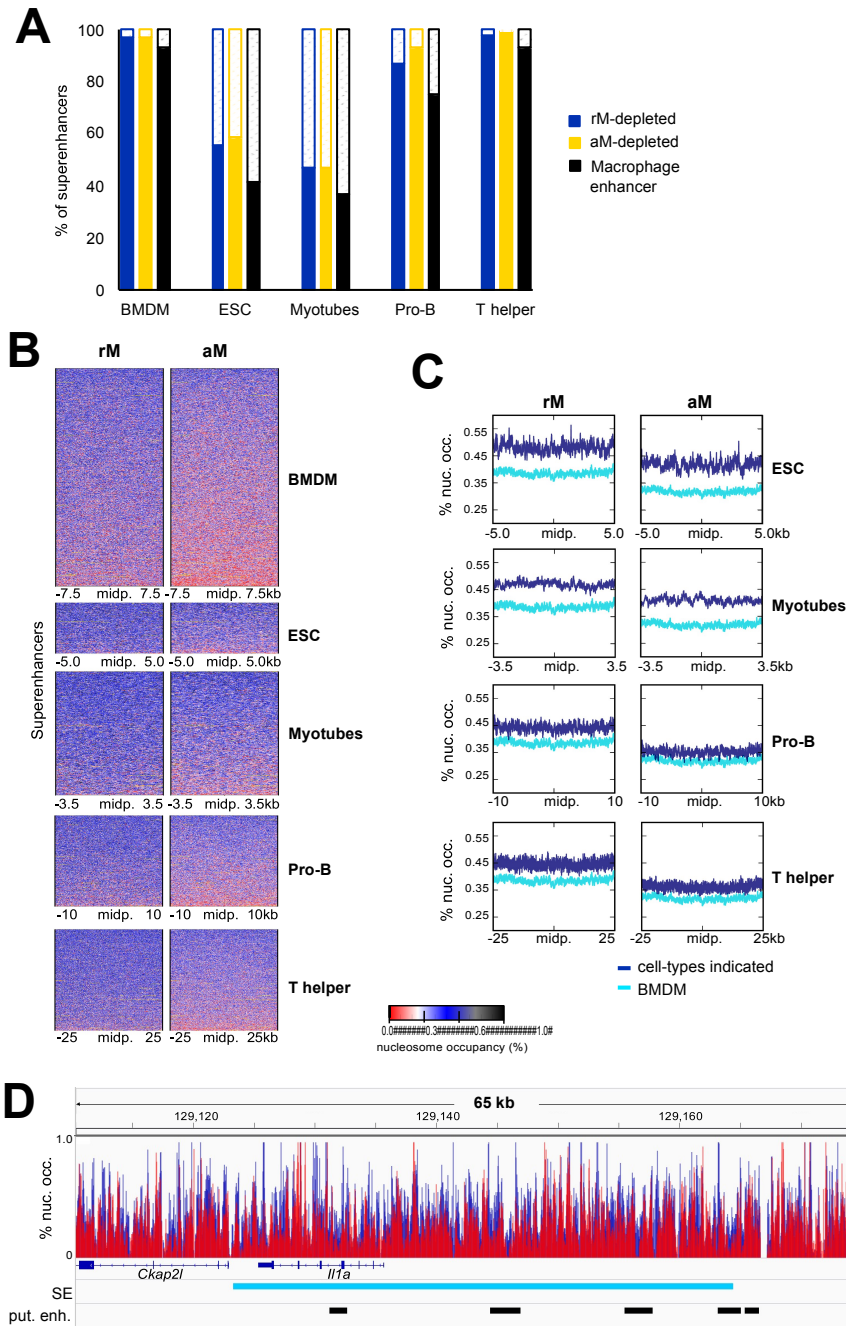
and IRF5 have been shown to play distinct roles in regulating pro-inflammatory gene expression (62-63). In summary, our results show that different motifs for LPS-activated TFs can in part explain the response of different types of poised enhancers to LPS. In addition, identification of partially depleted regions allows us to separate LPS-responsive from non-responsive enhancers already in resting cells, which cannot be done when considering histone marks and PU.1 binding alone. Quantitative analysis of nucleosome occupancy by GNO-seq in combination with our thresholding approach therefore has the potential to allow identification of functional enhancer elements in other systems.

Nucleosome depletion at super-enhancers

Previous studies identified super-enhancers (SEs) in different cell-types (41). SEs span large genomic regions and are associated with high levels of mediator binding in ChIP-seq experiments. In addition, expression of genes regulated by SEs is particularly sensitive to inhibition of the co-activator Brd4 by the BET-bromodomain inhibitor JQ1 and recent studies showed that genes regulated by SEs include master miRNAs that regulate cell-identity (64). To determine what makes these large SE regions highly accessible to binding of the transcriptional machinery we investigated whether SEs are particularly accessible in chromatin. We determined whether macrophage-specific SEs are associated with defined partially depleted regions in rM and with regions of nucleosome eviction in aM, using intermediate threshold conditions that captured 50% of all putative enhancers of Ostuni et al. (*i.e.*, 80% occupancy, 1,000 bp length and 1 bp gap allowed in rM and 20% occupancy, 140 bp length, 3 bp gap allowed in aM). Using these thresholds we found that most SEs specific to BMDMs were associated with

partially depleted regions in rM and regions of nucleosome eviction in aM (Fig. 4.6A, blue and yellow bars). Moreover, most macrophage-specific SEs also encompassed at least one putative macrophage enhancer of Ostuni et al. (black bars). In contrast, we found less association of SEs specific to ESCs or Myotubes with nucleosome-depleted regions in macrophages, and these SEs were also less likely to encompass a macrophage-specific enhancer. Strikingly, SEs identified in Pro-B and T helper cells (Th) were strongly associated with nucleosome-depleted regions in macrophages and with macrophage enhancers, and closely resembled macrophage-specific SEs.

Figure 4.6. Nucleosome occupancy at super-enhancers.



(A) The fraction of SEs identified in BMDMs, ESCs, myotubes, Pro-B and T helper (Th) cells identified by Whyte et al. (41) that are associated with depleted regions in rM (blue), aM (yellow) or with putative enhancers (black) are shown.

Figure 4.6. (cont'd)

(B) Heatmaps of nucleosome occupancy in SEs are shown in rM and aM after alignment of SEs by their midpoint. Surrounding regions included in each heatmap are based on SE sizes in different cell- types.

(C) Average nucleosome occupancy at SEs from cell-types indicated (dark blue) is shown compared to macrophage-specific SEs (cyan) in rM and aM, respectively. SEs were aligned by their midpoint and average occupancy over the whole region is shown in each panel.

(D) Nucleosome occupancy in rM (blue) and aM (red) in a region encompassing a macrophage- specific SE (sky blue) at the *Ii1a* locus. Putative enhancers of Ostuni et al. are indicated in black.

To further investigate whether entire SE regions are broadly associated with nucleosome depletion we determined nucleosome occupancy in rM and aM over the whole lengths of SEs from different cell-types. Our data show that average nucleosome occupancy in macrophage- specific SEs was lower over the whole regions in rM (~38%) than occupancy in SEs specific to other cell-types (~45-50% see Fig. 4.6B and C, compare cyan to dark blue lines), and lower than occupancy in randomly selected regions of the genome (~ 45% in rM in Suppl. Fig. 4.S7C). Note that these occupancies are average occupancies over large regions, and do not reflect occupancies of individual nucleosomal peak positions at specific sites. These differences were most striking when we compared macrophage-specific SEs to SEs from ESC and Myotubes, while SEs from Pro-B and T helper cells more closely resembled those of macrophages. In addition, we found that nucleosome occupancy further decreased upon LPS

induction, and occupancy in SEs from macrophages reached the lowest overall levels (~35% in aM). Again SEs from Pro-B and T helper cells most closely resembled SEs from macrophages also under inducing conditions. These results suggest that chromatin at macrophage-specific SEs is highly accessible in BMDMs and becomes even more accessible upon LPS induction. Our findings also indicate that SEs from more closely related cell-types resemble each other in terms of nucleosome occupancy, which may suggest that some SEs may be co-opted in related cells. Nevertheless, we noted that inspection of individual SEs revealed normal nucleosome positioning and most regions retained some level of nucleosome binding, while nucleosomes were evicted only from short sites that often overlapped macrophage enhancers of Ostuni et al. (see for example the SE at *I1a* locus in Fig. 4.6D).

Discussion

Nucleosome removal at promoters

Previous studies had suggested that promoters have to be cleared of nucleosomes to allow expression of genes upon LPS induction of mouse macrophages similar to findings at inducible genes in yeast (14,65). Support for this idea came from the finding that expression of most secondary and some primary immune response genes depends on the SWI/SNF family remodeler BAF/PBAF suggesting that nucleosomes have to be actively removed at promoters (25). Here we show that very few genes have highly occupied nucleosomes at their promoters that are removed upon LPS induction.

Instead, we find two types of genes: at many genes promoters are already significantly depleted presumably due to low-level basal transcription in resting macrophages and induction leads to complete nucleosome clearance and increased gene expression (Fig.

4.2). Low-level transcription presumably produces functional transcripts at these genes, since the transcripts identified by Mancino et al. were polyadenylated and detected along the entire ORFs in resting macrophages (22). Further support for the notion that these mRNAs are continuously produced by *de novo* transcription comes from another study that found newly synthesized transcripts associated with chromatin at these genes (19). However, we cannot exclude the possibility that non-functional transcripts may also be synthesized by paused Pol II at some of these genes. Pausing has been shown to control inducible gene expression in *Drosophila* and has been proposed to lead to nucleosome displacement at promoters (66). However, whether Pol II pausing plays a significant role in promoter nucleosome depletion at inducible genes in macrophages is unclear (67-68). At the second type of genes promoters were occupied by high levels of nucleosomes in resting macrophages, and significantly, nucleosomes remained associated with a large fraction of these promoters under inducing conditions (Fig. 4.3). In particular we identified a group of 179 genes that are only lowly expressed in rM but become highly expressed in response to LPS, which retain promoter nucleosomes under inducing conditions. This group of genes includes many cytokine and pro-inflammatory genes previously classified as LPS-induced (25) and a gene ontology analysis revealed enrichment for biological processes associated with the response of macrophages to bacterial stimulation including inflammation and cell motility and for molecular functions associated with cytokine and chemokine activity (Fig. 4.3F). These results extend our previous findings at *I12b* and *I1a* to a whole class of highly induced genes (17). We had previously hypothesized that promoter nucleosomes may rapidly reform at these genes after one round of transcription to

control access of the transcriptional machinery to their promoters. It remains to be determined what distinguishes this class of genes from others and what controls rapid reassembly of promoter nucleosomes, but we speculate that such tight regulation of promoter accessibility by chromatin may be reserved for genes whose uncontrolled expression might have adverse effects on the cell or organism.

Previous studies suggested that the underlying DNA-sequence affects nucleosome occupancy, and AT-richness was shown to contribute to relatively low promoter occupancy in the yeast *S. cerevisiae* (51,57,69). In contrast, mammalian promoters are usually devoid of AT-rich sequences and instead are GC-rich, sometimes with CpG-islands (19,25,47,50). We confirmed high overall GC content at the promoters of the Refseq genes of Fig. 4.2 compared to the rest of the genome (McAndrew, M.J. and Floer, M., data not shown), which supports the notion that promoter nucleosomes have to be removed at promoters by an active process. At most genes we found that the promoter regions that became completely nucleosome-free upon induction corresponded to a single nucleosomal site, while surrounding regions upstream of the promoters and in the 5' ORFs were often partially depleted but retained some level of nucleosome binding. Only in rare cases did we find broad nucleosome removal over a whole gene locus (e.g., *Tnf* Fig. 4.2K, and a number of chemokine ligand genes). Such broad nucleosome eviction had previously been thought to be restricted to heat shock genes, where it was shown to precede transcription (58-59). It remains to be determined what causes nucleosome depletion from entire gene loci and what are the consequences on gene expression. Nevertheless, we noted that high levels of expression in response to LPS did not require such broad nucleosome depletion, and

occurred even at genes that retained most of their nucleosomes (Fig. 4.2E and Suppl. Fig. 4.S6). Together our data revealed considerable variation in the nucleosome changes associated with LPS-induced gene expression, which highlights the importance of a quantitative analysis of nucleosome occupancy when measuring chromatin accessibility.

We also noted that LPS induction was associated with a small decrease in nucleosome occupancy genome-wide, but the functional relevance of this broad increase in chromatin accessibility remains to be determined (Suppl. Fig. 4.S5). Our recent study in B-cells found similar widespread decreases in nucleosome occupancy upon LPS activation and we showed that this was associated with chromatin decompaction in the genome (Kieffer-Kwon et al, manuscript accepted). Whether chromatin is also decompacted in LPS-induced macrophages remains to be determined.

Nucleosome depletion at enhancers

Our findings of nucleosome changes at macrophage enhancers are consistent with our previous studies showing that poised enhancers are partially depleted in resting macrophages and that nucleosomes are further evicted upon LPS induction (17). While PU.1 plays some role in this process (21,26-27), our data indicate that PU.1 may not be sufficient to create larger regions of partial depletion encompassing several nucleosomal sites within enhancers. This is supported by our finding that poised-not activated enhancers, which are bound by PU.1, are less likely to be associated with partially depleted regions in rM than poised-activated enhancers (Fig. 4.5C). PU.1 belongs to the family of pioneer TFs, which have been suggested to bind their sites in the presence of nucleosomes (60) and we recently showed that PU.1 is required for

recruitment of the remodeler BAF/PBAF during macrophage differentiation resulting in partial nucleosome depletion and priming of the Il12b and Il1a enhancers in rM (28). Our findings here are consistent with a role of BAF/PBAF in partial nucleosome depletion, and we hypothesize that remodeler recruitment to poised enhancers that are indeed functional in response to LPS may depend on other factors in addition to PU.1 (28). Strikingly, our approach allows us to distinguish different types of enhancer that cannot be distinguished solely by histone modifications and PU.1 binding, and underscores the importance of considering quantitative differences in nucleosome occupancy when analyzing enhancers.

A recent study that investigated gene induction as a result of the unfolded protein response had come to the conclusions that promoters and enhancers do not undergo changes in nucleosome occupancy upon induction (18). These findings are in contrast to our findings presented here, and while it is possible that there are cell-type and signal-dependent differences, we believe that in the absence of input and reference normalization in the approach of Mueller et al. quantitative differences in occupancy cannot be detected. In a related study we also found significant changes in occupancy at enhancers and promoters upon activation in B-cells, indicating that such changes are not restricted to macrophages (Kieffer- Kwon et al, manuscript accepted).

Conclusion

In summary, our findings highlight the significant advance GNO-seq provides, which improves quantification of nucleosome occupancy over previous MNase-seq and histone ChIP-seq methods. GNO-seq, in conjunction with the thresholding approach we have applied, allows further characterization of functional transcriptional regulatory

elements that goes beyond the information provided by localization of histone modifications and TF binding in the genome. GNO-seq provides information complementary to approaches such as DNase-seq and ATAC-seq and has the potential to become a useful tool when identifying functional enhancers in other systems where the TFs and inducing agents may be unknown.

Acknowledgments

We thank Dr. Mike Halbisen (BMB Dept., MSU) for initial mapping of lambda reads and help with the bioinformatics analysis. We also thank Dr. Mohita Tagore (now at Sloan Kettering Institute, New York), Drs. Shinhan Shiu, Nicholas Panchy, Sahra Uygun and other members of the Shiu lab (Dept. Plant Bio., MSU) for help with bioinformatics analyses. We thank the ICER/HPCC staff at MSU for troubleshooting. We thank Dr. Giacchino Natoli (European Institute of Oncology, Milan) for helpful discussions of the gene expression analysis in LPS stimulated macrophages. We thank Dr. David Arnosti and Dr. Shinhan Shiu (at BMB Dept., MSU) for reading of the manuscript and thoughtful comments, and Dr. Erik Martinez-Hackert for many stimulating discussions.

APPENDICES

APPENDIX A:

Supplementary Experimental Procedures

Supplementary Experimental Procedures

deepTools bamCoverage analysis

The BAM files of rM and aM were analyzed either with or without the MNase option in deepTools bamCoverage including a reference normalization step using the scaling factors described in *Experimental Procedures* (bin size `-bs = 1`, `--MNase`, `--scaleFactor = 1/lambda` reads per Million reads for each sample) (33). The MNase option of bamCoverage considers only the three nucleotides at the center of each paired-end fragment as the nucleosome dyad, and moreover limits the size of paired-end fragments considered in the analysis to 130-200 bp.

DANPOS analysis

The BAM files of the MNase-fractions of rM and aM were analyzed using DANPOS2 (42). We performed Dpos analysis using default settings for paired-end data, except that a scaling factor was applied for reference normalization of each MNase-fraction (`-c = scale factor`, *i.e.* `1/lambda` reads per Million reads) as described in *Experimental Procedures* (32). Dpos shifts paired-end reads toward the 3' end for half of the fragment size, and adjusts the read lengths to half of the nucleosome size.

Random genomic sampling for nucleosome occupancy determination

A total of 100,000 regions of 6 kb were generated using bedTools random and shuffled into regions with sufficient GNO-seq coverage as described in *Experimental Procedures*. We then removed any regions overlapping enhancers identified by Ostuni et al. (23) and promoters (*i.e.*, 500 bp upstream of all Refseq TSS) from these regions using bedTools intersect (default settings; `-v` option with `-a random` and `-b enhancers and promoters`), which yielded a total of 73,752 random regions.

Analysis of genes repressed in rM and induced in the presence of LPS

Boxplots of expression data in LPS induced cells (FPKM at 2 h LPS taken from (22)) of genes found in clusters C1-4 were made in R.

Heatmaps and average nucleosome occupancy plots after alignment at enhancer midpoints

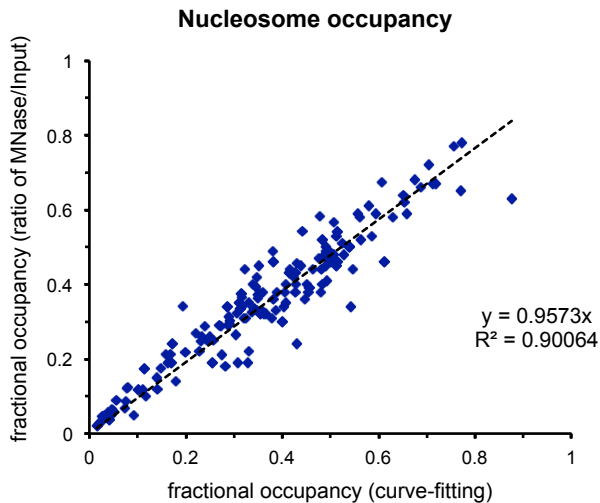
Enhancers in each category were aligned at their midpoint and nucleosome occupancy in rM and aM in the surrounding regions was plotted using deepTools computeMatrix (--referencePoint = center, bin size -bs = 1). Heatmaps and average occupancy plots were generated using deepTools plotHeatmap after sorting by occupancy in aM.

APPENDIX B:

Supplementary Figures

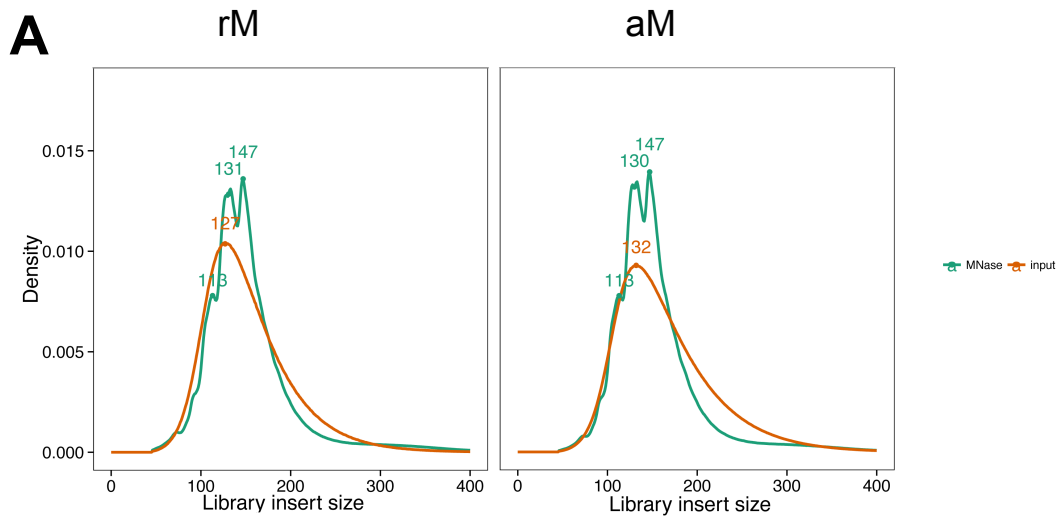
Supplementary Figures

Figure 4.S1. Correlation between fractional nucleosome occupancies obtained as the ratio of MNase over Input-fractions and occupancies obtained by curve-fitting.



MNase-digestion in rM was performed and data analyzed by qRT-PCR as described in *Experimental Procedures*. The values of MNase and Input-fractions at many genomic locations were calculated as the average of the qRT-PCR values corresponding to the three MNase and Input samples defined as described in the legend of Fig. 4.1B. Fractional occupancies calculated as the ratio of these values are plotted versus the fractional occupancies derived from curve-fitting as described (14). The genomic locations used for qRT-PCR amplification can be given upon request.

Figure 4.S2. Fragment sizes of inserts in Illumina libraries.



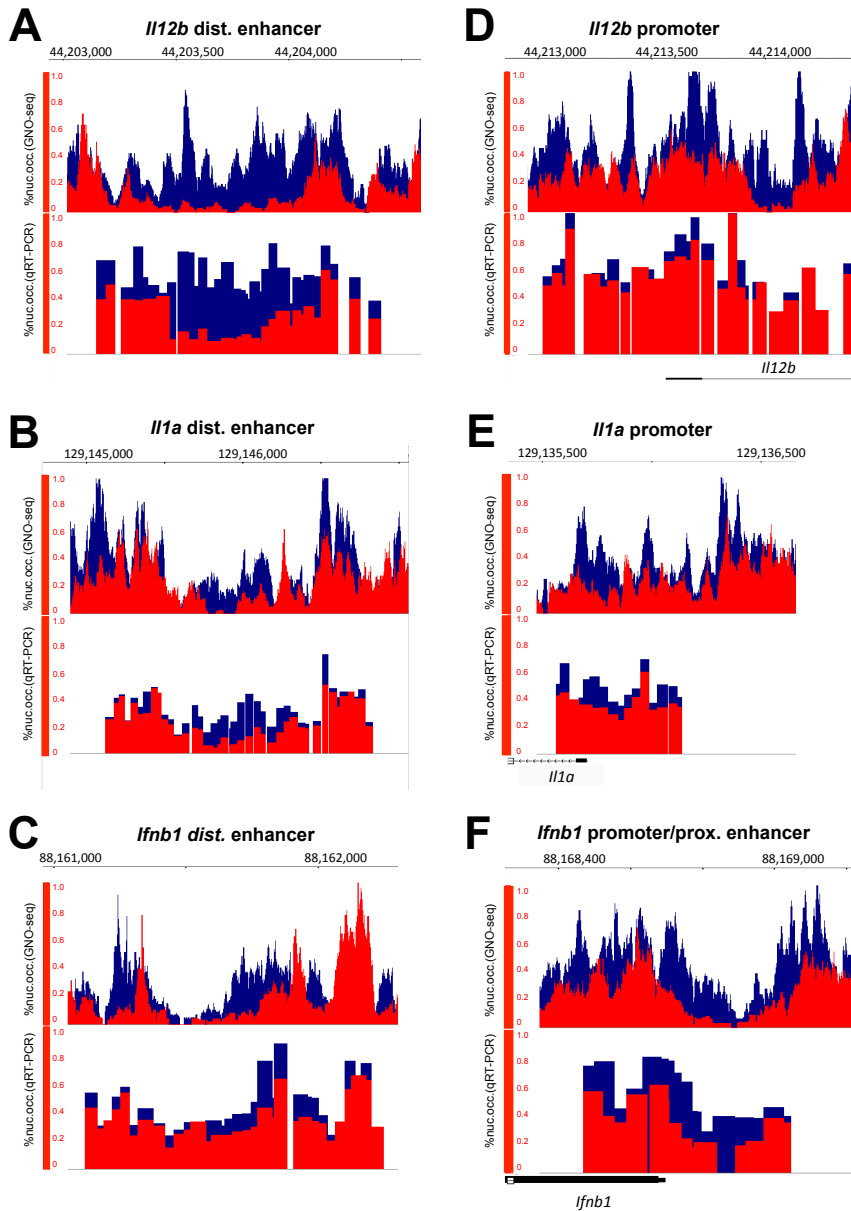
B

	Input	MNase
rM	428,097,485	352,600,810
aM	324,512,362	365,595,205

(A) Fragment sizes of inserts in Illumina libraries. Illumina libraries were prepared as described in *Experimental Procedures* and fragment sizes in the MNase (green) and Input-fractions (orange) are shown for libraries made from resting (rM) and activated macrophages (aM).

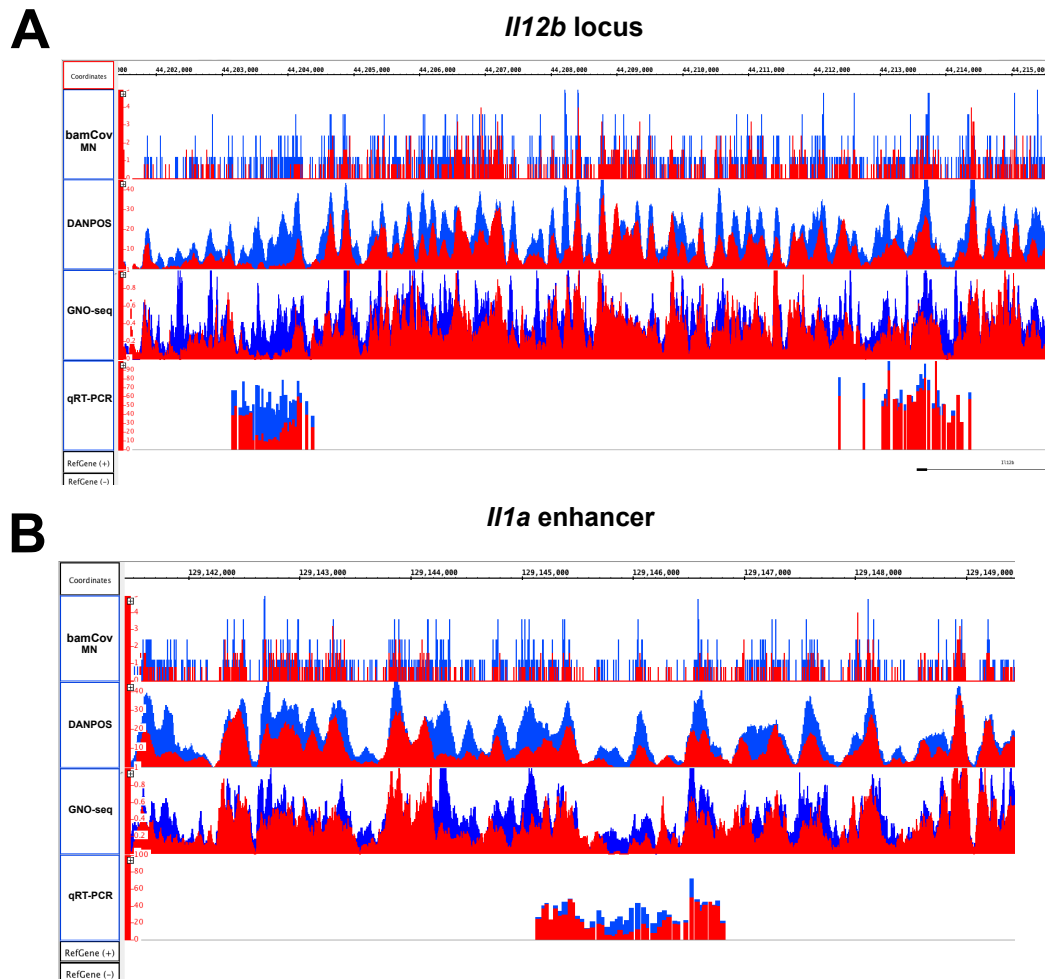
(B) Number of paired-end Illumina reads obtained for each fraction.

Figure 4.S3. GNO-seq analysis at enhancers and promoters of three pro-inflammatory genes.



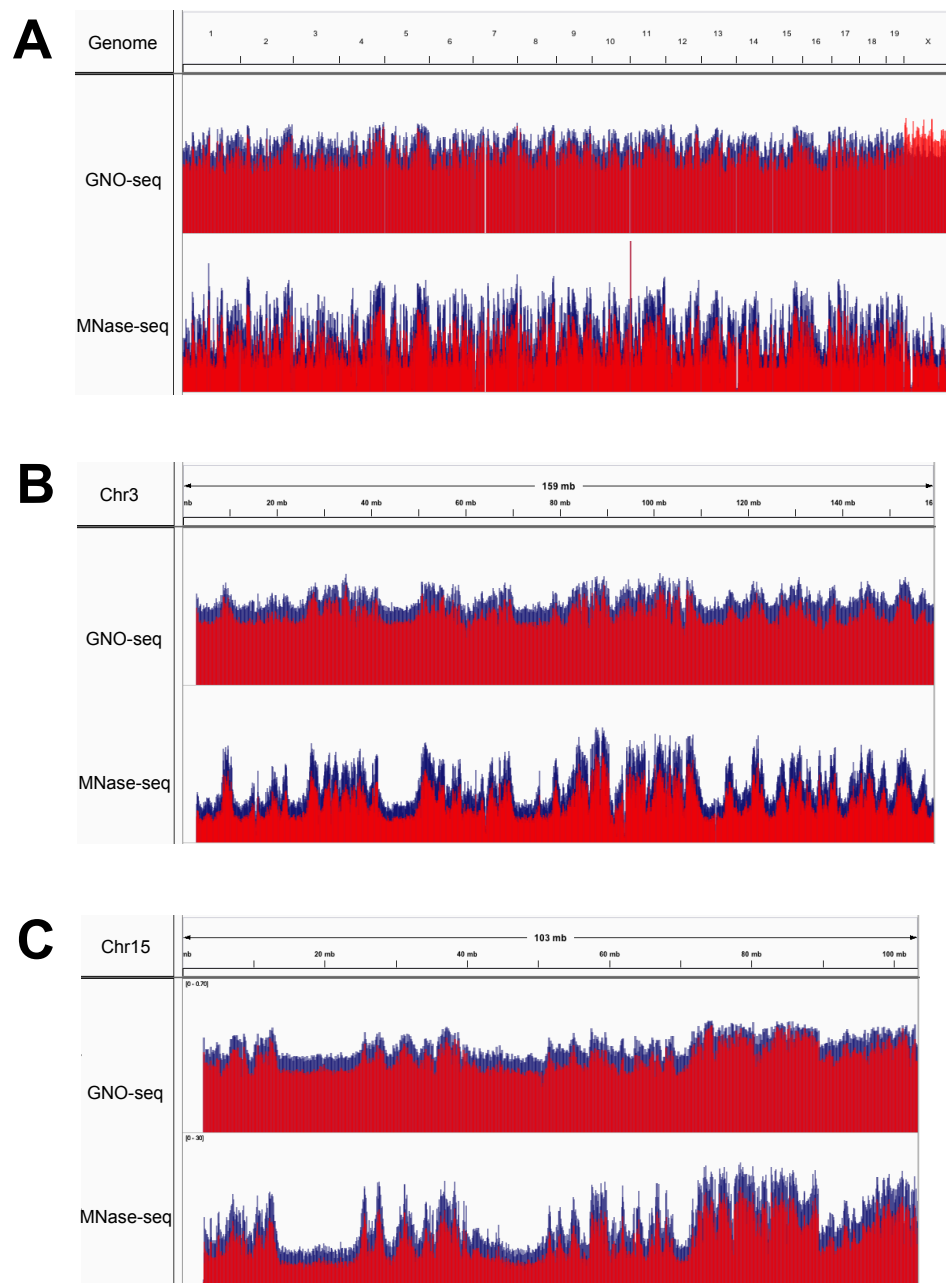
(A-F) Nucleosome occupancy determined by GNO-seq in rM (blue) and aM (red) is shown at the genomic locations indicated in each panel using the genome browser IGV (35). Underneath each panel nucleosome occupancy determined by the qRT-PCR assay as previously described (17) is shown for comparison.

Figure 4.S4. Nucleosome occupancy at *Il12b* and *Il1a* determined by the MNase option of deepTools bamCoverage, DANPOS and GNO-seq, and compared to the qRT-PCR based assay.



(A) and **(B)** Reference normalized MNase-seq data for rM (blue) and aM (red) was analyzed as described in *Suppl. Experimental Procedures* and occupancies at the enhancer and promoter of *Il12B* (A) and the enhancer of *Il1a* (B) are shown using the genome browser IGB.

Figure 4.S5. Nucleosome occupancy in the genome analyzed by GNO-seq and deepTools bamCoverage without dyad alignment.

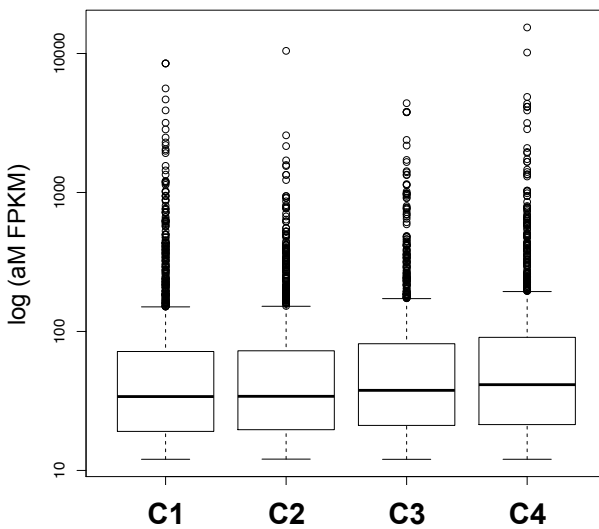


(A) Nucleosome occupancy was determined in rM (blue) and aM (red) as described in *Suppl. Experimental Procedures* and occupancy in the whole mouse genome is shown using IGV.

Figure 4.S5. (cont'd)

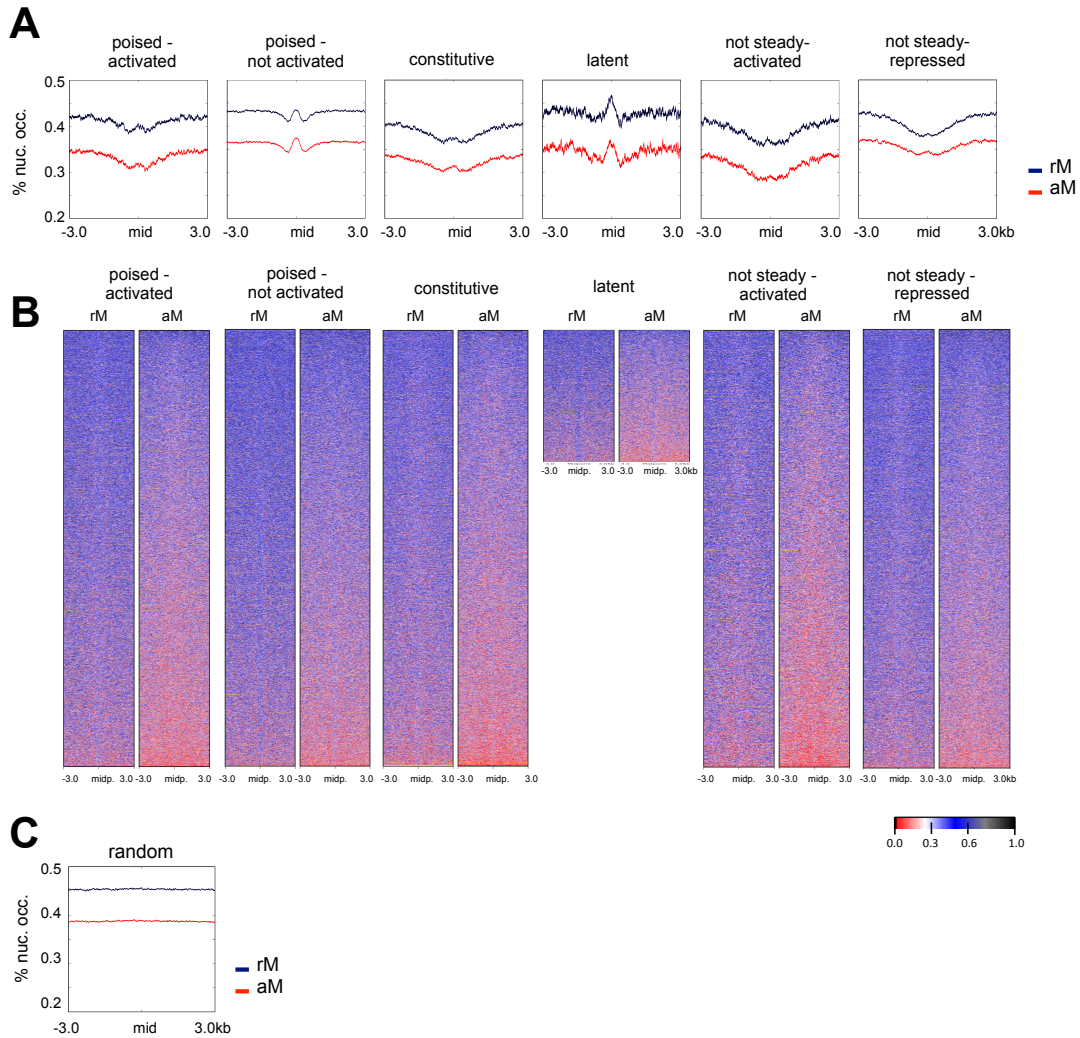
(B) and **(C)** Nucleosome occupancy was determined as in (A) and chromosomes 3 and 15 are shown.

Figure 4.S6. Expression of genes highly expressed in the presence of LPS.



Boxplots show the distribution and median gene expression in FPKM of genes in clusters C1-4 of Fig. 2C. Expression data of BMDMs grown for 2 h in LPS was taken from Mancino et al (22).

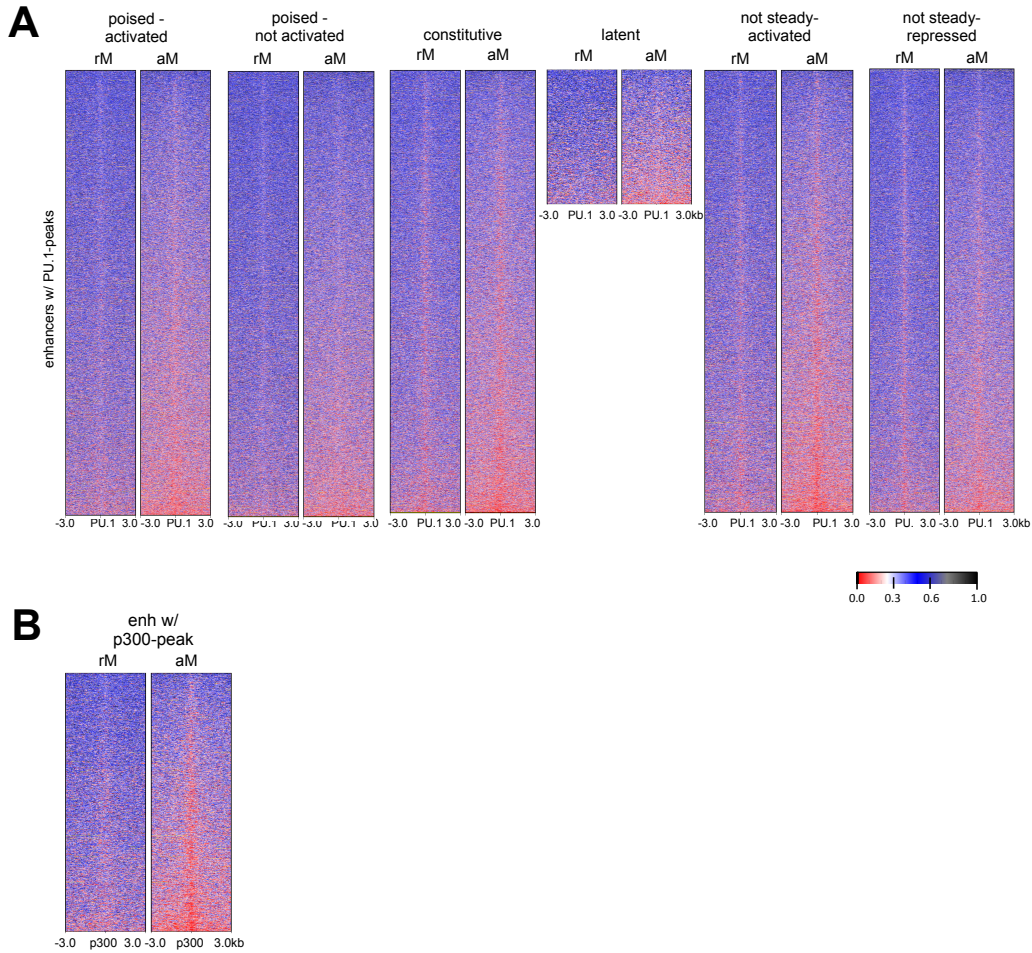
Figure 4.S7. Nucleosome occupancy at enhancers aligned at their midpoint.



(A) and **(B)** Nucleosome occupancy was determined by GNO-seq in rM (blue) and aM (red) at *bona fide* enhancers identified by (23) and separated into categories as described (Table 4.1). Average nucleosome occupancy plots (A) and heatmaps (B) after alignment of enhancers at their midpoints are shown.

(C) Average nucleosome occupancy in random genomic regions outside of promoter and enhancer regions is shown in rM (blue) and aM (red).

Figure 4.S8. Nucleosome occupancy at enhancers aligned at their PU.1 or p300 peaks.



(A) Enhancers of Ostuni et al. that contain a PU.1 peak identified as described in the legend of Fig. 4.4 were separated into categories (see Table 4.1) and heatmaps of nucleosome occupancy in rM and aM are shown after alignment at the PU.1 peaks.

(B) Enhancers of Ostuni et al. that contain a p300 peak identified as described in the legend of Fig. 4 and heatmaps of rM and aM are shown after alignment at the p300 peaks.

Table 4.S1. Threshold conditions defining partially depleted regions in rM and regions of nucleosome eviction in aM.

A						B											
occ. (%)	length (bp)	gap (bp)	# loci	# enh	% enh	occ. (%)	length (bp)	gap (bp)	# loci	# enh	% enh	occ. (%)	length (bp)	gap (bp)	# loci	# enh	% enh
70	2,000	0	3,859	1,537	2	20	600	0	2,623	710	1	30	200	0	853,228	36,859	53
70	2,000	1	6,004	2,224	3	20	500	0	6,035	1,647	2	25	160	0	1,004,226	37,110	53
70	1,200	1	73,230	12,376	18	25	600	0	7,103	2,057	3	30	190	0	957,175	38,717	56
70	1,200	2	93,268	14,951	21	30	600	0	13,448	3,593	5	25	150	0	1,141,237	39,105	56
70	1,200	3	114,173	17,401	25	20	400	0	17,399	3,629	5	20	100	0	1,381,123	39,117	56
75	1,200	1	114,960	18,889	27	25	500	0	18,391	4,008	6	20	140	10	1,299,838	40,230	58
70	1,000	1	145,664	19,131	28	30	500	0	33,706	6,576	9	20	100	1	1,482,644	40,559	58
75	1,200	2	144,308	22,224	32	20	300	0	63,793	8,325	12	30	180	0	1,072,534	40,582	58
70	1,000	2	177,930	22,269	32	20	300	1	74,912	9,170	13	25	140	0	1,299,083	41,094	59
70	1,000	3	210,512	25,076	36	20	300	2	86,631	10,057	14	20	100	2	1,578,063	41,825	60
75	1,200	3	174,498	25,369	36	20	300	3	99,425	10,902	16	30	170	0	1,202,540	42,435	61
80	1,200	1	181,966	26,230	38	30	400	0	92,617	11,938	17	25	140	1	1,407,029	42,679	61
75	1,000	1	213,615	26,829	39	20	250	0	130,698	12,601	18	20	100	3	1,667,439	42,930	62
70	800	1	298,377	29,046	42	20	250	1	151,000	13,750	20	25	130	0	1,482,040	43,144	62
80	1,200	2	222,104	30,233	43	20	250	2	172,160	14,865	21	25	140	2	1,506,659	44,027	63
75	1,000	2	257,480	30,527	44	25	300	0	174,189	15,660	23	30	160	0	1,349,764	44,268	64
70	800	2	349,647	32,437	47	20	250	3	194,209	15,900	23	20	100	5	1,828,340	44,733	64
80	1,200	3	261,019	33,762	49	25	300	1	204,019	17,172	25	25	120	0	1,696,153	45,142	65
75	1,000	3	300,501	33,840	49	25	300	2	234,872	18,489	27	25	140	3	1,598,840	45,233	65
80	800	3	398,765	35,441	51	20	200	0	277,323	19,012	27	20	140	20	1,695,962	45,285	65
75	800	1	407,131	37,391	54	25	300	3	265,828	19,699	28	30	150	0	1,515,090	46,080	66
80	1,000	2	366,351	38,737	56	20	190	0	323,145	20,531	30	25	140	5	1,761,962	47,193	68
75	800	2	470,491	40,986	59	30	300	0	275,260	21,562	31	25	110	0	1,950,893	47,299	68
80	1,000	3	416,444	42,011	60	25	250	0	322,939	21,739	31	30	140	0	1,703,142	47,964	69
75	800	3	529,021	44,071	63	20	180	0	377,086	22,192	32	25	100	10	2,141,205	48,044	69
80	800	1	546,142	45,048	65	25	250	1	369,299	23,397	34	25	100	0	2,255,839	49,286	71
80	800	2	614,730	48,511	70	30	300	1	321,237	23,463	34	30	140	1	1,832,689	49,387	71
80	800	3	675,376	51,260	74	20	170	0	439,777	23,951	34	30	130	0	1,919,450	49,756	72
80	600	3	1,114,344	59,931	86	25	250	2	416,058	24,860	36	25	140	10	2,073,328	50,523	73
80	400	3	1,874,913	66,596	96	30	300	2	367,906	25,124	36	25	100	1	2,386,199	50,591	73
						20	160	0	514,020	25,790	37	30	140	2	1,948,462	50,657	73
						25	250	3	462,033	26,210	38	30	120	0	2,169,813	51,524	74
						30	300	3	413,133	26,650	38	25	100	2	2,501,537	51,577	74
						20	150	0	600,613	27,767	40	30	140	3	2,053,256	51,752	74
						30	250	0	482,896	28,558	41	20	100	20	2,535,054	51,872	75
						25	200	0	605,136	29,653	43	25	100	3	2,603,405	52,577	76
						20	140	0	703,905	29,865	43	30	110	0	2,465,801	53,342	77
						30	250	1	550,009	30,475	44	30	140	5	2,231,986	53,563	77
						25	190	0	686,987	31,413	45	25	100	5	2,775,725	53,992	78
						20	140	1	774,258	31,470	45	25	140	20	2,448,648	54,665	79
						20	130	0	826,981	32,018	46	30	100	0	2,818,509	55,051	79
						30	250	2	615,643	32,153	46	30	100	1	2,962,610	56,145	81
						20	140	2	842,303	32,851	47	25	100	10	3,068,138	56,455	81
						25	180	0	779,296	33,241	48	30	140	10	2,546,508	56,525	81
						30	250	3	678,383	33,680	48	30	100	2	3,085,253	57,108	82
						20	140	3	908,369	34,093	49	30	100	3	3,189,925	57,874	83
						20	120	0	975,458	34,368	49	30	100	5	3,356,596	59,117	85
						25	170	0	884,410	35,200	51	25	100	20	3,342,784	59,417	85
						20	140	5	1,033,302	36,190	52	30	140	20	2,876,959	59,990	86
						20	110	0	1,157,464	36,653	53	30	100	10	3,612,190	61,164	88
												30	100	20	3,792,226	63,443	91

REFERENCES

REFERENCES

1. Buenroostro JD, Giresi PG, Zaba LC, Chang HY, Greenleaf WJ (2013) Transposition of native chromatin for fast and sensitive epigenomic profiling of open chromatin, DNA-binding proteins and nucleosome position. *Nature methods* 10: 1213-1218.
2. Hesselberth JR, Chen X, Zhang Z, Sabo PJ, Sandstrom R, Reynolds AP, Thurman RE, Neph S, Kuehn MS, Noble WS, Fields S, Stamatoyannopoulos JA (2009) Global mapping of protein- DNA interactions in vivo by digital genomic footprinting. *Nature methods* 6: 283-289.
3. Sabo PJ, Kuehn MS, Thurman R, Johnson BE, Johnson EM, Cao H, Yu M, Rosenzweig E, Goldy J, Haydock A, Weaver M, Shafer A, Lee K, Neri F, Humbert R, Singer MA, Richmond TA, Dorschner MO, McArthur M, Hawrylycz M, Green RD, Navas PA, Noble WS, Stamatoyannopoulos JA (2006) Genome-scale mapping of DNase I sensitivity in vivo using tiling DNA microarrays. *Nature methods* 3: 511-518.
4. Albert I, Mavrich TN, Tomsho LP, Qi J, Zanton SJ, Schuster SC, Pugh BF (2007) Translational and rotational settings of H2A.Z nucleosomes across the *Saccharomyces cerevisiae* genome. *Nature* 446: 572-576.
5. Carone BR, Hung JH, Hainer SJ, Chou MT, Carone DM, Weng Z, Fazzio TG, Rando OJ (2014) High-resolution mapping of chromatin packaging in mouse embryonic stem cells and sperm. *Developmental cell* 30: 11-22.
6. Iwafuchi-Doi M, Donahue G, Kakumanu A, Watts JA, Mahony S, Pugh BF, Lee D, Kaestner KH, Zaret KS (2016) The Pioneer Transcription Factor FoxA Maintains an Accessible Nucleosome Configuration at Enhancers for Tissue-Specific Gene Activation. *Molecular cell* 62: 79-91.
7. Kaplan N, Moore IK, Fondufe-Mittendorf Y, Gossett AJ, Tillo D, Field Y, LeProust EM, Hughes TR, Lieb JD, Widom J, Segal E (2009) The DNA-encoded nucleosome organization of a eukaryotic genome. *Nature* 458: 362-366.
8. Teif VB, Vainshtein Y, Caudron-Herger M, Mallm JP, Marth C, Hofer T, Rippe K (2012) Genome-wide nucleosome positioning during embryonic stem cell development. *Nature structural & molecular biology* 19: 1185-1192.
9. Henikoff JG, Belsky JA, Krassovsky K, MacAlpine DM, Henikoff S (2011) Epigenome characterization at single base-pair resolution. *Proceedings of the National Academy of Sciences of the United States of America* 108: 18318-18323.

10. Kubik S, Bruzzone MJ, Jacquet P, Falcone JL, Rougemont J, Shore D (2015) Nucleosome Stability Distinguishes Two Different Promoter Types at All Protein-Coding Genes in Yeast. *Molecular cell* 60: 422-434.
11. Mieczkowski J, Cook A, Bowman SK, Mueller B, Alver BH, Kundu S, Deaton AM, Urban JA, Larschan E, Park PJ, Kingston RE, Tolstorukov MY (2016) MNase titration reveals differences between nucleosome occupancy and chromatin accessibility. *Nature communications* 7: 11485.
12. Weiner A, Hughes A, Yassour M, Rando OJ, Friedman N (2010) High-resolution nucleosome mapping reveals transcription-dependent promoter packaging. *Genome research* 20: 90-100.
13. Xi Y, Yao J, Chen R, Li W, He X (2011) Nucleosome fragility reveals novel functional states of chromatin and poises genes for activation. *Genome research* 21: 718-724.
14. Bryant GO, Prabhu V, Floer M, Wang X, Spagna D, Schreiber D, Ptashne M (2008) Activator control of nucleosome occupancy in activation and repression of transcription. *PLoS biology* 6: 2928-2939.
15. Berrozpe G, Bryant GO, Warpinski K, Ptashne M (2013) Regulation of a Mammalian gene bearing a CpG island promoter and a distal enhancer. *Cell reports* 4: 445-453.
16. Floer M, Wang X, Prabhu V, Berrozpe G, Narayan S, Spagna D, Alvarez D, Kendall J, Krasnitz A, Stepansky A, Hicks J, Bryant GO, Ptashne M (2010) A RSC/nucleosome complex determines chromatin architecture and facilitates activator binding. *Cell* 141: 407-418.
17. Gjidoda A, Tagore M, McAndrew MJ, Woods A, Floer M (2014) Nucleosomes Are Stably Evicted from Enhancers but Not Promoters upon Induction of Certain Pro-Inflammatory Genes in Mouse Macrophages. *PLoS one* 9: e93971.
18. Mueller B, Mieczkowski J, Kundu S, Wang P, Sadreyev R, Tolstorukov MY, Kingston RE (2017) Widespread changes in nucleosome accessibility without changes in nucleosome occupancy during a rapid transcriptional induction. *Genes & development* 31: 451-462.
19. Bhatt DM, Pandya-Jones A, Tong AJ, Barozzi I, Lissner MM, Natoli G, Black DL, Smale ST (2012) Transcript dynamics of proinflammatory genes revealed by sequence analysis of subcellular RNA fractions. *Cell* 150: 279-290.
20. Ghisletti S, Barozzi I, Mietton F, Polletti S, De Santa F, Venturini E, Gregory L, Lonie L, Chew A, Wei CL, Ragoussis J, Natoli G (2010) Identification and

characterization of enhancers controlling the inflammatory gene expression program in macrophages. *Immunity* 32: 317-328.

21. Heinz S, Benner C, Spann N, Bertolino E, Lin YC, Laslo P, Cheng JX, Murre C, Singh H, Glass CK (2010) Simple combinations of lineage-determining transcription factors prime cis-regulatory elements required for macrophage and B cell identities. *Molecular cell* 38: 576-589.
22. Mancino A, Termanini A, Barozzi I, Ghisletti S, Ostuni R, Prosperini E, Ozato K, Natoli G (2015) A dual cis-regulatory code links IRF8 to constitutive and inducible gene expression in macrophages. *Genes & development* 29: 394-408.
23. Ostuni R, Piccolo V, Barozzi I, Polletti S, Termanini A, Bonifacio S, Curina A, Prosperini E, Ghisletti S, Natoli G (2013) Latent enhancers activated by stimulation in differentiated cells. *Cell* 152: 157-171.
24. Piccolo V, Curina A, Genua M, Ghisletti S, Simonatto M, Sabo A, Amati B, Ostuni R, Natoli G (2017) Opposing macrophage polarization programs show extensive epigenomic and transcriptional cross-talk. *Nature immunology* 18: 530-540.
25. Ramirez-Carrozzi VR, Braas D, Bhatt DM, Cheng CS, Hong C, Doty KR, Black JC, Hoffmann A, Carey M, Smale ST (2009) A unifying model for the selective regulation of inducible transcription by CpG islands and nucleosome remodeling. *Cell* 138: 114-128.
26. Barozzi I, Simonatto M, Bonifacio S, Yang L, Rohs R, Ghisletti S, Natoli G (2014) Coregulation of transcription factor binding and nucleosome occupancy through DNA features of mammalian enhancers. *Molecular cell* 54: 844-857.
27. Tagore M, McAndrew MJ, Gjidoda A, Floer M (2015) The lineage-specific transcription factor PU.1 prevents polycomb-mediated heterochromatin formation at macrophage-specific genes. *Molecular and cellular biology* 35: 2610-2625.
28. McAndrew MJ, Gjidoda A, Tagore M, Miksanek T, Floer M (2016) Chromatin Remodeler Recruitment during Macrophage Differentiation Facilitates Transcription Factor Binding to Enhancers in Mature Cells. *Journal of biological chemistry* 291: 18058-18071.
29. Bolger AM, Lohse M, Usadel B (2014) Trimmomatic: a flexible trimmer for Illumina sequence data. *Bioinformatics* 30: 2114-2120.
30. Langmead B, Salzberg SL (2012) Fast gapped-read alignment with Bowtie 2. *Nature methods* 9: 357-359.

31. Li H, Handsaker B, Wysoker A, Fennell T, Ruan J, Homer N, Marth G, Abecasis G, Durbin R (2009) The Sequence Alignment/Map format and SAMtools. *Bioinformatics* 25: 2078-2079.
32. Orlando DA, Chen MW, Brown VE, Solanki S, Choi YJ, Olson ER, Fritz CC, Bradner JE, Guenther MG (2014) Quantitative ChIP-Seq normalization reveals global modulation of the epigenome. *Cell reports* 9: 1163-1170.
33. Ramirez F, Ryan DP, Gruning B, Bhardwaj V, Kilpert F, Richter AS, Heyne S, Dundar F, Manke T (2016) deepTools2: a next generation web server for deep-sequencing data analysis. *Nucleic acids research* 44: W160-165.
34. Pohl A, Beato M (2014) bwtool: a tool for bigWig files. *Bioinformatics* 30: 1618-1619.
35. Thorvaldsdottir H, Robinson JT, Mesirov JP (2013) Integrative Genomics Viewer (IGV): high- performance genomics data visualization and exploration. *Briefings in bioinformatics* 14: 178- 192.
36. Kent WJ, Zweig AS, Barber G, Hinrichs AS, Karolchik D (2010) BigWig and BigBed: enabling browsing of large distributed datasets. *Bioinformatics* 26: 2204-2207.
37. Neph S, Kuehn MS, Reynolds AP, Haugen E, Thurman RE, Johnson AK, Rynes E, Maurano MT, Vierstra J, Thomas S, Sandstrom R, Humbert R, Stamatoyannopoulos JA (2012) BEDOPS: high-performance genomic feature operations. *Bioinformatics* 28: 1919-1920.
38. Quinlan AR, Hall IM (2010) BEDTools: a flexible suite of utilities for comparing genomic features. *Bioinformatics* 26: 841-842.
39. Smedley D, Haider S, Durinck S, Pandini L, Provero P, Allen J, Arnaiz O, Awedh MH, Baldock R, Barbiera G, Bardou P, et al. (2015) The BioMart community portal: an innovative alternative to large, centralized data repositories. *Nucleic acids research* 43: W589-598.
40. Ashburner M, Ball CA, Blake JA, Botstein D, Butler H, Cherry JM, Davis AP, Dolinski K, Dwight SS, Eppig JT, Harris MA, Hill DP, Issel-Tarver L, Kasarskis A, Lewis S, Matese JC, Richardson JE, Ringwald M, Rubin GM, Sherlock G (2000) Gene ontology: tool for the unification of biology. The Gene Ontology Consortium. *Nature genetics* 25: 25-29.
41. Whyte WA, Orlando DA, Hnisz D, Abraham BJ, Lin CY, Kagey MH, Rahl PB, Lee TI, Young RA (2013) Master transcription factors and mediator establish super-enhancers at key cell identity genes. *Cell* 153: 307-319.

42. Chen K, Xi Y, Pan X, Li Z, Kaestner K, Tyler J, Dent S, He X, Li W (2013) DANPOS: dynamic analysis of nucleosome position and occupancy by sequencing. *Genome research* 23: 341-351.
43. Chen K, Hu Z, Xia Z, Zhao D, Li W, Tyler JK (2015) The Overlooked Fact: Fundamental Need for Spike-In Control for Virtually All Genome-Wide Analyses. *Molecular and cellular biology* 36: 662-667.
44. Loven J, Orlando DA, Sigova AA, Lin CY, Rahl PB, Burge CB, Levens DL, Lee TI, Young RA (2012) Revisiting global gene expression analysis. *Cell* 151: 476-482.
45. De Toma I, Rossetti G, Zambrano S, Bianchi ME, Agresti A (2014) Nucleosome loss facilitates the chemotactic response of macrophages. *Journal of internal medicine* 276: 454-469.
46. Ruvinsky A, Marshall Graves JA (2005) *Mammalian Genomes*: CABI Publishing.
47. Fenouil R, Cauchy P, Koch F, Descostes N, Cabeza JZ, Innocenti C, Ferrier P, Spicuglia S, Gut M, Gut I, Andrau JC (2012) CpG islands and GC content dictate nucleosome depletion in a transcription-independent manner at mammalian promoters. *Genome research* 22: 2399-2408.
48. Lee W, Tillo D, Bray N, Morse RH, Davis RW, Hughes TR, Nislow C (2007) A high-resolution atlas of nucleosome occupancy in yeast. *Nature genetics* 39: 1235-1244.
49. Valouev A, Ichikawa J, Tonthat T, Stuart J, Ranade S, Peckham H, Zeng K, Malek JA, Costa G, McKernan K, Sidow A, Fire A, Johnson SM (2008) A high-resolution, nucleosome position map of *C. elegans* reveals a lack of universal sequence-dictated positioning. *Genome research* 18: 1051-1063.
50. Valouev A, Johnson SM, Boyd SD, Smith CL, Fire AZ, Sidow A (2011) Determinants of nucleosome organization in primary human cells. *Nature* 474: 516-520.
51. Wang X, Bryant GO, Floer M, Spagna D, Ptashne M (2011) An effect of DNA sequence on nucleosome occupancy and removal. *Nature structural & molecular biology* 18: 507-509.
52. Agalioti T, Lomvardas S, Parekh B, Yie J, Maniatis T, Thanos D (2000) Ordered recruitment of chromatin modifying and general transcription factors to the IFN-beta promoter. *Cell* 103: 667- 678.
53. Burd CJ, Ward JM, Crusselle-Davis VJ, Kissling GE, Phadke D, Shah RR, Archer TK (2012) Analysis of chromatin dynamics during glucocorticoid receptor activation. *Molecular and cellular biology* 32: 1805-1817.

54. Korber P, Luckenbach T, Blaschke D, Horz W (2004) Evidence for histone eviction in trans upon induction of the yeast PHO5 promoter. *Molecular and cellular biology* 24: 10965-10974.
55. Scruggs BS, Gilchrist DA, Nechaev S, Muse GW, Burkholder A, Fargo DC, Adelman K (2015) Bidirectional Transcription Arises from Two Distinct Hubs of Transcription Factor Binding and Active Chromatin. *Molecular cell* 58: 1101-1112.
56. Yuan GC, Liu YJ, Dion MF, Slack MD, Wu LF, Altschuler SJ, Rando OJ (2005) Genome-scale identification of nucleosome positions in *S. cerevisiae*. *Science* 309: 626-630.
57. Zhang Z, Wippo CJ, Wal M, Ward E, Korber P, Pugh BF (2011) A packing mechanism for nucleosome organization reconstituted across a eukaryotic genome. *Science* 332: 977-980.
58. Petesch SJ, Lis JT (2008) Rapid, transcription-independent loss of nucleosomes over a large chromatin domain at Hsp70 loci. *Cell* 134: 74-84.
59. Zhao J, Herrera-Diaz J, Gross DS (2005) Domain-wide displacement of histones by activated heat shock factor occurs independently of Swi/Snf and is not correlated with RNA polymerase II density. *Molecular and cellular biology* 25: 8985-8999.
60. Zaret KS, Carroll JS (2011) Pioneer transcription factors: establishing competence for gene expression. *Genes & development* 25: 2227-2241.
61. Cai DH, Wang D, Keefer J, Yeaman C, Hensley K, Friedman AD (2008) C/EBP alpha:AP-1 leucine zipper heterodimers bind novel DNA elements, activate the PU.1 promoter and direct monocyte lineage commitment more potently than C/EBP alpha homodimers or AP-1. *Oncogene* 27: 2772-2779.
62. Honma K, Udono H, Kohno T, Yamamoto K, Ogawa A, Takemori T, Kumatori A, Suzuki S, Matsuyama T, Yui K (2005) Interferon regulatory factor 4 negatively regulates the production of proinflammatory cytokines by macrophages in response to LPS. *Proceedings of the National Academy of Sciences of the United States of America* 102: 16001-16006.
63. Takaoka A, Yanai H, Kondo S, Duncan G, Negishi H, Mizutani T, Kano S, Honda K, Ohba Y, Mak TW, Taniguchi T (2005) Integral role of IRF-5 in the gene induction programme activated by Toll-like receptors. *Nature* 434: 243-249.
64. Suzuki HI, Young RA, Sharp PA (2017) Super-Enhancer-Mediated RNA Processing Revealed by Integrative MicroRNA Network Analysis. *Cell* 168: 1000-1014 e1015.

65. Reinke H, Horz W (2003) Histones are first hyperacetylated and then lose contact with the activated PHO5 promoter. *Molecular cell* 11: 1599-1607.
66. Gilchrist DA, Dos Santos G, Fargo DC, Xie B, Gao Y, Li L, Adelman K (2010) Pausing of RNA polymerase II disrupts DNA-specified nucleosome organization to enable precise gene regulation. *Cell* 143: 540-551.
67. Adelman K, Kennedy MA, Nechaev S, Gilchrist DA, Muse GW, Chinenov Y, Rogatsky I (2009) Immediate mediators of the inflammatory response are poised for gene activation through RNA polymerase II stalling. *Proceedings of the National Academy of Sciences of the United States of America* 106: 18207-18212.
68. Gupte R, Muse GW, Chinenov Y, Adelman K, Rogatsky I (2013) Glucocorticoid receptor represses proinflammatory genes at distinct steps of the transcription cycle. *Proceedings of the National Academy of Sciences of the United States of America* 110: 14616-14621.
69. Zhang Y, Moqtaderi Z, Rattner BP, Euskirchen G, Snyder M, Kadonaga JT, Liu XS, Struhl K (2009) Intrinsic histone-DNA interactions are not the major determinant of nucleosome positions in vivo. *Nature structural and molecular biology* 16: 847-852.

Chapter 5: Global nucleosome occupancy increases during differentiation of hematopoietic stem and progenitor cells into macrophages

Authors who contributed to this study were: Michael McAndrew, Mohita Tagore, Alison Gjidoda, Tyler Miksanek, and Monique Floer.

Introduction

Recent studies suggest that chromatin of pluripotent stem cells may be more accessible to DNA binding proteins, and that binding of certain factors in stem cells and early progenitors may keep cell-type specific genes accessible only in a specific cell-lineage. Genome-wide nucleosome binding has been assessed in different mammalian cell types, and an MNase (micrococcal nuclease) -seq analysis in embryonic stem cells (ESCs), mouse embryonic fibroblasts (MEFs) and neural progenitor cells (NPCs) indicated that ESC differentiation was associated with changes in nucleosome positioning (1). This study also showed that relative nucleosome occupancy (*i.e.*, sensitivity to MNase digestion) at binding sites for various transcription factors (TFs) differed in these cell types, and the investigators concluded that many TFs were preferentially associated with nucleosome-depleted sites. How nucleosomes are depleted from these sites has remained unclear. Previous studies have also shown that total chromatin of ESCs is more accessible to digestion by Dnase I or MNase than that of differentiated cells, and that the number of Dnase I hypersensitive sites decreased as cells differentiated (2,3). Furthermore, it has been suggested that the genome of ESCs may be largely accessible to the transcriptional machinery, since much of the genome was found to be transcribed at low levels (4). A larger fraction of the genome was also associated with “active” histone modifications and a smaller fraction was associated with heterochromatin marks in ESCs compared to differentiated cells (5). Compaction of chromatin has long been a measure for the differentiation state of a cell (6), and a recent study using super-resolution nanoscopy indicated that chromatin became more compacted as ESCs differentiated (7). Intriguingly, it was also found that cellular histone

levels (both mRNA and protein) were low in ESCs and increased as cells differentiated (7,8), but whether low levels of histone proteins result in low nucleosome occupancy in ESCs has not been investigated. Together these findings suggest that chromatin of multipotent stem cells is qualitatively different from that of differentiated cells, and that chromatin may undergo global changes during differentiation. This notion is consistent with two of our previous studies, the first of which showed that in the absence of binding of the lineage-specific or pioneer TF PU.1 to macrophage-specific enhancers in hematopoietic progenitors (HSPCs), the associated genes became wrapped into heterochromatin as cells differentiated and the genes could not be induced in fully differentiated cells (9). Heterochromatin formation was associated with an increase in nucleosome occupancy, as well as with binding of the polycomb repression complex (PRC2) and with the appearance of repressive histone modifications (*i.e.* H3K27me3). We have also shown that cell-type-specific enhancers of inducible pro-inflammatory genes are primed and rendered accessible in mature macrophages through the action of BAF/PBAF chromatin remodelers, which are likely recruited to these regulatory elements by the lineage-specific TF PU.1 during differentiation (10). How PU.1 and other lineage-specific TFs initially access their binding sites in stem and progenitor cells has remained unclear, however. In order to determine whether low nucleosome occupancy in stem and progenitor cells might facilitate lineage-specific TF binding early in the process of differentiation, we have investigated chromatin accessibility in undifferentiated multipotent HSPCs and ESCs. Surprisingly, we find that the cell-type specific changes at enhancers described in our previous studies occur as nucleosome

occupancy increases globally, and our results suggest that low nucleosome occupancy may be a universal feature of undifferentiated cells.

Experimental Procedures

Cell isolation and culture

Bone marrow cells were isolated as described from 6-8 week old C57BL/6 female mice (NCI/Charles River) with IACUC oversight (11). To obtain BMDMs, cells were differentiated into macrophages by growth in the presence of M-CSF as described (11,12). BMDMs were induced with LPS as described (11). HSPCs were isolated using the EasySep™ Mouse Hematopoietic Progenitor Cell Isolation Kit (Stemcell Technologies) per manufacturer's instructions, with an additional red blood lysis step prior to progenitor isolation. Briefly, $2-3 \times 10^7$ cells were resuspended in 1 ml red blood cell lysis buffer (Sigma) and mixed gently for 2 min. The buffer was diluted with 9 ml IMDM medium (Gibco), and cells were centrifuged at $400 \times g$ for 5 min. For the differentiation timecourse experiment cells were harvested on day 3, 5, 7 and 9. On day 3 and 5 many cells had not yet attached to the tissue culture plates and we collected only attached cells for our experiments. Unattached cells include undifferentiated cells and cells that do not survive these growth conditions (*i.e.*, the presence of M-CSF). We found that viability of unattached cells on day 3 was around 70%. By day 7 most cells had attached. For ESC experiments, R1 ESCs from ATCC (passage 11, a gift from the laboratory of Jason Knott) were first resuscitated onto a feeder layer of mitotically inactivated mouse embryonic fibroblasts (ATCC) in standard ES cell media (DMEM (Gibco) with 20% ESC-grade fetal bovine serum (Atlanta Biologicals S10250), 1x β -Mercaptoethanol, 1x non-essential amino acids, and 1 μ L/mL leukemia inhibitory factor

(Millipore ESG1106). Cells were passaged onto 0.1% gelatin twice to remove MEFs, then transferred to 2i ES cell media (standard ES cell media containing 1 μ M PD0325901 and 3 μ M GSK3 inhibitor Chir99021 (Stemgent)) for at least two passages. Mouse embryonic fibroblasts (MEFs) were provided by the laboratory of Amy Ralston, and were isolated as described in (13).

Quantitative nucleosome occupancy assay

The assay was performed essentially as described in (11) except that cross-linked chromatin from 0.5 to 1 x 10⁷ cells was used per experiment and the MNase (NEB) concentrations were adjusted to a range from 0.0027 U to 13.3 U. Bar graphs and overlays were generated using the IGB genome browser. The primer pairs for the amplicons in the *I12b* and *I1a* enhancers, and in the control regions can be given upon request. Intergenic region 1 corresponds to a region upstream of the *I1a* enhancer; intergenic 2 to a region between the constitutively expressed *Gmeb2* and *Stmn3* genes; intergenic 3 to a region in the Hox cluster, between the *Hoxd11* and *Hoxd10* genes; intergenic 4 to a region in the lymphocyte antigen locus, between *Ly6a* and *Ly6c1*; and intergenic 5 to a region upstream of the stress induced *Rps6ka5* gene.

Quantitation of total cellular chromatin protected against digestion by MNase

Total DNA remaining after digestion of chromatin from different cells with increasing concentrations of MNase was isolated using a QIAquick 96 PCR Purification Kit and quantified by SYBR Green on a FLUOstar Omega microplate reader (BMG Labtech). Briefly, 5 μ l of DNA was added to a solution of 95 μ l TE (10 mM Tris-HCl pH 8.0, 1 mM EDTA) containing 1x SYBR Green Gel loading dye (Lifetech). Analysis was performed in opaque 96-well microplates (PerkinElmer) using an excitation wavelength of 485 nm

and an emission wavelength of 520 nm. Data was analyzed using MARS Data Analysis Software (BMG Labtech).

Flow cytometry

Analysis was performed on a BD Biosciences LSR II flow cytometer. 1×10^5 cells were used per antibody. Cells were fixed with 1% formaldehyde for 10 min. and washed with PBS once. To block nonspecific Fc receptor binding, cells were incubated with 2.42G supernatant for 10 min., followed by a wash with PBS. Staining was performed in permeabilization buffer (PBS, 5% FBS, 0.1% sodium azide, 0.5% Triton X-100) for 30 min. in the dark with the lineage antibody cocktail provided in the EasySep™ Hematopoietic Progenitor Cell Isolation Kit probing for CD5, CD11b, CD19, CD45R/B220, Ly6G/C(Gr-1), TER119, 7-4 (19856; Stemcell Technologies) followed by secondary incubation with Streptavidin-PE (Lifetech), as well as for anti-CD117/KIT (60025; Stemcell Technologies) and anti-SCA1 (60032; Stemcell Technologies) followed by secondary incubation with anti-mouse-FITC (55499; MP Biomedicals). Cells were subsequently washed twice in flow wash buffer (PBS, 5% FBS, 0.1% sodium azide).

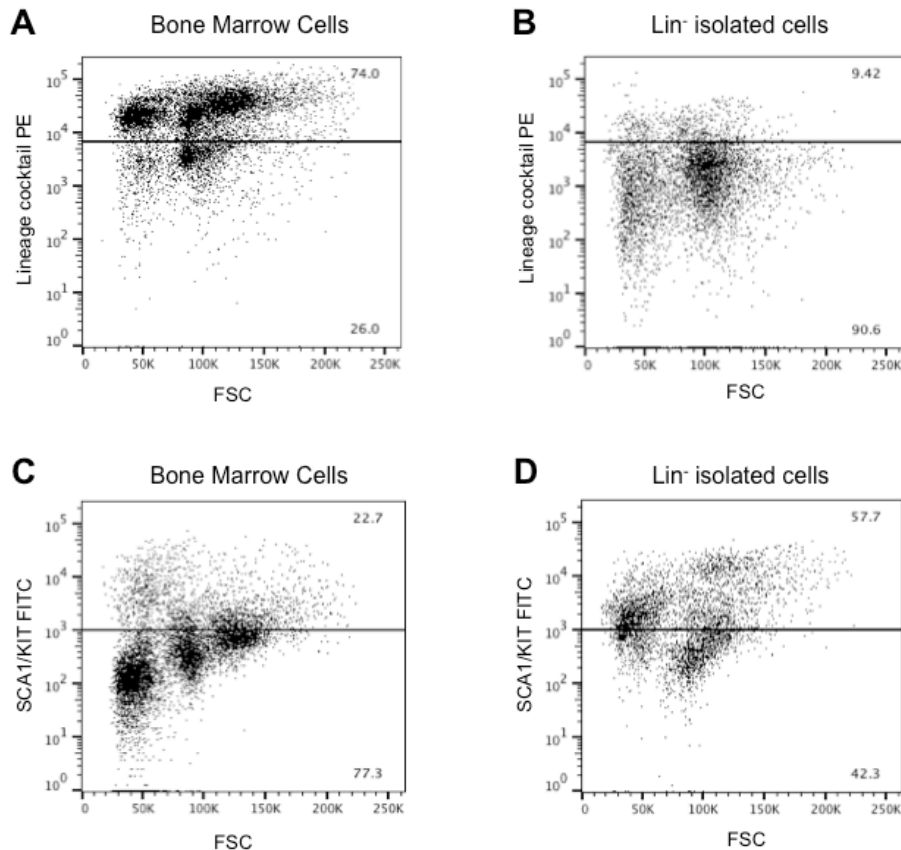
Results

Nucleosome occupancy at macrophage-specific enhancers increases during differentiation

To investigate how accessible chromatin is established at the enhancers of *Il12b* and *Il1a* during macrophage differentiation, we analyzed changes in nucleosome occupancy using the assay described (11) during a timecourse of *in vitro* differentiation of HSPCs into macrophages. Nucleosome occupancy was analyzed in HSPCs isolated by Lin⁻

selection from the bone marrow of adult female mice, and in cells grown for 3, 5, 7 and 9 days in the presence of M-CSF. We determined HSPC enrichment in total bone marrow via flow cytometry after negative selection using a cocktail of antibodies against multiple cell surface markers of differentiation (see Fig. 5.1 and *Experimental Procedures*). M-CSF promotes macrophage differentiation and yields fully differentiated bone marrow derived macrophages (BMDMs) after 9 days that respond to induction by LPS (11).

Figure 5.1. Isolation of HSPCs.



Isolation of Lin⁻ HSPCs was determined by flow cytometry as described in *Experimental Procedures*.

Figure 5.1. (cont'd)

(A) and (B) Total bone marrow (A) and HSPCs isolated from bone marrow (B) were analyzed for lineage-positive cells using the antibody cocktail used for isolation.

(C) and (D) Total bone marrow (C) and HSPCs (D) were analyzed for hematopoietic progenitor markers by staining with antibodies targeting SCA1 and KIT.

We found that nucleosome occupancy at the *Il12b* and *Il1a* enhancers was low in HSPCs (20-30%, Fig. 5.2A and B, cyan lines). This is in contrast to nucleosome occupancy at these sites in fully differentiated macrophages, which we had previously shown to be around 60% at preferred positions in the *Il12b* enhancer and between 40 and 60% in the *Il1a* enhancer (Fig. 5.2A and B, dark blue lines). As cells differentiated into macrophages, nucleosome occupancy at the enhancers increased gradually and preferred nucleosomal positions became more highly occupied (Fig. 5.2C-H).

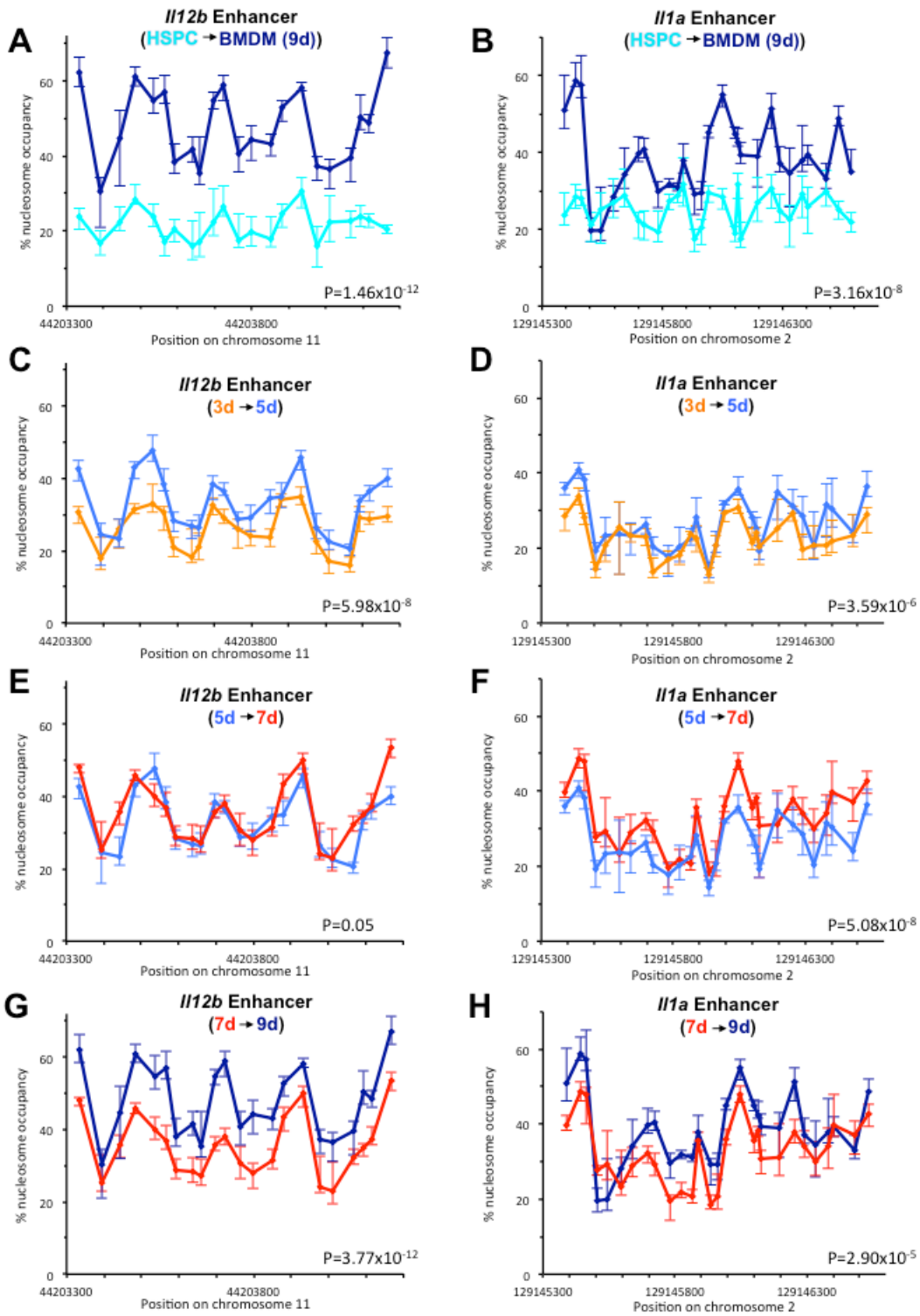
Differences in occupancy from one timepoint to the next were statistically significant as indicated by the P-values of paired, two-tailed Student's t-tests, with the exception of changes at the *Il12b* enhancer between days 5 and 7.

In Fig. 5.2J and K the changes at each enhancer over the timecourse of differentiation are shown as bar graphs in an overlay plot, where the width of each bar corresponds to the size of an amplicon. HSPCs and cells differentiated for 5 and 9 days are shown, which reveals that nucleosomes already formed at their preferred positions in HSPCs and occupancy at these positions increased as cells differentiated. A boxplot summarizing the changes at both enhancers shows that median occupancy increased from 24% to 40%, and occupancy at preferred nucleosomal peak positions increased from 32% to 65% (upper whiskers of boxplots in Fig. 5.2L). We also analyzed

nucleosome occupancy at regions in the promoters of both genes as well as at control loci and found that nucleosome occupancy in progenitors was low at all the locations tested (Fig. 5.2M shows a selection of the genomic regions we examined). At most locations nucleosome occupancy increased as cells differentiated, and occupancy at many regions reached levels higher than those found at the enhancers of *Il12b* and *Il1a*. For example, nucleosome occupancy at the promoters of *Il12b*, *cKit*, *Ikzf3*, *Sox2* and *Nanog*, as well as at five example intergenic regions, reached 70-100% in mature BMDMs. The intergenic control regions were selected to include regions in the vicinity of actively transcribed genes (*i.e.*, intergenic region 1 is upstream of the *Il1a* enhancer, and intergenic region 2 is between the two constitutively transcribed genes *Gmeb2* and *Stmn3*), as well as regions that are presumably silenced in macrophages (*i.e.*, intergenic region 3 is in the HOX cluster between *Hoxd11* and *Hoxd10*, and intergenic region 4 is in the lymphocyte antigen locus between *Ly6a* and *Ly6c1*). We also included a region upstream of a stress-inducible gene (*i.e.*, intergenic region 5 is upstream of *Rps6ka5*). Nucleosome occupancy at all these regions reached similar, high levels in BMDMs. In contrast, we found that the promoters of genes constitutively expressed in macrophages (*e.g.*, *Cd14*, *Cd18*, *Irf8* and *Egr1*) were lowly occupied in HSPCs, but occupancy further decreased during the timecourse of macrophage differentiation suggesting that promoter nucleosomes were evicted when these genes were expressed in the macrophage lineage. Together our results indicate that nucleosome occupancy is low in HSPCs and increases at most regions as cells differentiate, except at genes expressed in the macrophage lineage. While regulatory regions of genes that are constitutively expressed in macrophages became essentially nucleosome-free,

occupancy at the enhancers of genes that can only be induced in mature macrophages (i.e., *Il12b* and *Il1a*) reached intermediate levels between 40 and 60% in fully differentiated cells.

Figure 5.2. Nucleosome occupancy in HSPCs and differentiating BMDMs.



HSPCs and cells differentiated *in vitro* into macrophages by growth in the presence of M-CSF for different times were obtained as described in Experimental Procedures.

Figure 5.2. (cont'd)

HSPCs (cyan) and cells grown in the presence of M-CSF for 3 (orange), 5 (sky blue), 7 (red), and 9 days/BMDMs (dark blue) are shown. Nucleosome occupancy was analyzed using the quantitative assay described (11). Error bars show the confidence intervals of measurements at each genomic location derived from curve-fitting of MNase digestion data. Each dot in these graphs represents the midpoint of an amplicon. P-values indicate statistical significance of differences in the enhancers as determined by Student's t-tests.

(A) Nucleosome occupancy in HSPCs and fully differentiated BMDMs is shown at an enhancer 10 kb upstream of *Il12b*

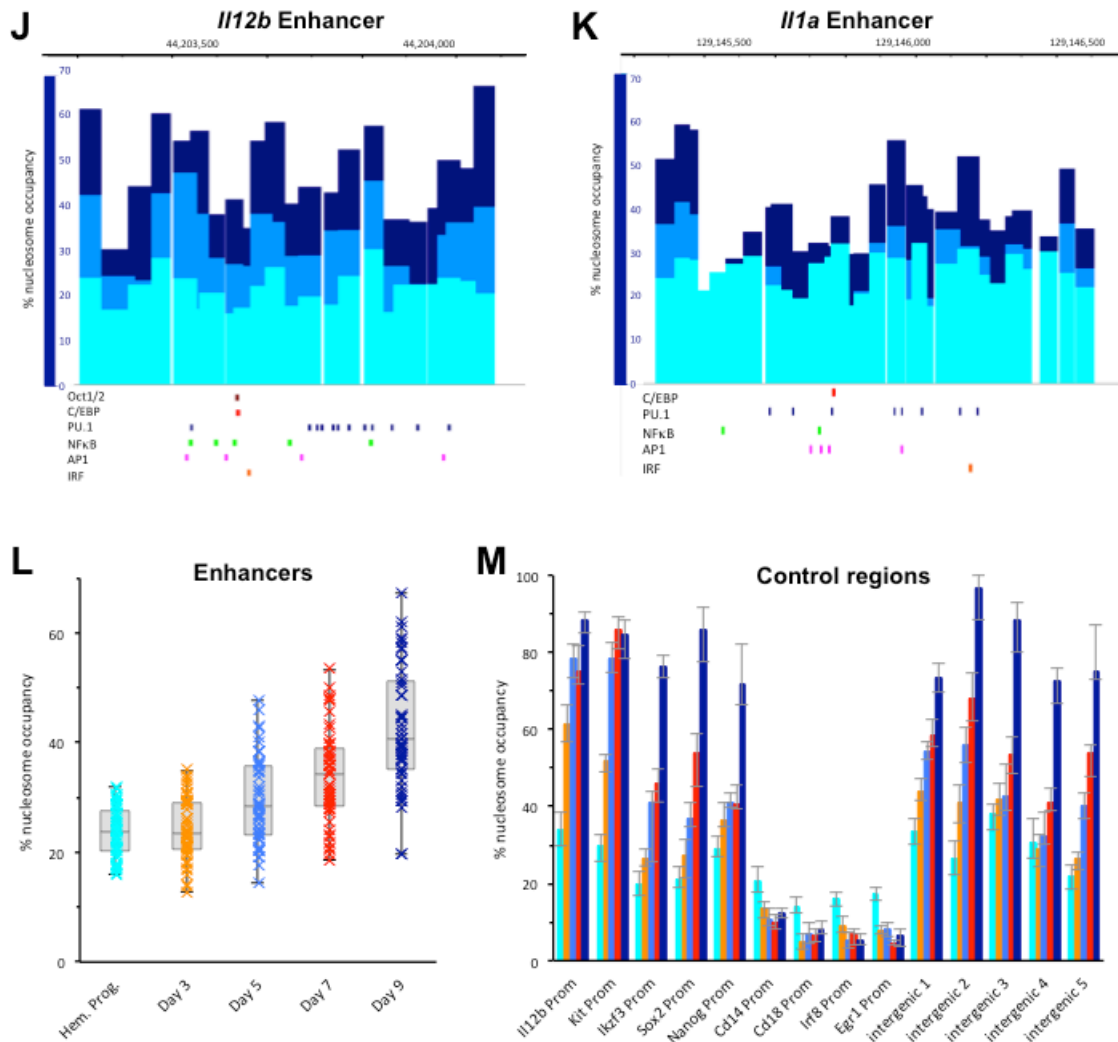
(B) Nucleosome occupancy in HSPCs and fully differentiated BMDMs is shown at an enhancer 10 kb upstream of *Il1a*.

(C) and **(D)** Nucleosome occupancy at the enhancers on days 3 and 5.

(E) and **(F)** Nucleosome occupancy at the enhancers at day 5 and 7.

(G) and **(H)** Nucleosome occupancy at the enhancers at day 7 and day 9 (BMDMs).

Figure 5.2. (cont'd)



(J) and **(K)** The same data from Fig. 5.2A-H is shown as bar graphs, where the width of each bar corresponds to the size of an amplicon. Occupancy in HSPCs and cells differentiated for 5 days and in BMDMs is shown at the enhancers. Consensus sites for TFs are indicated.

(L) A boxplot shows a summary of the changes in nucleosome occupancy at both enhancers.

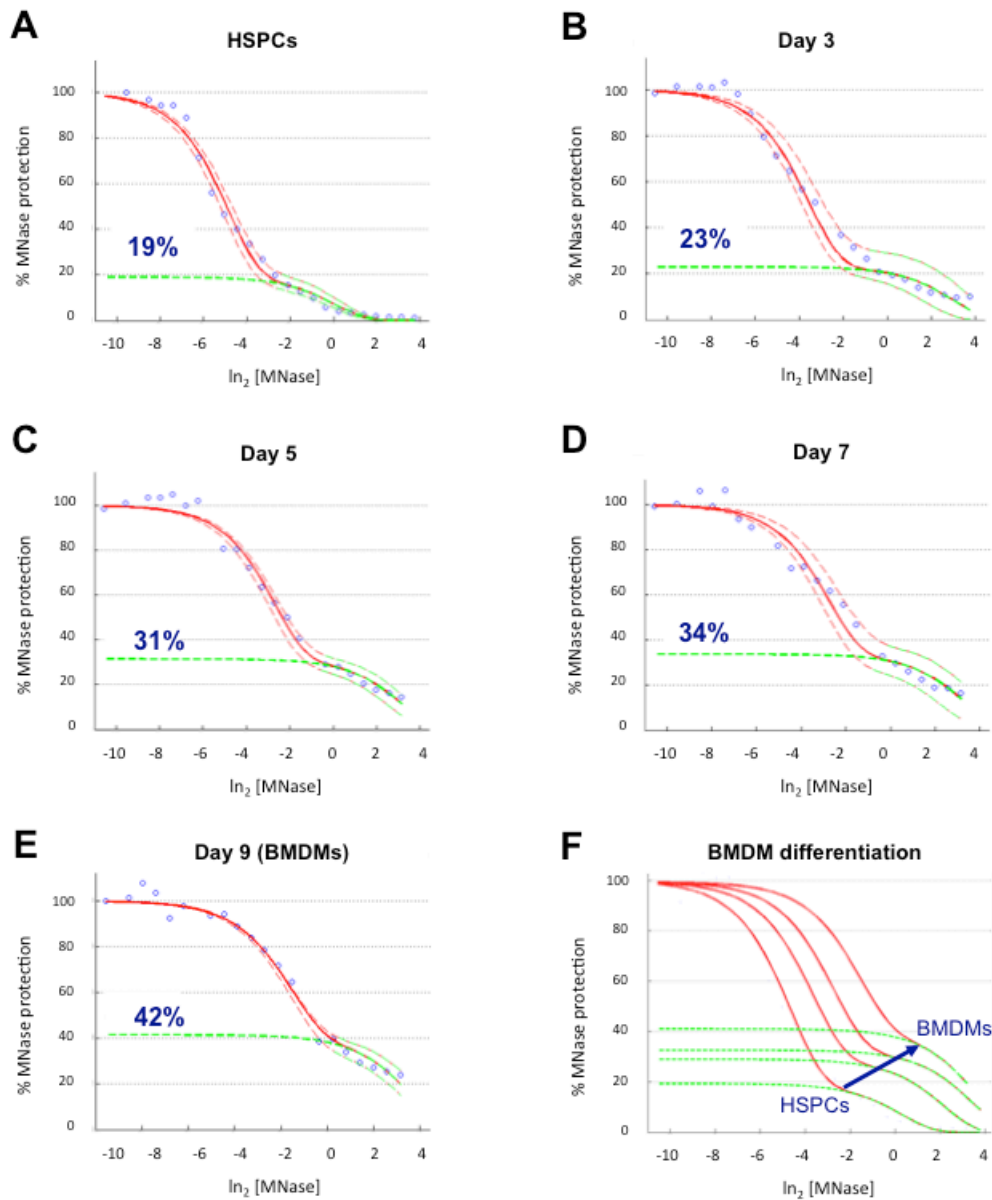
Figure 5.2. (cont'd)

(M) Nucleosome occupancy is shown at the genomic regions indicated in cells as in (A-H). Exact locations of the amplicons are described in Experimental Procedures. A Student's t-test shows statistical significance of differences between HSPCs and BMDMs ($p < 0.05$).

Protection of total cellular chromatin against MNase increases as HSPCs differentiate into macrophages

Our results at individual loci suggested the intriguing possibility that nucleosome occupancy may be low genome-wide in HSPCs and increase as cells differentiate. To further investigate this we determined whether differentiation led to increased protection against MNase of *total* cellular chromatin. We analyzed the total DNA remaining after digestion of chromatin with increasing concentrations of MNase as described in Experimental Procedures and found that the fraction of total genomic DNA that was protected against digestion by MNase steadily increased as cells differentiated (Fig. 5.3A-F). In HSPCs about 19% of total genomic DNA was protected, while levels of protection reached 42% in fully differentiated BMDMs. We note that the percent protection in this analysis does *not* represent the fractional occupancy of defined nucleosomal positions, but rather provides a measure for the median nucleosome occupancy of the genome including linker and nucleosome-free regions. Together, our results indicate that nucleosome occupancy may be universally low in undifferentiated progenitors and may increase as cells differentiate.

Figure 5.3. Protection of total cellular chromatin against digestion by MNase in HSPCs and in differentiating BMDMs.



Chromatin of cells obtained as described in the legend of Fig. 5.2 was digested with increasing concentrations of MNase, total DNA remaining after digestion was determined, and data was analyzed by curve-fitting as described in Experimental Procedures in (A) HSPCs, and cells grown in the presence of M-CSF for (B) 3 days, (C)

Figure 5.3. (cont'd)

5 days, (D) 7 days and (E) 9 days (BMDMs). (F) Overlay of the same data from HSPCs and cells grown in the presence of M-CSF for 3, 7, and 9 days shows increased protection.

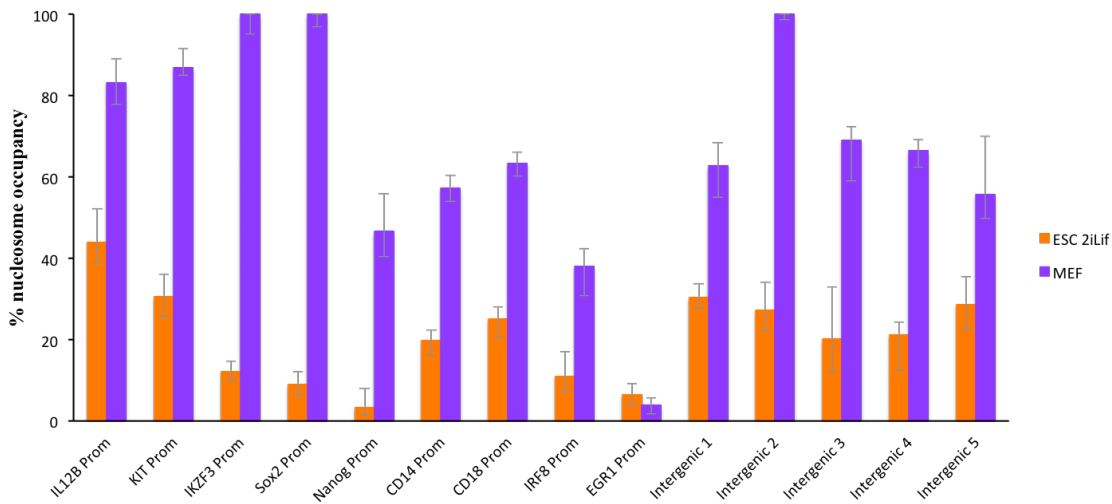
Nucleosome occupancy is lower in ESCs than in differentiated cells

In order to determine whether low nucleosome occupancy might be a universal feature of multipotent undifferentiated cells, we extended our analyses to ESCs. The ESCs were grown and passaged in 2i medium (see Experimental Procedures), as it has been suggested that this maintains “ground-state” pluripotency, and results in a more homogenous population of cells than growth in standard ESC media (14). However, we note that occupancy at control locations was similar in cells grown in standard ESC media (McAndrew, M.J. and Floer, M., unpublished data). We used primary mouse embryonic fibroblasts (MEFs, see Experimental Procedures) as differentiated control cells for these experiments and found that occupancy was low at all of the regions tested in ESCs. Similar to our results in mature macrophages, occupancy in MEFs reaches intermediate to high levels of occupancy at nearly all of the locations tested except at the *Egr1* promoter, presumably because of *Egr1*'s role as an active tumor suppressor in these cells (15). Occupancy in ESCs was also lower than in mature BMDMs (compare orange bars in Fig. 5.4A to dark blue bars in Fig. 5.2M), except at the promoters of genes that are constitutively expressed in BMDMs (e.g., *Cd14*, *Cd18*, *Irf8* and *Egr1*). Taken together with our results in HSPCs and differentiating bone marrow cells, our analysis of nucleosome occupancy in ESCs and MEFs suggests that low

nucleosome occupancy may be a universal feature of undifferentiated multipotent cells, and that nucleosome occupancy increases during the process of differentiation.

Figure 5.4. Nucleosome occupancy in ESCs and differentiated MEFs.

Nucleosome occupancy is shown at the control regions from Figure 5.2M in ESCs (orange bars) and MEFs (purple bars).



Discussion

Our analysis indicates that nucleosome occupancy increases globally as cells differentiate from HSPCs into BMDMs. We find using our quantitative assay that nucleosome occupancy at all the locations tested was low in HSPCs and increased as cells differentiated (Fig. 5.2). Moreover, we find that nucleosome occupancy was also low at these locations in ESCs when compared to either differentiated MEFs or mature macrophages (Fig. 5.4). Our results also show that protection of total chromatin against MNase increased as HSPCs differentiated into mature macrophages (Fig. 5.3), suggesting that nucleosome occupancy may change globally during differentiation. The increases in nucleosome occupancy we have observed at many genomic locations during macrophage differentiation cannot be solely a consequence of transcriptional

repression of genes, since we also found increased occupancy at intergenic regions not involved in transcriptional regulation in BMDMs. Nevertheless, some increases may indeed be a consequence of repression, such as those found at the promoter of *cKit*, which is expressed in HSPCs and turned off in the macrophage lineage. Similarly, we believe that further depletion of nucleosomes at promoters of genes that become constitutively expressed in the macrophage lineage is likely a consequence of their activation (e.g., *Cd14*, *Cd18*, *Irf8* and *Egr1*). On the other hand, the low levels of nucleosome occupancy we have observed at many locations in HSPCs are unlikely to be a direct consequence of active gene expression, since we found low occupancy at intergenic regions and at promoters of genes that are not expressed in these cells (e.g., *Il12b*, *Ikzf3*, *Sox2* and *Nanog*) (Fig. 5.1M) (16). Rather, it is possible that low nucleosome occupancy may facilitate low levels of spurious transcription from many genomic locations, an idea consistent with the finding in yeast that reduced nucleosome occupancy led to transcriptional upregulation of the genome (17). The global increases in nucleosome occupancy suggested by our findings (Fig. 5.2-5.4) may limit transcription to genes used only in a specific cell-type, while the majority of the genome becomes silenced. What might regulate such global changes in nucleosome occupancy remains to be determined, but we hypothesize that this may be a consequence of changes in histone expression. Intriguingly, recent studies showed that histone proteins become limiting in aging cells (18,19) and loss of nucleosomes in aging yeast resulted in increased global transcription (17). Not only do these studies suggest that histone expression may change as a consequence of various cellular processes such as aging or differentiation, but also that these changes may be directly correlated with spurious

transcription from previously silenced loci. Low levels of transcription from much of the genome have also been detected in ESCs (4), and our finding that nucleosome occupancy is lower in ESCs than in either MEFs or mature BMDMs (Fig. 5.4) is consistent with a number of previous studies which suggested that chromatin in ESCs is qualitatively different than in differentiated cells (3,7,8), and that chromatin becomes more highly compacted during differentiation (7). Increased chromatin compaction has also been observed during hematopoiesis (see for example (6)) and has long been used by histologists to assess the differentiation stage of different blood cells. Our results suggest that the low chromatin compaction observed may be a consequence of low genome-wide nucleosome occupancy in these cells, and that low nucleosome occupancy may be a hallmark of multipotent progenitors and stem cells. This may render their DNA more accessible to any DNA-binding TF, which may ultimately be the reason for their plasticity and stemness. Our results are consistent with and add important context to the model of remodeler-assisted competition proposed in (10), which posits that BAF/PBAF chromatin remodelers are recruited to macrophage-specific enhancers during differentiation by the lineage-specific TF PU.1, increasing nucleosome turnover at these regulatory elements such that they are accessible to signal-induced TFs in the presence of LPS. Based on our analyses in undifferentiated multipotent cells, as well as cells collected at various points during differentiation, we propose that pioneer transcription factors bind to lineage-specific regulatory elements and recruit BAF/PBAF when overall nucleosome occupancy in the genome is low during the early stages of differentiation, thus keeping enhancers accessible while the rest of the genome becomes wrapped into highly occupied nucleosomes. However, it remains to

be determined whether nucleosome occupancy indeed changes genome-wide during differentiation. The recently developed GNO-seq (described in Chapter 4) is an ideal method to investigate genome-wide occupancy in HSPCs and ESCs, as the use of external spike-in controls and Input fractions during sequencing allows for direct comparison between different cell types.

REFERENCES

REFERENCES

1. Teif VB, Vainshtein Y, Caudron-Herger M, Mallm JP, Marth C, Hofer T, Rippe K (2012) Genome-wide nucleosome positioning during embryonic stem cell development. *Nature structural & molecular biology* 19: 1185-1192.
2. Schaniel C, Ang YS, Ratnakumar K, Cormier C, James T, Bernstein E, Lemischka IR, Paddison PJ (2009) Smarcc1/Baf155 couples self-renewal gene repression with changes in chromatin structure in mouse embryonic stem cells. *Stem cells* 27: 2979-2991.
3. Stergachis AB, Neph S, Reynolds A, Humbert R, Miller B, Paige SL, Vernot B, Cheng JB, Thurman RE, Sandstrom R, Haugen E, Heimfeld S, Murry CE, Akey JM, Stamatoyannopoulos JA (2013) Developmental fate and cellular maturity encoded in human regulatory DNA landscapes. *Cell* 154: 888-903.
4. Efroni S, Duttagupta R, Cheng J, Dehghani H, Hoepfner DJ, Dash C, Bazett-Jones DP, Le Grice S, McKay RD, Buetow KH, Gingeras TR, Misteli T, Meshorer E (2008) Global transcription in pluripotent embryonic stem cells. *Cell stem cell* 2: 437-447.
5. Meshorer E, Yellajoshula D, George E, Scambler PJ, Brown DT, Misteli T (2006) Hyperdynamic plasticity of chromatin proteins in pluripotent embryonic stem cells. *Developmental cell* 10: 105-116.
6. Kernell AM, Bolund L, Ringertz NR (1971) Chromatin changes during erythropoiesis. *Experimental cell research* 65: 1-6.
7. Ricci MA, Manzo C, Garcia-Parajo MF, Lakadamyali M, Cosma MP (2015) Chromatin fibers are formed by heterogeneous groups of nucleosomes in vivo. *Cell* 160: 1145-1158.
8. Karnavas T, Pintonello L, Agresti A, Bianchi ME (2014) Histone content increases in differentiating embryonic stem cells. *Frontiers in physiology* 5: 330.
9. Tagore, M., McAndrew, M. J., Gjidoda, A., Floer, M. (2015) The lineage-specific transcription factor PU.1 prevents polycomb-mediated heterochromatin formation at macrophage-specific genes. *Molecular and cellular biology* 35, 2610-2625.
10. McAndrew MJ, Gjidoda A, Tagore M, Miksanek T, Floer M (2016) Chromatin Remodeler Recruitment during Macrophage Differentiation Facilitates Transcription Factor Binding to Enhancers in Mature Cells. *The Journal of biological chemistry* 291: 18058-18071.

11. Gjidoda A, Tagore M, McAndrew MJ, Woods A, Floer M (2014) Nucleosomes Are Stably Evicted from Enhancers but Not Promoters upon Induction of Certain Pro-inflammatory Genes in Mouse Macrophages. *PLoS one* 9: e93971.
12. Nociari, M., Ocheretina, O., Schoggins, J. W., Falck-Pedersen, E. (2007) Sensing infection by adenovirus: Toll-like receptor-independent viral DNA recognition signals activation of the interferon regulatory factor 3 master regulator. *Journal of virology* 81, 4145-4157.
13. Parenti, A., Halbisen, Michael A., Wang, K., Latham, K., Ralston, A. (2016) OSKM Induce Extraembryonic Endoderm Stem Cells in Parallel to Induced Pluripotent Stem Cells. *Stem cell reports* 6, 447-455.
14. Ying, Q.-L., Wray, J., Nichols, J., Battle-Morera, L., Doble, B., Woodgett, J., Cohen, P., and Smith, A. (2008) The ground state of embryonic stem cell self-renewal. *Nature* 453, 519-523.
15. Kronen-Herzig, A., Mittal, S., Yule, K., Liang, H., English, C., Urcis, R., Soni, T., Adamson, E. D., and Mercola, D. (2005) Early growth response 1 acts as a tumor suppressor in vivo and in vitro via regulation of p53. *Cancer research* 65, 5133-5143.
16. Tanaka Y, Era T, Nishikawa S, Kawamata S (2007) Forced expression of Nanog in hematopoietic stem cells results in a gammadeltaT-cell disorder. *Blood* 110: 107-115.
17. Hu Z, Chen K, Xia Z, Chavez M, Pal S, Seol JH, Chen CC, Li W, Tyler JK (2014) Nucleosome loss leads to global transcriptional up-regulation and genomic instability during yeast aging. *Genes & development* 28: 396-408.
18. Feser J, Truong D, Das C, Carson JJ, Kieft J, Harkness T, Tyler JK (2010) Elevated histone expression promotes life span extension. *Molecular cell* 39: 724-735.
19. O'Sullivan RJ, Kubicek S, Schreiber SL, Karlseder J (2010) Reduced histone biosynthesis and chromatin changes arising from a damage signal at telomeres. *Nature structural & molecular biology* 17: 1218-1225.

Chapter 6: Conclusions and future directions

The goal of this study was to characterize chromatin structure at distal regulatory elements involved in the inducible pro-inflammatory gene expression program of mouse macrophages. Our studies at individual pro-inflammatory enhancers, as well as the genome-wide studies we have conducted, have provided key insights into the mechanisms by which accessibility is maintained at enhancers in mature macrophages, ensuring rapid nucleosome removal, transcription factor binding, and gene activation in stimulated cells.

Our study in chapter 2 focuses on the promoters and distal enhancers of two inducible pro-inflammatory cytokines, IL12B and IL1A, in mouse macrophages. Using the quantitative nucleosome occupancy assay developed by Bryant et. al (1), we show that these enhancers display intermediate nucleosome occupancy (40-60%), suggesting that they may be rendered accessible even in resting cells by lineage-specific transcription factors (2,3) and/or chromatin remodelers (4). We did detect binding of the lineage-specific transcription factors PU.1 and C/EBP β at these enhancers even before induction with LPS, suggesting a role for these factors in the maintenance of enhancer accessibility. Upon induction, 2-3 nucleosomes are removed from the enhancers, and this removal is concurrent with the recruitment of both lineage-specific (PU.1, C/EBP β) and signal-induced (NF- κ B, AP-1, IRF3) transcription factors, indicating that nucleosome removal may be required for transcription factor binding and subsequent gene induction. We did not detect nucleosome removal at the IL12B or IL1A promoters, despite a clear increase in gene expression and recruitment of the transcriptional machinery to these promoters. This may be explained by studies from ourselves and others which have indicated that the expression of these and other inducible genes is

highly stochastic (4,5,6), perhaps due to rapid nucleosome reformation at promoters. Further investigation into the kinetics of nucleosome reformation at inducible promoters, as well as the factors that prevent promoters in cells with active (i.e. cleared of nucleosomes and bound by transcription factors) enhancers from firing would provide valuable insight into the regulation of inducible gene expression.

In chapter 3, we continue to investigate the role of both lineage-specific transcription factors and chromatin remodelers in the maintenance of enhancer accessibility. Using an shRNA knockdown approach in differentiating macrophages, we find that BAF/PBAF nucleosome remodelers are required to maintain intermediate (40-60%) occupancy at the IL12B and IL1A enhancers via the proposed model of remodeler-assisted competition. Further, using an inducible cell line expressing an estrogen receptor fusion of the lineage-specific transcription factor PU.1, we show that the recruitment of BAF/PBAF remodelers to these enhancers is correlated with PU.1 binding at these loci, suggesting that PU.1 may directly recruit remodelers to cell-type specific regulatory elements. Quantitative nucleosome occupancy analysis in the absence of BAF/PBAF upon induction with LPS also indicates that histone eviction is at least partially regulated by chromatin remodelers, as enhancer nucleosomes are not completely removed under these conditions. Further, this lack of nucleosome removal results in impaired gene expression, suggesting that histone eviction at regulatory elements is in fact required for inducible gene expression. Although other lineage-specific transcription factors such as C/EBP β have been shown to interact directly with chromatin remodelers (7), further study is needed to determine whether the recruitment of BAF/PBAF complexes to inducible enhancers is mediated directly by PU.1. It is also as yet unclear whether the

remodeler-assisted competition model proposed requires BAF, PBAF, or both chromatin remodeling complexes. In yeast, the SWI/SNF complex has been shown to remove nucleosomes from inducible gene promoters (8,9), while the RSC complex positions nucleosomes at regulatory elements (10,11) and partially unwraps nucleosomes to allow transcription factor binding (12). The homologous BAF and PBAF complexes require further study to determine whether there might be a similar delineation of function at regulatory elements.

In Chapter 4, we describe the development of the GNO-seq method, an extension of the quantitative nucleosome occupancy assay that allows us to determine fractional nucleosome occupancies genome-wide using next-generation sequencing technology. Using this technique, we find that the promoters of most induced genes are nucleosome depleted in resting macrophages before LPS treatment, and that nucleosome occupancy decreases further in activated macrophages. Consistent with our studies in chapter 2, however, we also identify a small subset of induced promoters which are not depleted in resting macrophages and remain associated with nucleosomes in activated cells. Further, we analyze chromatin signatures at LPS-responsive enhancers and detect intermediate occupancy at these loci in resting cells, particularly at known PU.1 binding sites, as well as further nucleosome depletion in activated macrophages, consistent with our results in chapters 2 and 3. Although GNO-seq represents an important advance over current MNase-seq methods, further testing of this novel method is required to determine its efficacy in generating nucleosome occupancy data from other (i.e. non-mouse) organisms. As the cost of sequencing genomes drops, complete genomic maps are being generated for many non-model organisms (8). GNO-

seq may be utilized to identify putative regulatory elements in these organisms, particularly if relevant TFs have not yet been identified.

In Chapter 5, we further investigate how enhancer accessibility may be maintained during macrophage differentiation. Surprisingly, we find that occupancy is low at all locations tested in hematopoietic stem and progenitor cells, and, utilizing differentiating cells collected at various intermediate timepoints, that occupancy increases in a stepwise fashion as cells mature. When we extended these analyses to embryonic stem cells, we found that occupancy was low in these cells when compared to either differentiated macrophages or mouse embryonic fibroblasts, suggesting that low nucleosome occupancy is an important feature of undifferentiated cells. Further investigation using the GNO-seq method is required to determine whether nucleosome occupancy is indeed low genome-wide in these cell types. At this time, it also remains unclear whether the low occupancy we observed is the result of decreased histone expression, decreased histone chaperone expression/activity, or some other unknown factor, and the implications for gene expression and regulation in undifferentiated cells require further investigation. The ensuing studies will not only help to further characterize multipotent progenitor cells: it is increasingly clear that induced pluripotent stem cells (iPSCs) retain an epigenetic memory of their previous differentiated state (14,15). Thus, a better understanding of chromatin structure in multipotent progenitor cells may help to optimize reprogramming protocols that can safely and efficiently generate iPSCs for therapeutic use.

REFERENCES

REFERENCES

1. Bryant, G. O., Prabhu, V., Floer, M., Wang, X., Spagna, D., Schreiber, D., and Ptashne, M. (2008) Activator control of nucleosome occupancy in activation and repression of transcription. *PLoS biology* 6, 2928-2939.
2. Heinz, S., Benner, C., Spann, N., Bertolino, E., Lin, Y. C., Laslo, P., Cheng, J. X., Murre, C., Singh, H., and Glass, C. K. (2010) Simple combinations of lineage-determining transcription factors prime cis-regulatory elements required for macrophage and B cell identities. *Molecular cell* 38, 576-589.
3. Ghisletti, S., Barozzi, I., Mietton, F., Polletti, S., De Santa, F., Venturini, E., Gregory, L., Lonie, L., Chew, A., Wei, C. L., Ragoussis, J., and Natoli, G. (2010) Identification and characterization of enhancers controlling the inflammatory gene expression program in macrophages. *Immunity* 32, 317-328.
4. McAndrew, M. J., Gjidoda, A., Tagore, M., Miksanek, T. & Floer, M. Chromatin Remodeler Recruitment During Macrophage Differentiation Facilitates Transcription Factor Binding to Enhancers in Mature Cells. *The Journal of biological chemistry* 291, 18058-18071.
5. Weinmann AS, Plevy SE, Smale ST (1999) Rapid and selective remodeling of a positioned nucleosome during the induction of IL-12 p40 transcription. *Immunity* 11: 665–675.
6. Shalek, A. K., Satija, R., Adiconis, X., Gertner, R. S., Gaublomme, J. T., Raychowdhury, R., Schwartz, S., Yosef, N., Malboeuf, C., Lu, D., Trombetta, J. J., Gennert, D., Gnirke, A., Goren, A., Hacohen, N., Levin, J. Z., Park, H., and Regev, A. (2013) Single-cell transcriptomics reveals bimodality in expression and splicing in immune cells. *Nature* 498, 236-240.
7. Kowenz-Leutz, E., and Leutz, A. (1999) A C/EBP beta isoform recruits the SWI/SNF complex to activate myeloid genes. *Molecular cell* 4, 735-743.
8. Bryant GO, Prabhu V, Floer M, Wang X, Spagna D, et al. (2008) Activator control of nucleosome occupancy in activation and repression of transcription. *PLoS biology* 6: 2928–2939.
9. Reinke H, Horz W (2003) Histones are first hyperacetylated and then lose contact with the activated PHO5 promoter. *Molecular cell* 11: 1599–1607.
10. Badis, G., Chan, E. T., van Bakel, H., Pena-Castillo, L., Tillo, D., Tsui, K., Carlson, C. D., Gossett, A. J., Hasinoff, M. J., Warren, C. L., Gebbia, M., Talukder, S., Yang, A., Mnaimneh, S., Terterov, D., Coburn, D., Li Yeo, A., Yeo, Z. X., Clarke, N. D., Lieb, J. D., Ansari, A. Z., Nislow, C., and Hughes, T. R. (2008) A library of yeast

transcription factor motifs reveals a widespread function for Rsc3 in targeting nucleosome exclusion at promoters. *Molecular cell* 32, 878-887.

11. Hartley, P. D., and Madhani, H. D. (2009) Mechanisms that specify promoter nucleosome location and identity. *Cell* 137, 445-458
12. Floer, M., Wang, X., Prabhu, V., Berrozpe, G., Narayan, S., Spagna, D., Alvarez, D., Kendall, J., Krasnitz, A., Stepansky, A., Hicks, J., Bryant, G. O., and Ptashne, M. (2010) A RSC/nucleosome complex determines chromatin architecture and facilitates activator binding. *Cell* 141, 407-418.
13. Ellegren, H. (2014) Genome sequencing and population genomics in non-model organisms. *Trends in ecology & evolution* 29, 51-63.
14. Kim K, Doi A, Wen B, Ng K, Zhao R, Cahan P, Kim J, Aryee MJ, Ji H, Ehrlich LI, Yabuuchi A, Takeuchi A, Cunniff KC, Hongguang H, McKinney-Freeman S, Naveiras O, Yoon TJ, Irizarry RA, Jung N, Seita J, Hanna J, Murakami P, Jaenisch R, Weissleder R, Orkin SH, Weissman IL, Feinberg AP and Daley GQ: Epigenetic memory in induced pluripotent stem cells. *Nature* 467: 285-90, 2010.
15. Polo JM, Liu S, Figueroa ME, Kulalert W, Eminli S, Tan KY, Apostolou E, Stadtfeld M, Li Y, Shioda T, Natesan S, Wagers AJ, Melnick A, Evans T and Hochedlinger K: Cell type of origin influences the molecular and functional properties of mouse induced pluripotent stem cells. *Nature Biotechnol* 28: 848-55, 2010.